Transcriptional control of somatosensory neuron diversification in *Drosophila*

Megan M. Corty

Submitted in partial fulfillment of the
requirements for the degree of
Doctor of Philosophy
under the Executive Committee
of the Graduate School of Arts and Sciences

COLUMBIA UNIVERSITY

2011

ABSTRACT

Transcriptional control of somatosensory neuron diversification in *Drosophila*

Megan M. Corty

Primary sensory neurons deliver information from the periphery to specific circuits in the central nervous system. It is vital that each sensory neuron detects the appropriate type of stimulus and conveys that information to appropriate regions of the sensory neuropil to target second-order neurons. Molecular programs that coordinate sensory morphology in the periphery with axon projection patterns centrally are poorly understood. I have used the multidendritic (md) sensory neurons of the *Drosophila melanogaster* peripheral nervous system to identify genetic and molecular programs that coordinate dendrite and axonal morphogenesis in individual sensory neurons. The homeodomain transcription factor Cut is expressed in neurons with complex dendrite morphologies that innervate the epidermis and ventral axon projections in the CNS, and is absent from putative proprioceptive neurons that have simpler dendrites and target to more dorsal CNS regions. In this thesis I demonstrate that, in defined subsets of sensory neurons, loss of Cut leads to dendritic transformation to a proprioceptive-type arbor that is accompanied by a dorsal shift in the termination of their axons in the CNS. Mechanistically, I show that Cut functions at least in part by repressing the expression of the POU domain transcription factors Pdm1 and Pdm2 (Pdm1/2), which are normally expressed only in proprioceptive neurons. Gain and loss of function studies further suggest instructive roles for Pdm1/2 in the development of proprioceptive dendritic arborization and axonal targeting. Together these results identify a transcriptional program that coordinately specifies proprioceptive dendrite morphology and sensory axon targeting to modality-

specific domains of the CNS. Using a candidate based approached I have identified three molecular regulators of proprioceptive neuron dendrite morphology. In addition, gene profiling of sensory neurons forced to express Pdm2 has identified over 600 genes that show changes in expression when Pdm2 is misexpressed and that may mediate the effects of Pdm1/2 in directing proprioceptive dendrite and axon development. These profiling experiments pave the way for the identification of novel regulators of dendrite and axon morphogenesis that link transcriptional programs to specific morphologies with consequences for sensory circuit function.

Table of Contents

Acknowledgments

I would like to thank my mentor, Wes Grueber, for his support, encouragement, and mentorship over the past five years. In addition I want to thank all members of the Grueber lab, past and present, for advice and discussions, scientific and otherwise. I would especially like to thank Ben Matthews, and Brikha Shrestha for their assistance and advice on my projects. The Grueber lab has been a fantastic place to do science and learn what it means to truly become a scientist. I also need to thank the individuals who directly contributed to the work presented in this thesis: Rehana Bhuiyan and Michael Newman, two dedicated summer students that contributed to the behavior experiments and array candidate screening described in Chapters 1 and 3, respectively; Rich Blazeski, for his technical expertise and work on the EM analysis of dmd1; Kristie Gordon and the staff at the Flow Cytometry Core Facility; and Vladan Miljkovic at the Genomic Services Core for technical assistance.

Many of the antibodies used in this research were provided by the Developmental Studies Hybridoma Bank at the University of Iowa, and fly stocks were provided by the Bloomington Drosophila Stock Center, and the Drosophila Genetic Research Center in Kyoto. Fly stocks and reagents were also generously shared by other members of the Drosophila community including: Fernando Diaz-Benjumea, Tom Clandinin, Barry Dickson, Chris Doe, Stephen Cohen, Cynthia Hughes, Tzumin Lee, Liqun Luo, Richard Mann, and Gary Struhl, Jessica Triesman.

This work was supported by an NSF Graduate Research Fellowship (M. Corty) as well as NIH grant NS061908 from the NINDS, the Searle Scholars Program, the Klingenstein Foundation, and the McKnight Endowment Fund (W. Grueber).

In addition I would not have been able to complete this work without the help and support of my friends and family. To my fellow grad students and close friends, particularly the Neurobiology and Behavior incoming class of 2005, the McCabe lab women (especially Ellen Penney and Erin Savner), Heidi Smith, the wine night ladies, The Fernald lab girls, and my NYC social director Payal Dalal, thanks for keeping me sane and never thirsty…..

Finally to my family, my parents Jean and Andy, my brother Mike and new sister-in-law Kelly, thank you so much for your support and understanding as I completed this thesis. Knowing I had your love and support meant the world to me.

Dedication

I'd like to dedicate my thesis to my parents, who instilled in me a love of learning from a young age and who have always supported all of my endeavors—educational, scientific, and otherwise. And in particular, I dedicate this thesis to my mom who has weathered all the ups and downs of my education and life for the past 30 years with inordinate amounts of encouragement. Thank you.

Introduction

Portions of this chapter have been adapted from a published review: Corty, M.M.*, Matthews, B.J.*, and Grueber, W.B. (2009) Molecules and mechanisms of dendrite development in *Drosophila*. Development 136: 1049-61, with permission of my co-authors.

Introduction

Since the development of the Golgi stain, which revealed the complex and diverse morphologies of individual nerve cells, a central question in neurobiology has been to understand how specific morphologies arise during development to impact neuronal function. Neurons are the fundamental unit of the nervous system, and their specific morphological features underlie neuronal connectivity and function. Dendrites represent the input portion of a neuron and show remarkable diversity in form across neuronal types. The particular shapes of dendrites matter for nervous system function. Their targets and complexity influence the nature and range of inputs that a neuron receives. In addition, the complexity of a dendritic arbor can impact the processing and integration of electrical signals (London and Häusser, 2005). The precise targeting of axons—the output end of neurons—is likewise required to ensure the specific information collected by a neuron's dendrites is passed on to an appropriate synaptic partner. Thus, dendrite morphogenesis and axonal targeting within individual neurons must be matched for proper nervous system wiring and function.

Neurons are among the most morphologically diverse cell types and the vast diversity of neuronal morphologies—ranging from neurons with a single dendrite to Purkinje neurons with complex space-filling dendritic arbors—is indicative of the wide variety of neuronal types that underlie the diversity of neuronal function in the nervous system. Despite the vast diversity in neuronal form across cell types, neurons with similar developmental origins or functions often share a common morphology (Masland, 2004). These observations raise the question of how diverse morphologies are generated in a cell-type specific manner. Morphologically similar neurons often share common

gene expression, suggesting that intrinsic genetic programs might control key class-specific aspects of dendrite and axon morphogenesis. Moreover, observations that neurons transplanted to new environments can maintain morphological features and connectivity patterns dictated by their birthplace (e.g. Kelsch et al., 2007) offer support for intrinsic cell-autonomous control of dendrite and axonal development.

Studies of dendrite development and axonal targeting have increasingly implicated transcription factors (TFs) as key determinants of class-specific dendritic morphology (Jan and Jan 2010; Parrish et al. 2007) and axon targeting in both invertebrate and vertebrate systems (Dalla Torre di Sanguinetto et al. 2008; Polleux et al. 2007). It is also well established that extrinsic factors such as secreted guidance cues and growth factors (O'Donnell et al., 2009), interactions with neighboring dendrites and axons (Grueber and Sagasti, 2010), and neural activity (Wong and Ghosh, 2002) play major roles in dendrite and axon development. Understanding how intrinsic transcriptional programs and extrinsic patterning cues interact to guide dendrite and axon morphogenesis is a key question for a comprehensive understanding of the mechanisms of neuronal patterning. Evidence points to combinatorial codes of transcription factors that control intrinsic growth programs and as well as the competence of dendrites and axons to respond to activity and appropriate extracellular cues, presumably by regulating the expression of cell surface molecules such as guidance cue receptors or cell adhesion molecules.

Identifying the TFs that give rise to specific dendrite morphologies and underlie precise axonal targeting, and understanding how these TFs instruct neuronal morphogenesis is an important goal in trying to understand nervous system development.

In this introduction, I focus on what is known about the transcriptional regulation of cell-type specific dendritic and axonal development. This includes the identification of specific TFs that control class-specific morphogenesis and targeting and, where they are known, the mechanisms by which these TFs instruct class-specific patterning. I will address the roles of TFs in dendrite and axon development separately followed by a discussion of what is known about the coordinate regulation of axons and dendrites by individual TFs. I focus primarily on studies carried out in *Drosophila* but refer to known or emerging areas of conservation in vertebrate systems where they can provide specific insight. To set the context for the studies presented in this thesis, I will begin with a brief overview of the *Drosophila* peripheral nervous system.

The *Drosophila* PNS: a model system for studying neural development

The sensory neurons of the *Drosophila* PNS have provided a model system for understanding neuronal specification and cell fate decisions for decades. More recently, advances in our ability to visualize individual neuronal morphologies have made these neurons excellent models for the systematic study of morphological development *in vivo*. *Drosophila* larvae are segmentally repeated animals, and each abdominal hemisegment contains 44 sensory neurons with highly stereotyped lineages, morphologies, and positions in one of four clusters along the dorso-ventral (DV) body axis that allow for the unambiguous identification of the same neuron from segment to segment and animal to animal (Figure 1A-B). PNS neurons can be divided into three main morphological types: the **e**xternal **s**ensory (es) organs, **ch**ordotonal (ch) organs, and the **m**ultiple **d**endrite (md) neurons (Figure 1D). Es and ch neurons have single dendrites, and the md neurons, as

their name suggests have multiple dendrites. The md neurons are a diverse population that includes several subdivisions: the bipolar dendrite (bd) neurons, the tracheal dendrite (td) neurons, and the dendritic arborization (da) neurons. Md-bd and md-td neurons have dendrites associated with trachea, glia, and other connective tissue and have relatively simple dendritic arbors compared to the md–da neurons. The da neurons extend their dendrites in roughly two-dimensions along and within the epidermis as free nerve endings (Kim et al., unpublished), and are among the best-characterized and most studied neurons in the *Drosophila* PNS. The da neurons have been subdivided into four classes (I-IV) based on increasing dendritic complexity (Grueber et al., 2002). Studies of these neurons have provided a number of important insights to about the molecules and mechanisms that underlie dendrite development and morphological diversity, the majority of which have conserved roles in vertebrate systems.

In addition to a stereotyped dendritic arbor, each type of PNS neuron has a stereotyped axonal projection domain in the ventral nerve cord (VNC), which is equivalent to the vertebrate spinal cord)(Figure 1 A, C). As is the case with peripheral neurons in vertebrates, insect neurons with distinct sensory functions target to discrete regions of the central neuropil, which presumably aligns afferents with the appropriate post-synaptic partners for each modality. In insects, the dorsal neuropil is associated with proprioceptive afferents while the ventral regions are targeted by tactile and nociceptive afferents (Grueber et al. 2007; Merritt and Whitington, 1995; Murphey et al. 1989; Schrader and Merritt, 2000). Analysis of the axonal projection patterns of the da neuron subclasses revealed that neurons with similar dendritic arborization patterns have similar axon terminal locations in the VNC (Grueber et al., 2007) suggesting they have common

or similar second order targets. These findings reinforce the theory that neurons with similar morphologies have similar functions. Compared to the study of PNS neuron dendrite development, we know much less about the specific mechanisms that guide axon termination choices in the VNC. Thus far it has been determined that the classic midline repellent system of secreted Slit and Robo receptors helps to determine the medial-lateral positioning of sensory axon terminals (Grueber et al., 2007; Zlatic et al., 2003), and Semaphorin-Plexin signaling specifies the positioning on the dorso-ventral axis for at least some sensory neurons (Zlatic et al., 2009).

Despite what is known about the development and dendritic arborization patterns of md sensory neurons, relatively little is known about their specific sensory functions. As a group they are believed to have proprioceptive or mechanosensory functions, and recent work is finally beginning to narrow down the exact functions of a subset of these cells (Hughes and Thomas, 2007; Hwang et al., 2007; Song et al., 2007). Determining the specific sensory modalities of each morphological class is an important future goal; as such knowledge would contribute greatly to our understanding of how dendritic arbor form impacts function and how sensory feedback is used to modulate behavior.

Transcriptional control of dendrite development

Transcription factors (TFs) are important determinants of dendritic morphology in both invertebrate and vertebrate systems (Jan and Jan, 2010; Parrish et al., 2007b). In invertebrate systems, TFs that control class-specific branching patterns and dendrite targeting have received intense study and appear to create combinatorial codes to control these processes in distinct classes of neurons (Grueber et al., 2003; Jinushi-Nakao et al.,

2007; Kim et al., 2006; Komiyama and Luo, 2007). In vertebrates, transcription factors have been found to influence the shape and size of dendritic arbors of specific populations of neurons by regulating the timing of neurite outgrowth, promoting or inhibiting dendrite outgrowth and branching, and contributing to refinement of those arbors by regulating activity-dependent growth and pruning (Cobos et al., 2007; Hand et al., 2005; Ramos et al., 2007).

Transcriptional control of class-specific dendrite morphology in *Drosophila*

Dendritic arbors show tremendous morphological diversity that reflects the inputs that a neuron receives and impacts the processing of signals within the arbor. Identification of the developmental programs that endow different neurons with distinct shapes is therefore an important goal. Much attention has been focused on how intrinsic transcriptional programs of dendritic growth and branching control characteristic cell-type specific morphogenesis, and much of this work has been performed using the *Drosophila* peripheral nervous system (PNS).

As described above the embryonic and larval PNS consists of a well-defined array of sensory neurons in each hemisegment that includes some neurons with a single dendrite (es neurons and ch neurons) and some with more extensively branched arbors (md neurons). The dendritic arborization (da) neurons are one type of md neuron that themselves show diverse dendritic morphologies (Grueber et al., 2002; Sweeney et al., 2002) and have been categorized into four classes (I-IV) with increasingly complex arborizations (Grueber et al., 2002). Thus, the variations in dendrite morphology in this system range from the general (single dendrite vs. multiple dendrite) to specific (different subtypes of multidendritic morphologies). The distinction between a single-dendrite

morphology of external sensory neurons and a multiple dendrite morphology is specified by the zinc finger transcription factor Hamlet. The *hamlet* gene is expressed in the immediate precursors of external sensory neurons (and briefly in postmitotic external sensory neurons), where it acts to repress dendritic branching. Lack of expression in the immediate precursors of multidendritic neurons permits these neurons to form highly-branched arborizations (Moore et al., 2002).

Genetic screens, as well as studies of genes expressed in all, or specific subsets, of da neurons, have identified transcription factors that function to further diversify dendritic branching morphology. The homeodomain protein Cut is expressed at distinct increasing levels in class II, IV, and III neurons, respectively (Blochlinger et al., 1990; Grueber et al., 2003). The distinct expression levels of Cut in each class are responsible for class-specific arbor features (Grueber et al., 2003) (Figure 2). Loss of Cut from cells that express it leads to a simplification of dendrites; whereas its misexpression leads to morphological switches towards the dendritic pattern of the higher-level neurons (Grueber et al., 2003). Although Cut acts to increase branching in most classes of da neurons when overexpressed, the highest levels of Cut do not correlate with the greatest number of branches, but rather with the presence of numerous actin-based filopodia-like extensions. One possibility is that Cut levels are more closely associated with branch dynamics than growth (Grueber et al., 2003; Sugimura et al., 2003), and in this way influence the ability of neurons to build more complex scaffolds. Given the enormous diversity of neuronal morphology, level-dependent transcriptional regulation of morphogenesis, such as is demonstrated by Cut could provide a mechanism of diversification not possible with simple binary (expression or no expression)

transcriptional states. Identification of key transcriptional targets and determining how different levels of Cut affect targets are among the key questions that remain to be addressed to understand how Cut contributes to the development of diverse arbors.

The Broad, Tramtrack, Bric a brac (BTB) zinc finger transcription factor Abrupt is expressed in just one class of da neurons—the class I neurons (Figure 2) where it is required to limit dendritic branching (Li et al., 2004; Sugimura et al., 2004). Correspondingly, the expression of Abrupt in the other, more complex, classes strongly suppresses dendritic complexity (Li et al., 2004; Sugimura et al., 2004). The transcriptional mechanisms that underlie dendrite simplification by Abrupt are still unknown. Abrupt is expressed in a complementary pattern to the homeodomain protein Cut (Grueber et al., 2003; Li et al., 2004; Sugimura et al., 2004), and while ectopic expression of Cut can reduce Abrupt levels in class I neurons, there is no strong evidence that cross-regulation is responsible for their exclusive expression patterns (Sugimura et al., 2004).

Recent studies of the Collier/Olfactory-1/Early B-Cell Factor (COE) transcription factor Knot/Collier suggest that dendritic arbor patterns are specified in individual cells by combinatorial use of transcription factors. Knot is expressed, together with Cut, in class IV neurons **(**Figure 2) and is required for the development of their highly branched space-filling arborizations. Its postmitotic misexpression in other da neuron classes is sufficient to transform them toward a class IV-like branching pattern (Crozatier and Vincent, 2008; Hattori et al., 2007; Jinushi-Nakao et al., 2007). Although Cut can exert a moderate positive effect on the amplitude of Knot expression (Jinushi-Nakao et al., 2007), the consequences of such regulation for arbor morphology are not clear.

Conversely, Knot activity counteracts the formation of the class III-like actin-based dendritic extensions that are induced by Cut overexpression (Jinushi-Nakao et al., 2007). These results suggest that a code for the two most complex morphologies – $Cut^{hi}/knot^{-}$ (class III) and $Cut^{intermediate}/Knot^{+}$ (class IV) – acts to promote several of the differences in their class-specific dendritic branching patterns. One possibility arising from overexpression experiments is that Cut promotes F-actin based dendrite extensions, while Knot promotes growth of microtubule-based arbor (Jinushi-Nakao et al., 2007). This hypothesis is supported by the finding that the cortex of mice lacking the Cut homologs Cux1 and Cux2 have decreased levels of β-actin mRNA and protein (Cubelos et al., 2010). However, selective control of actin-based processes by Cut is inconsistent with certain mutant phenotypes that show severe truncation of entire dendritic arbors (Grueber et al., 2003), suggesting that other mechanisms are important. Knot might also regulate physiological features of class IV neurons given that it also regulates expression of an ion channel subunit encoded by *pickpocket* (and transgenic reporters of *pickpocket* expression) in these cells (Ainsley et al., 2003; Crozatier and Vincent, 2008; Hattori et al., 2007; Jinushi-Nakao et al., 2007).

Spineless, a conserved basic helix loop helix-Period/Ahr/Single-minded (bHLH-PAS) transcription factor, has a unique influence on dendrite diversification. When da neurons are mutant for *spineless*, all four da neuron classes exhibit similar morphologies that are of similar intermediate branching complexity (Kim et al., 2006). Spineless is expressed at similar levels in all four da neurons classes, and most da neurons (with the exception of class IV neurons) do not show an overexpression phenotype (Kim et al., 2006). Thus, in different cells Spineless can act to either limit or promote branching,

perhaps permitting the perhaps permitting the diversification of a common (maybe a ground or default state) dendritic morphology of intermediate complexity (Kim et al., 2006). How Spineless might accomplish this is not clear. Given that Spineless seems not to control the expression of Cut or Abrupt in da neurons (Kim et al., 2006), and that both Cut and Abrupt are sufficient to drive class-specific branching when overexpressed in Spineless-expressing neurons, it is conceivable that Spineless might normally regulate factors that balance the execution of class-specific programs. Furthermore, the molecular mechanism by which Spineless acts is not known given that its typical heterodimeric partner, Tango (Emmons et al., 1999), is not required cell autonomously during dendrite morphogenesis (Kim et al., 2006), raising the possibility that class-specific co-factors may contribute to its apparently opposite functions in distinct da classes.

Targets of transcription factors that control dendrite morphology

To fully understand how intrinsic transcriptional programs contribute to the development of diverse morphologies, we must understand the nature of the genes they regulate to mediate these effects. In the *Drosophila* PNS system, downstream targets of identified TFs remain largely unknown. To date only one target of Cut transcriptional regulation in da neurons has been reported. A recent study demonstrated that Cut can positively regulate *turtle (tutl)*, a gene encoding an evolutionarily conserved member of the Tutl/Dasm1/IgSF9 group of immunoglobulin-superfamily proteins. Cut can bind to the *tutl* locus, and overexpression of Cut in class I neurons can lead to increased expression of Tutl (Sulkowski et al., 2011). The authors also found that decreased dosage of *tutl* can limit the ability of Cut to produce excess branch formation in overexpression

experiments (Sulkowski et al., 2011). Despite these findings, it remains unclear how endogenous regulation of *tutl* by Cut might contribute to class-specific morphogenesis *in vivo*. Tutl is expressed in all classes of da neurons (Long et al., 2009) with higher levels of expression in the more complex class III and IV neurons compared to class I and II neurons (Sulkowski et al., 2011), but Cut is not required for Tutl expression in these neurons (Long et al., 2009; Sulkowski et al., 2011). It is possible that that *turtle* might be a level-dependent target of Cut that is relevant only at Cut levels found in forced overexpresion experiments. There are conflicting reports about the effects of Tutl in the highest expressing class III neurons—either no effect at all of *tutl* mutation (Long et al., 2009) or a modest but significant reduction in branching (Sulkowski et al., 2011). In either case the effect of *tutl* mutation on class III neurons is much less severe than *cut* mutation indicating that *tutl* is just one of many genes that mediate Cut's effects on dendrites.

Knot has been shown to promote branching by positively regulating the expression of Spastin (Jinushi-Nakao et al., 2007), an ATPase that has microtubule-severing activity (Roll-Mecak and Vale, 2005). The authors of this study suggested that appropriate levels of microtubule severing activity might be needed to promote complex dendritic branching by creating opportunities for new microtubule polymerization (Jinushi-Nakao et al., 2007). These results and interpretation are seemingly at odds with a recent study that has identified a novel Kruppel-like factor named Dar1 that promotes dendrite branching by negatively regulating Spastin (Ye et al., 2011). Can these conflicting findings be reconciled? Knockdown of Spastin in class IV neurons reduces branching (Jinushi-Nakao et al., 2007), but overexpression of Spastin can have a similar

effect (Ye et al., 2011). This suggests that a precisely controlled level of Spastin is required to maintain a balance between the stabilization and severing of microtubules that allows for growth. This model fits the data provided—loss of Dar1 leads to unchecked Spastin expression that leads to high levels of microtubule severing that do not allow for growth (Ye et al., 2011). However, too little Spastin cannot support the complex branching of class IV neurons; so Knot might be used to moderately increase Spastin levels specifically in these most complex highly arborized neurons (Jinushi-Nakao et al., 2007). Additional studies, including analysis of the effects of different Spastin expression levels on growth and branching, will be needed to confirm this interpretation.

The small number of distinct morphological classes and the ability to genetically manipulate individually identifiable neuron across animals has made the *Drosophila* md-da neuron system particularly useful for identifying specific transcription factors that contribute to class-specific morphological features. The overexpression of mammalian homologs of either Cut or Knot can at least partially mimic the effect of its *Drosophila* counterpart (Grueber et al., 2003; Jinushi-Nakao et al., 2007), and the rodent homologs of Cut and Knot (Cux and Ebf transcription factors, respectively) are expressed in the developing brain (Cobos et al., 2006; Garel et al., 1997) suggesting there might be conserved roles for these genes in vertebrates. The roles of Knot homologs in dendrite development have not yet been studied. Interestingly, two recent studies, discussed below, have demonstrated roles for the Cut homologs Cux1 and Cux2 in vertebrate dendrite development.

Transcriptional control of class-specific dendrite morphology in vertebrates

In the last few years, candidate-based approaches stemming from selective expression patterns of individual transcription factors in vertebrate nervous systems have identified several TFs that have important roles in cell-type specific morphological development, a few of which I will briefly review here.

Pyramidal cells and inhibitory GABAergic non-pyramidal interneurons are the two major types of neurons in the mammalian neocortex. Basic pyramidal neuron dendritic morphology is characterized by a single apical dendrite and numerous basal dendrites, whereas non-pyramidal interneurons have diverse dendritic morphologies (Markram et al., 2004). The basic helix-loop-helix (bHLH) transcription factor Neurogenin2 (Ngn2) is expressed in developing pyramidal neurons, and is important for neuronal proliferation and specification of these cells (Schuurmans et al., 2004). Ngn2 also has a later role in migration and acquisition of the unipolar pyramidal cell dendritic morphology (Hand et al., 2005). These distinct functions of Ngn2 depend on a specific post-translational modification: phosphorylation of tyrosine 241 (Y241) of Ngn2 is required for the regulation of migration and neurite outgrowth, but not for neuronal differentiation (Hand et al., 2005). Presumably this modification changes the partners with which Ngn2 associates to modulate transcription for the control of distinct processes. Thus, it is not only sustained expression of Ngn2 throughout postmitotic development that allows it to play different roles at different stages of development. As many TFs in the nervous system appear to have separable early and late roles, it will be important to determine how widespread such post-translational molecular changes are amongst TFs with distinct early and late roles in neuronal development.

Programs that regulate cortical layer-specific differences in pyramidal neuron morphology are also beginning to be uncovered. Comparisons of global gene expression patterns in microdissected upper and lower neocortical layers, which have distinct dendritic and axonal morphologies (Cheng et al., 2005) identified Zinc finger protein 312 (Zfp312/Fez1/Fezl), which is likely to function as a transcription factor. Zfp312 was enriched in layer V and VI pyramidal neuron nuclei (as well as a few other areas of the brain), and siRNA knockdown demonstrated a role in the specification of deep layer V apical dendritic orientation and basal dendrite branching and growth (Cheng et al., 2005). Upper-layer pyramidal neuron morphology is not affected by Zfp312 knockdown, so this transcription factor might specify morphological differences in different cortical layers by regulating other transcription factors or guidance and growth cues (Cheng et al., 2005). Whereas Zfp312 regulates layer V and VI morphogenesis, recent studies have identified Cux1 and Cux2, the mouse homologs of *Drosophila* Cut, in regulating upper layer cortical neuron dendrite morphology (Cubelos et al., 2010).

In mice, Cux1 and Cux2 are expressed in upper layer (II/III) but not lower layer cortical neurons (Nieto et al., 2004). One recent study suggests that Cux1 and Cux2 promote dendritic growth and branching in these upper (II/III) layer cortical neurons, as evidenced by analysis of mutant animals and targeted knockdown of Cux1 and Cux2 in slices (Cubelos et al., 2010). Dendritic length and branching was reduced in single mutants, but the effects were stronger when both genes were affected suggesting additive effects of the two TFs. In addition, Cux1 and Cux2 can promote spine development and synapse formation in these neurons. These findings are similar to those in *Drosophila* that describe a growth-promoting role for Cut (Grueber et al., 2003).

Another report finds that Cux1 acts to decrease neuronal complexity of pyramidal neurons. In these experiments, knockdown of Cux1 (but not Cux2) in cultured rat pyramidal neurons led to increased dendritic complexity, suggesting that Cux1 acts as a negative regulator of dendrite growth and complexity in these neurons with Cux2 having no effect (Li et al., 2010). The reasons for these conflicting results are not yet clear. Cubelos and colleagues carried out their analyses in a defined population of upper layer somatosensory neurons from whole animals or in slices and based their conclusions on similar results in both knockout and RNAi experiments. Li and colleagues analyzed a more heterogeneous population of dissociated neurons in culture exclusively with RNAi, so these conflicting results could be due to experimental or species differences.

In rat cortical neurons, Cux1 was shown to negatively regulate the cyclin-dependent kinase inhibitor p27 to suppress dendrite complexity (Li et al., 2010). By contrast, positive regulation of *Xlr3b* and *Xlr4b,* genes likely involved in chromatin modification, is required for Cux1 and Cux2 roles in promoting synapse development(Cubelos et al., 2010). Despite the differences in direction, these studies demonstrate that Cux1 and Cux2 have conserved roles as postmitotic regulators of dendrite development. Do Cux1 and Cux2 perhaps also have level dependent effects on dendrite morphogenesis, as in *Drosophila*? In somatosensory cortex, where these studies were carried out, neurons express both Cux1 and Cux2 at approximately equal levels. Other populations of upper layer neurons express Cux2 at high levels but only low levels of Cux1. Interestingly, these neurons have less complex dendritic morphologies than somatosensory neurons. Overexpression of Cux1 in these neurons caused a significant increase in dendritic complexity (Cubelos et al., 2010), suggesting that Cux1 and Cux2

levels may dictate dendritic complexity in vertebrate neurons, similar to their role in *Drosophila* da neurons, though this has not yet been tested directly.

Gene expression analysis has also begun to identify candidate regulators of GABAergic interneuron anatomical diversity (Cobos et al., 2006; Hardt et al., 2008). Several transcription factors, including Dlx homeobox transcription factors and Cux transcription factors are expressed in subsets of GABAergic interneurons (Cobos et al., 2006; Cubelos et al., 2008b). Dlx1/2 genes set the timing of interneuron arborization relative to migration which affects their finally morphologies (Cobos et al., 2007). Cux TFs are expressed specifically in the Reelin-expressing subpopulation of interneurons and have an early role in their specification (Cubelos et al., 2008). Cux TF continue to be expressed post-mitotically in these cells, suggesting they might play additional roles in the maturation of these neurons, but specific roles in morphogenesis in this population have yet not been described.

As these studies suggest, the transcriptional codes that mediate dendritic morphogenesis are likely to be complex, and the genes studied so far, along with the few known downstream targets, represent a preliminary stage in our understanding of the transcriptional control of dendritic diversification. In addition, other mechanisms that modify chromatin structure, including histone modification and ATP-dependent chromatin remodeling, add another level of transcriptional control over dendrite morphogenesis (Nott et al., 2008; Parrish et al., 2007a; Parrish et al., 2006; Tea and Luo; Wu et al., 2007). Such mechanisms have the potential to further diversify the effects of individual transcription factors in different neuronal types.

Transcriptional control of dendritic guidance and targeting

The development of functional circuits is aided by cell-type specific dendritic targeting. Dendritic guidance and targeting programs polarize arbors to innervate particular regions of the nervous system, and thus impact the inputs that a neuron receives. Studies in vertebrate and invertebrate systems indicate that a first level of targeting control arises from intrinsic programs that are linked to cell lineage and identity (Jefferis et al., 2001; Kelsch et al., 2007; Komiyama et al., 2003; Komiyama and Luo, 2007). These programs, in turn, likely dictate how dendrites respond to attractive or repulsive cues in their environment.

Combinatorial codes of transcription factors direct dendritic targeting in the *Drosophila* antennal lobe

An extensive analysis of intrinsic factors that control dendritic targeting has been undertaken in the *Drosophila* antennal lobe (AL), a region of the brain where olfactory information from olfactory receptor neurons (ORNs) is transmitted to second-order olfactory neurons called projection neurons (PNs) (Figure 3). About 150-200 PNs are produced from three major lineages: the anterodorsal (adPN), lateral (lPN), and ventral (vPN) lineages. PN dendrites target one or a few, out of approximately 50, AL glomeruli in a lineage-dependent manner (Jefferis et al., 2001). Intrinsic transcriptional programs control lineage-specific dendritic targeting of PNs by directing both global and local positioning in the AL. Based on analysis of several families of transcription factors (including POU domain, homeodomain, BTB-Zn finger, and LIM-homeodomain families), it has been shown that some transcription factors, such as Cut, likely specify

the general AL domain targeted by PN dendrites (Komiyama and Luo, 2007). Other transcription factors, including the POU-domain proteins Acj6 and Drifter, are expressed in a lineage specific manner (Acj6 in adPNs and Drifter in lPNs) and specify local glomerular choice (Komiyama et al., 2003; Komiyama and Luo, 2007).

An example of how global and local transcriptional programs act in combination to mediate lineage-specific targeting is provided by studies of PNs innervating the DL1 glomerulus (Komiyama and Luo, 2007). DL1 is targeted by a subset of adPNs that express the Acj6 transcription factor, and in *acj6* mutant clones, dendrites are no longer restricted to DL1 glomerular boundaries (Komiyama et al., 2003; Komiyama and Luo, 2007) (Figure 3C). Misexpression of Cut in *acj6* mutant clones shifts dendrites to distant glomeruli in the medial portion of the AL but these glomeruli are ones that are normally targeted by adPNs, indicating that some lineage information is preserved (Komiyama and Luo, 2007) (Figure 3E). By contrast, if Cut is misexpressed in *acj6* clones together with the lPN-specific transcription factor Drifter, the dendrites innervate medial (Cut) lPN (Drifter) target glomeruli (Komiyama and Luo, 2007) (Figure 3F). Thus, precise PN targeting arises from combinations of transcription factors that specify coarse and local positioning of dendrites to guide them to the most appropriate target.

Additional transcription factors that control PN targeting include the LIM-HD factors Islet and Lim1 and the LIM binding co-factor Chip (Komiyama and Luo, 2007), as well as the homeodomain transcription factor Empty spiracles (Ems), a fly homolog of mouse Emx1/2 that affects the targeting of adPNs at least partly by regulating *acj6* (Lichtneckert et al., 2008). Glomerular targeting in the AL also relies on the *longitudinals lacking (lola)* gene. The *lola* locus encodes at least 20 alternative isoforms, most of

which are transcription factors of the BTB-Zinc-finger family (Goeke et al., 2003; Spletter et al., 2007). PNs that lack all *lola* isoforms show disrupted glomerular targeting, ectopic targeting phenotypes, and misregulation of at least some genes important for PN targeting, such as Lim1 (Spletter et al., 2007). The expression of single Lola isoforms does not rescue the loss of function phenotypes, and produces additional dendrite defects, including disrupted process extension and elaboration outside of normal glomerular boundaries (Spletter et al., 2007). Thus, Lola isoforms are not simply interchangeable, and *lola* molecular diversity is important for proper dendritic targeting. Together, the transcription factors identified so far probably represent a subset of those required for complex glomerular map formation in the AL, and perhaps a full instructive code for glomerular targeting could be reconstructed with the identification of additional factors.

With the identification of transcription factors that control dendritic targeting, an important question that arises is how these factors are linked to the expression of specific guidance receptors, cell adhesion molecules, or components of receptor signaling pathways that affect targeting choices. Links between transcription factor activity and the expression of specific axon guidance factors have been identified in several systems (Kania and Jessell, 2003; Labrador et al., 2005; Lee et al., 2008; Wilson et al., 2008; Zlatic et al., 2003), but so far such relationships have not been established for dendritic targeting.

Extrinsic factors shaping dendrite development

Studies of stereotyped axon guidance decisions have identified core cues and receptors (Garbe and Bashaw, 2004; Huber et al., 2003), and data so far indicate that in both vertebrate and invertebrate systems, several of these same families of molecules also

function in guidance and targeting of dendrites, including Semaphorins (Komiyama et al., 2007; Polleux et al., 2000), Robo and Slit (Furrer et al., 2003; Furrer et al., 2007; Godenschwege et al., 2002; Ou et al., 2008; Whitford et al., 2002), and Netrin and DCC/Frazzled/UNC-40 (Furrer et al., 2003; Ou et al., 2008; Suli et al., 2006).

Positive (adhesive) and negative (repulsive) interactions can also act locally between dendritic branches to delimit the territories that they cover. Interactions between dendrites can function to maintain dendrites within a specific territory. For example, N-cadherin is required among PNs targeting to glomeruli in the AL in order form and maintain compact targeting of a single glomerulus (Zhu and Luo, 2004). By contrast, repulsive interactions between branches of the same cell can help to ensure that branches spread out evenly within their territory. This is exemplified by the studies of DsCAM as a mediator of self-avoidance (Matthews et al., 2007; Matthews and Grueber, 2011). Responsiveness to such extrinsic cues may be largely determined by cell intrinsic programs of TFs that regulate the expression of the wide variety of molecules that have been shown to mediate dendrite growth and development including guidance cue receptors, cell adhesion molecules, other cell surface molecules.

Transcriptional control of axon targeting

During nervous system development axons must be directed to appropriate target regions where they will be able to form connections with the appropriate synaptic partners. Axons are guided to their targets by long and short range guidance cues as well as contact mediated mechanisms (Tessier-Lavigne and Goodman, 1996), but these extrinsic signals are only as good as a growth cone's ability to detect them. As with

dendrites, there is overwhelming evidence that intrinsic codes of transcription factors are used to specify axonal targeting. One way in which they might carry out this role is by orchestrating the precise regulation of guidance cue receptors, cell adhesion molecules, and other cell surface proteins that mediate growth cone and environment interactions. In fact, numerous studies have linked TFs that specify axon projections with specific molecular regulators of axon guidance. Evidence for TF control of cell-type specific axon targeting exists in many systems (e.g. the retina: Herrera et al., 2003; the cortex: Hand and Polleux, 2011; Chen et al., 2006), but the most comprehensive example of how TF codes can specify neuronal subtype identity and axonal trajectory and targeting comes from studies of motor neuron identity and targeting in the vertebrate spinal cord.

Combinatorial codes of Hox and Lim TFs specify vertebrate motor neuron targeting

Much of the work demonstrating that TF codes control axonal targeting has been done in the vertebrate spinal cord, investigating how specific motor neuron pools are specified to direct their axons to the appropriate target muscles in the periphery. Studies in this system have revealed that hierarchal and combinatorial actions of TFs direct motor neuron fate and axon targeting down to final muscle target choice. In this highly organized system, motor neuron fate is specified by position along the anterior-posterior (AP) axis primarily by specific combinations of Hox family transcription factors. Cross repressive interactions between different Hox genes create zones of unique expression for multiple Hox genes that delineate discrete populations of motor neurons into columns, sub-columns, and eventually specify motor neuron pools, which are comprised of motor neurons that will innervate the same target muscle (Dalla Torre di Sanguinetto et al.,

2008; Dasen et al., 2005; Dasen et al., 2008; Dasen et al., 2009). The "Hox codes" of each motor pool ultimately direct projection of axons to specific muscles and altering the pattern of Hox gene expression leads to predictable shifts in motor axon innervation of non-target muscles (Dasen et al., 2005).

Hox codes appear to specify motor neuron targeting by regulating additional downstream transcription factors (De Marco Garcia and Jessell, 2008), which in turn regulate axon guidance molecules that specify axon trajectory (at the level of columns) and connectivity (at the level of motor pools) creating a complex hierarchical code that results in highly specific targeting. The ensemble of Hox TF expression at each level of motor neuron organization (column, pool, etc) specifies the expression of these so-called "intermediate" TFs, which are also required for proper targeting. Thus far, it is mainly these intermediate TFs that have been found to directly regulate responsiveness to axon guidance pathways that lead to specific innervation patterns. For example, LIM-homeodomain family member, Lim1 is expressed in a subset of lateral motor column (LMC) neurons that project to dorsal muscles. This dorsal trajectory is dependent upon Lim1 regulation of EphA4 (Kania and Jessell, 2003). Islet1 is expressed in a complimentary fashion and specifies ventral motor neuron trajectory, in part by negatively regulating EphA4 and in part by positively regulating EphB1 (Kania and Jessell, 2003; Luria et al., 2008) (Figure 4). Targeting to specific muscles requires pool-specific transcription factors including Nkx6.1 and Runx1 but the downstream target genes of these TFs that control this specificity are not yet known (Dasen et al., 2003; De Marco Garcia and Jessell, 2008). Despite a different organization, the same principles and classes of TFs act to specify motor neuron fate and targeting in *Drosophila* (e.g.

Broihier et al., 2004; Labrador et al., 2005). These findings demonstrate the tight and specific regulation of motor neuron connectivity is in large part dictated by intrinsic transcriptional programs and that the overall logic of such control as well as the use of specific genes is highly conserved.

Cell type specific TF expression directs axon targeting in many additional systems, and in several cases the key downstream effectors of these transcriptional programs have been identified (Lee et al., 2008; Wilson et al., 2008; Zlatic et al., 2003). For example, retinal ganglion cells (RGCs) from the ventro-temporal retina need to project their axons ipsilaterally in the brain. Ipsilateral projection is specified by the zinc finger TF Zic2 (Herrera et al., 2003), which positively regulates EphB1 receptors in ventro-temporal RGCs neurons so that they do not cross the ephrinB-rich optic chiasm (Lee et al., 2008). Another example comes from studies of spinal cord projection neurons, which must also choose an ipsilateral or contralateral route to higher brain centers. One subset of projection neurons, the dl1c neurons, express the homeodomain TFs Lhx2 and Lhx9 and project their axons contralaterally. Analysis of *Lhx2* and *Lhx9* double mutants revealed that Lhx2 and Lhx9 are specifically required for contralateral axon projection by virtue of their ability to positively regulate Rig-1, a variant Robo receptor required for floor plate crossing (Sabatier et al., 2004; Wilson et al., 2008). It is of interest to note that identity of these neurons was unchanged (as assayed by the retained expression of several other cell type specific markers), providing evidence that Lhx2 and Lhx9 have specific roles in regulating axon guidance rather than just controlling cell identity that could lead to changes in projections (Wilson et al., 2008) .

A final example directly relevant to the work of this thesis, comes from studies in

Drosophila of the mechanisms that control the sensory axon termination in the ventral nerve cord. Chordotonal (ch) sensory neurons have stereotyped axon projections in the nerve cord, terminating at the intermediate fascicle on the mediolateral (ML) axis, which is distinct from the terminations of the multidendritic (md) sensory neurons that terminate on the medial fascicle. The proneural gene *atonal* is required for the formation of chordotonal (ch) sensory neurons (Jarman et al., 1993; Jarman et al., 1995), and also acts to specify the intermediate ML termination of their axon by positively regulating Robo3, a receptor that mediates repulsion from midline sources of Slit. Robo3 expression is normally limited to ch neurons. Misexpression of atonal in md neurons leads to widespread Robo3 expression and induces a lateral shift of their axons to a ch-like intermediate position (Zlatic et al., 2003). This study provides evidence for type-specific TF control of guidance molecules that are read out as type specific axon patterns. Atonal expression is not sufficient to dictate a complete conversion to a ch-like termination, as laterally shifted md neurons can maintain their characteristic positions on the DV axis (Zlatic et al., 2003). These results suggest that multiple TFs must work together to specify the precise location of axon terminals in this system. Furthermore they suggest that ML and DV positioning in the Drosophila VNC are independently regulated. This is supported by the finding that Slit and Netrin guidance pathways regulate ML positioning in the VNC, whereas Semaphorin signaling positions sensory neuron terminals along the DV axis (Zlatic et al., 2009). It will be of interest to determine whether ML and DV position can be controlled in a coordinate fashion by individual TFs, or if the use of combinations of TFs is conserved throughout the VNC.

Coordinating the development of dendrites and axons

Intrinsic transcriptional programs simultaneously control many key aspects of neuronal identity and functionality including axon and dendrite development. In the context of circuit formation, one interesting question is whether single TFs might control both dendrite and axon morphogenesis in the same cell to coordinate their development, and whether this can be done independently from an overall cell fate decision. Such a system would help to ensure proper integration of neurons into functional circuits, and recent findings demonstrating that dendrites and axons are capable of using the same growth and targeting strategies and even molecules, indicate that common regulatory programs could be used to simultaneously direct both processes.

Two examples of individual TFs found to have effects on both dendrite and axon development within the same neuron come from the study of PNs in the *Drosophila* antennal lobe. Loss of the Acj6 TF, which plays critical roles in PN dendrite targeting of the DL1 glomerulus as described above, also alters growth and targeting of DL1 PN axons (Komiyama et al., 2003). Likewise altering the expression pattern of Lola isoforms impacts both dendrite targeting and axon growth and targeting (Spletter et al., 2007). In the case of Lola, this may correspond to some degree of fate change, since it is noted that the expression patterns of gene expression are altered in *lola-/-* clones (Spletter et al., 2007). In the case of Acj6, mutant dendrites typically still target adPN targets, just not DL1, suggesting that at least general adPN identity is retained (Komiyama et al., 2003).

Although these examples represent the ability of single TFs to affect both dendrite and axonal patterning, it is not entirely clear whether the changes seen in axons and

dendrites are coordinated per se—that is, do the changes in dendritic patterning reflect and correspond to the new connectivity of the axon (or vice versa)? Or do the changes just represent non-specific defects in neurite outgrowth? PN glomerular choice is tightly coupled to specific axonal projection patterns in higher brain centers—so much so that axonal projections can be used to predict a neuron's glomerulus choice (Marin et al., 2002; Wong et al., 2002). Although Acj6-/- axons were missing one axonal branch, the majority of its stereotyped axon projection pattern was intact (Komiyama et al., 2003) and the authors did not note a switch to the axonal arborization pattern of any aberrantly targeted glomeruli. Similarly in the case of Lola, it was reported that the severity of dendritic and axonal phenotypes did not seem to correlate, suggesting that although aspects of dendrite and axon development are controlled by the same transcription factor, this does not lead to their coordinated development (Spletter et al., 2007).

Another example of a single TF that can have effects both dendrite and axon patterning comes from the vertebrate motor neuron system where expression of the ETS TF Pea3 controls both motor neuron dendrite patterning and axonal innervation of target muscles. Pea3 is expressed by motor pools that innervate the cutaneous maximus (CM) and latissimus dorsi (LD) muscles. Pea3 expression in motor neurons is required for wild type innervation of CM and LD muscles—without Pea3, motor neurons still innervate the appropriate muscles, however the innervation is incomplete (Livet et al., 2002). Interestingly Pea3 is also required for normal patterning of CM and LD motor neuron dendrites (Vrieseling and Arber, 2006). Pea3 expression in these motor neurons is induced by GDNF expression in the limb bud (near the muscle target)(Haase et al., 2002). In this case the changes in dendrite patterning do not appear to be a means to

compensate for or match aberrant axon patterning. But the concept that axon and dendrite patterning are co-regulated by target-induced TF expression raises the possibility that such a mechanism could allow for compensatory alterations in dendrite patterning depending on the final outcome of axon targeting to ensure matching.

In addition to the examples of TFs that can affect both axon and dendrites, there are also many examples of TFs that strictly control either axons or dendrites but not both. For example, in *Drosophila,* Spineless and the Kruppel-Like factor Dar1 exclusively affect class-specific dendrite development without affecting axonal projections (Kim et al., 2006; Ye et al., 2011), and Atonal overexpression can alter axonal targeting with little effect on dendrite morphology (Zlatic et al., 2003). It is currently difficult to know how common dual regulation of axons and dendrites by individual TFs might be, as genetic studies have not always examined both dendrite and axon phenotypes. Examples of both dual and separate regulation by TFs suggest that coordinate control may by achieved through simultaneous parallel regulation of discrete axon targeting and dendrite patterning programs by a single upstream TF.

Potential molecular mechanisms of coordinated control

Although coordinate regulation appears to be an elegant solution to ensure proper wiring, dendrites and axons have many differences that might pose challenges to such a strategy. The breaking of symmetry a key step in early morphogenesis establishes numerous differences of axonal vs. dendritic cell biology (Rolls, 2010; Rolls et al., 2007; Tahirovic and Bradke, 2009). Differences between axons and dendrites include differences in microtubule polarity, biased membrane trafficking, and precise sorting of

cargo to axons vs. dendrites that might pose challenges for coordinate regulation (Stone et al., 2008; Ye et al., 2007; Horton et al., 2005). In addition dendrites and axons from the same neuron will likely be developing at different time points and at great distances from one another. The degree of difference in the complexity of axons and dendrites in some cells can be vast. (For example the class IV da neuron with a complex dendritic arbor, but a simple axon termination.) Given these differences between axons and dendrites, how might a single TF regulate both dendritic patterning and axon targeting in the same neuron?

One possibility is that a TF could control the expression of a common set of genes that affect both dendrite and axon morphogenesis. In theory this could even represent a single molecule, such as a guidance cue receptor that can work in both dendrites and axons to coordinate their development. . Many guidance and cell adhesion molecules have demonstrated roles in both axons and dendrites (Jan and Jan, 2010), and there are examples of single molecules differentially affecting the dendrites and axon of the same neurons (Polleux et al., 2007), which would expand the ability of common factors to have disparate effects in axons and dendrites. Another possibility, mentioned above, is that a TF that can coordinate axon and dendrite development through parallel regulation of separate axon and dendrite programs. In both cases, the cell biological differences between axons and dendrites might be useful for maintaining separate signaling compartments and controlling the distribution of cell surface molecules such as guidance receptors through differential trafficking. Identifying more examples of functionally relevant coordination of axonal and dendritic development by single TFs, and identifying the downstream targets that underlie this coordination should provide important insights

into the control of precise neural circuit formation.

Conclusion

Proper circuit formation is crucial for a functional nervous system and depends on the proper development of both dendrites and axons, which is under tight control by intrinsic programs and extrinsic cues. In recent years, our understanding of the genetic and molecular bases of dendritic and axonal growth, branching, targeting, has greatly expanded and has increasingly implicated tight transcriptional control as a key determinant of connectivity in the nervous system. In addition to the genes and pathways characterized in recent studies and reviewed here, the potential for our knowledge to grow is immense. A screen in *Drosophila* identified more 70 TFs that affect dendrite patterning from an RNAi-based approach (Parrish et al., 2006). There have also been several large-scale efforts to identify TF expression patterns that define discrete populations of neurons in brain (Gong et al., 2003; Gray et al., 2004), which will undoubtedly increase the number of TFs implicated in controlling class-specific dendritic and/or axonal development of vertebrate neurons. Despite the identification of a wide variety of TFs with specific influences on morphological development, the downstream targets that they regulate remain largely unknown. Thus it remains unclear how different transcriptional programs result in distinct and specific morphologies and targeting. Identification of more of these targets will be crucial for understanding the logic of nervous system wiring controlled by differential expression of TFs.

Figure 1: The Drosophila larval PNS

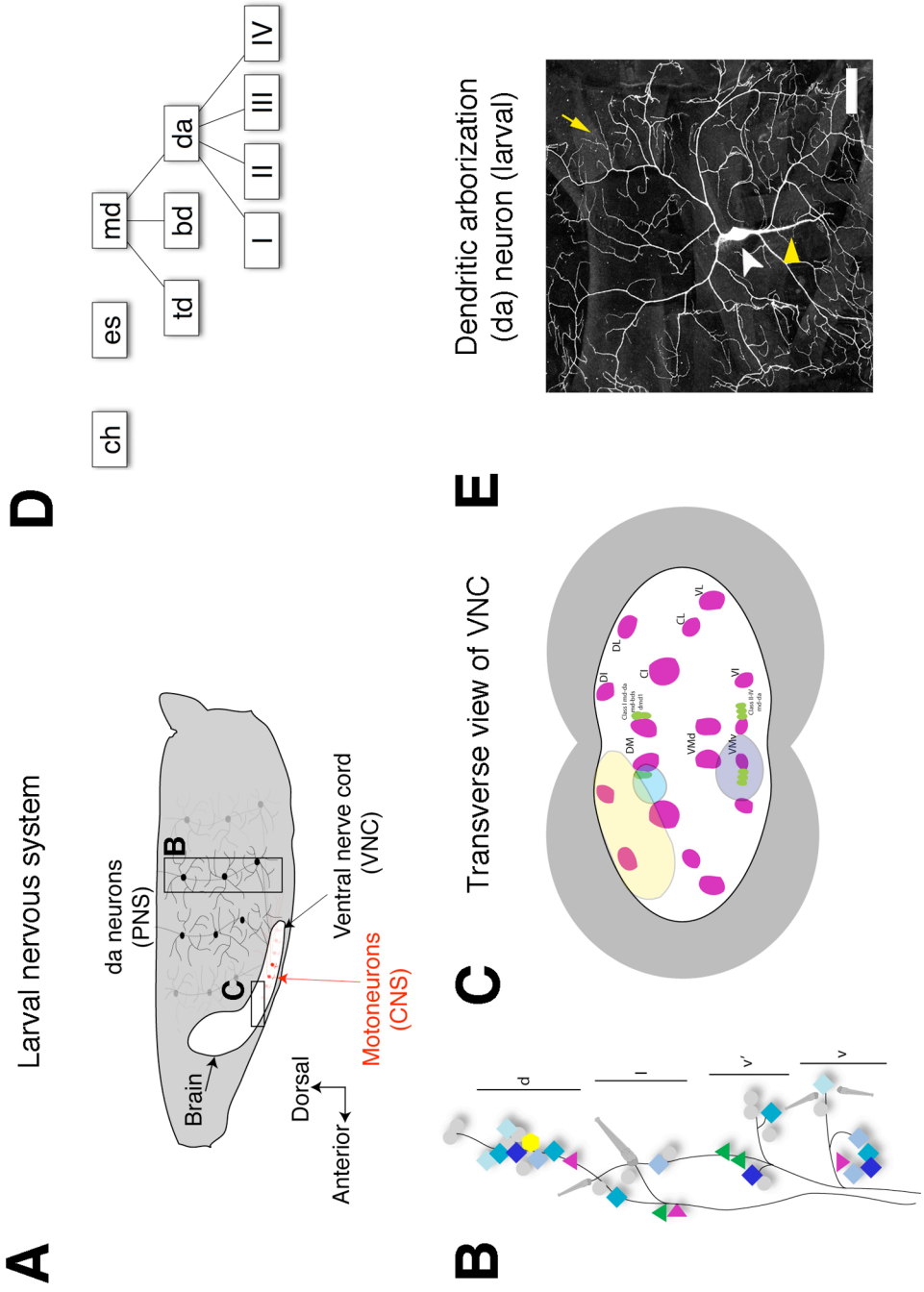

Figure 1: The *Drosophila* larval PNS

(A) Schematic of the entire larval nervous system showing the position within the body of the PNS neurons and the CNS. Boxed areas "B" and "C" are shown in detail in panels **(B)** and **(C)**.

(B) Schematic diagram showing of one hemisegment of the *Drosophila* larval PNS. Dorsal (d), lateral (l), ventral prime, (v'), and ventral (v) clusters are labeled. Es neurons are depicted as gray circles, chordotonal organs as gray triangles. Md neurons are depicted in color. Md-da neurons are represented by diamonds in increasing shades of blue to correspond to subclass (Class I <ClassII <ClassIII <ClassIV). Md-bd neurons are represented as magenta triangles. Md-td neurons are represented with green triangles.

(C) Schematic of a transverse section of the larval VNC. Central neuropil is white. An array of stereotyped longitudinal tracts can be visualized using an antibody against Fasciclin II (FasII). The stereotyped positions of these longitudinal tracts are depicted in magenta. Names of the tracts correspond to position in the D/V and M/L axis (i.e. D-dorsal, C-central, V-ventral, M-medial, I-Intermediate, L-Lateral). The wild type positions of axon terminals of the md neurons are depicted in green. Md-bds, dmd1, and class I md-da neurons terminate at the DM fascicle. Class II-IV terminate at the VM fascicle. Yellow shaded region corresponds to the location of motor neuron dendrites. Blue shaded region marks the typical termination of proprioceptive afferents. Purple shaded region marks the typical termination zone for tactile and nociceptive afferents. (Adapted from Grueber et al, 2007)

(D) Diagrammatic representation of the different subtypes of PNS neurons. External sensory (es) and chordotonal (ch) neurons have single dendrites. Multiple dendrite (md) neurons have multiple dendrites and are subdivided into 3 main groups—the tracheal dendrite neurons (td), bipolar dendrite neurons (bd) and the dendritic arborization neurons (da). The md-da neurons have been further subdivided into 4 discrete morphological classes.

(E) A class IV md-da neuron from a 3rd instar larvae. Class IV neurons have the most complex dendritic arbors of the md-da neurons. White arrowhead marks the cell body. Yellow arrowhead marks the axon. Yellow arrow points out the distal dendrites. Scale bar =50μm. (Image from Matthews et al, 2007)

Figure adapted from Corty et al., 2009.

Figure 2: Diversity of da neuron morphology and transcription factor expression

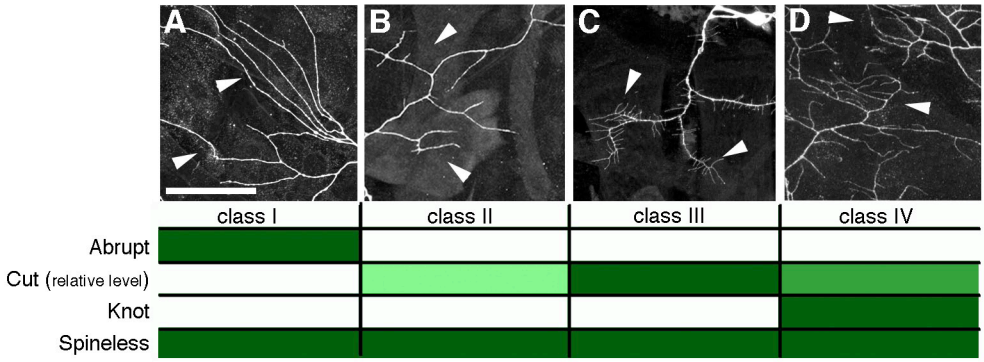

Figure 2: Diversity of da neuron morphology and transcription factor expression

(A-D) Terminal dendritic arbors of class I, II, III, and IV da neurons (left to right). Cells are classified according to increasing arbor complexity. The status of transcription factor expression of Cut, Knot, Abrupt, and Spineless are listed in a table below each morphological class. Filled boxes indicate expression; open boxes indicate no detectable expression. Progressively higher levels of Cut expression are indicated by progressively darker shadings. The degree of shading is not meant to indicate relative levels among the different transcription factors. Images in A-C reproduced, with permission, from Matthews et al. (Matthews et al., 2007).

Scale bar: 50μm for all images.

Figure adapted from Corty et al., 2009.

Figure 3: Transcriptional control of dendritic targeting in the *Drosophila* antennal lobe

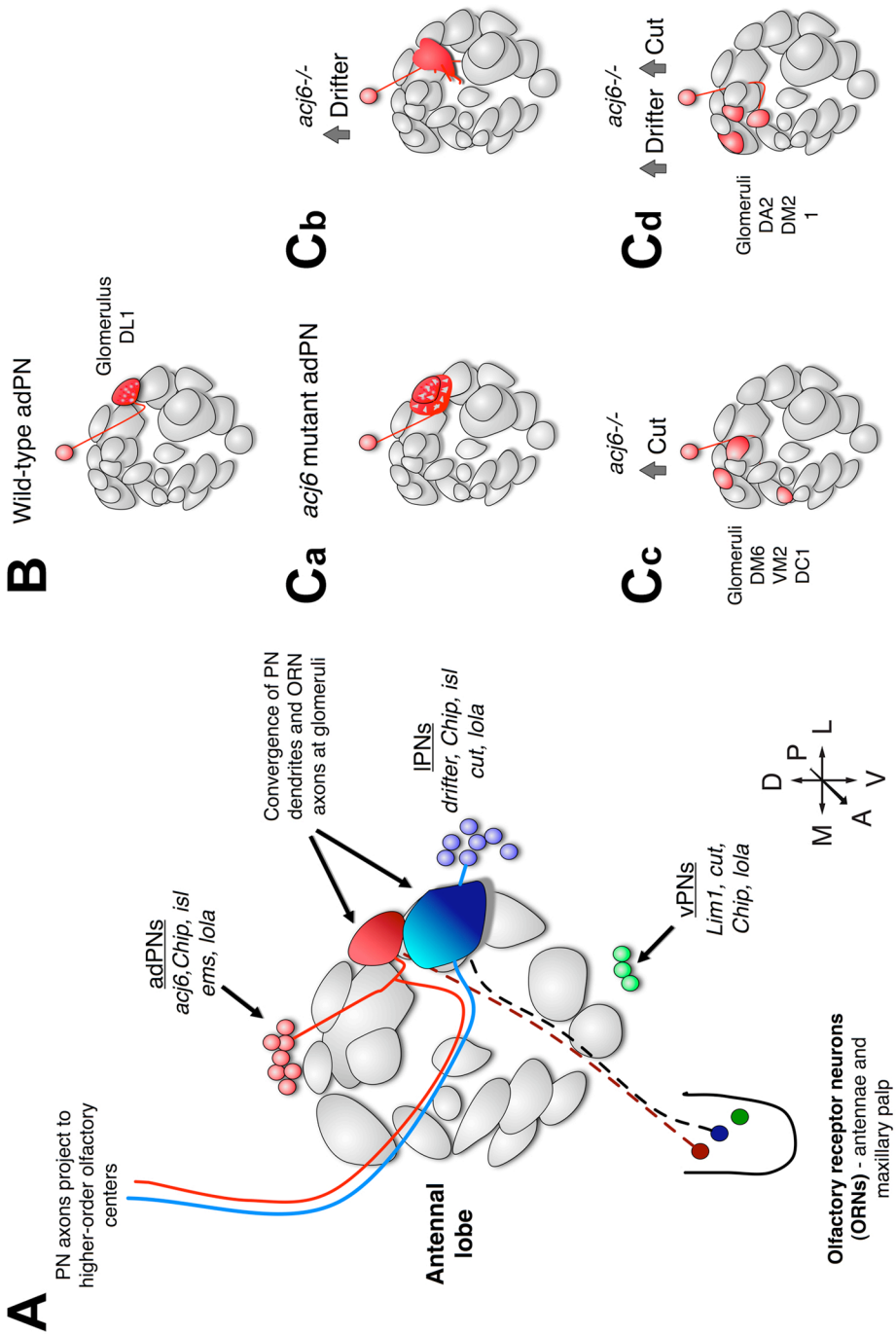

Figure 3: Transcriptional control of dendritic targeting in the Drosophila antennal lobe

(A) Schematic organization of the *Drosophila* antennal lobe (AL). For simplicity, only a subset of glomeruli are shown. Projection neurons (PNs) from anterodorsal (adPNs, red); lateral (lPNs, blue) and ventral, (vPNs, green) lineages project dendrites to glomeruli where they connect with ORN axons (a vPN projection is not shown here). PN axons extend to higher order olfactory centers in the brain. Transcription factors discussed in this review are shown. Schematic of glomerular organization based on data from Couto, 2005 and adapted with permission (Couto et al., 2005).

(B-F) Cell autonomous alterations in transcription factor expression re-direct dendrite targeting. **(B)** Wild type (WT) adPN dendrites (red) normally target to the DL1 glomerulus (filled in red in the antennal lobe). adPNs express *acj6* but not *drifter* or *cut*. **(C)** *acj6* mutants extend dendrites outside their normal glomerulus. **(D)** *acj6* mutant DL1 adPNs forced to express Drifter partially mistarget to more anterior glomeruli. **(E)** *acj6* mutant DL1 adPNs forced to express Cut target medial adPN glomeruli. **(F)** Expression of both Drifter and Cut in *acj6* mutant DL1 adPNs results in mistargeting of dendrites to medial lPN glomeruli. Schematic based on data from Komiyama et al. and Komiyama and Luo (Komiyama et al., 2003; Komiyama and Luo, 2007).

Figure adapted from Corty et al., 2009.

Figure 4: Transcription factors regulate guidance cue receptors to direct axon guidance and targeting

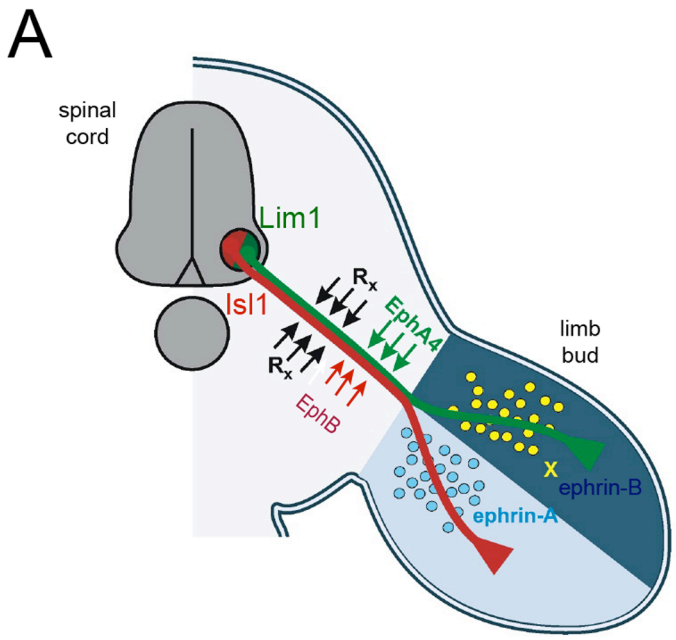

Figure 4: Transcription factors regulate guidance cue receptors to direct axon guidance and targeting

(A) Schematic showing how TF expression influence guidance receptor expression to control axon guidance decisions in the vertebrate spinal cord.
LMC motor neurons express either Lim1 or Isl1. Expression of Lim1 in dorsal motor neurons increases expression of EphA4 receptors leading them to avoid sources of ephrin-A in the ventral half of the limb bud, and thus project into the dorsal limb bud, where their ultimate target muscles are located. Similarly, Isl1 expression in ventral LMC neurons increase EhpB receptors to ensure that these neurons project into the ventral limb bud, away from sources of ephrin-B dorsally.

Figure adapted from Kania and Jessell, 2003.

Methods

Fly stocks and genetics

Fly Stocks

Chapter 1

For visualizing wild type dmd1 morphology I recombined *Nub-Gal4* (Calleja et al., 2000; provided by Stephen Cohen) with *UAS-mCD8:GFP* (Lee and Luo, 1999) (obtained from Bloomington Drosophila Stock Center, BDSC) using standard fly husbandry. Wild-type MARCM clones for visualizing wild-type dendrite and axon morphology were generated as described below by crossing females of the genotype *tub-Gal80, hs-FLP, FRT19A; 109(2)80-Gal4, UAS-mCD8:GFP* (Grueber et al., 2003) to males of the genotype *yw, FRT 19A (Lee and Luo, 1999)*. Flies, embryos, and larvae from the w^{1118} strain were used as wild type animals for *in situ* and EM experiments, as well as to obtain control genomic DNA. To examine glial cell distribution I crossed *w;; repo-Gal4 /TM3*(Sepp et al., 2000) or *w; moody-Gal4* (Stork et al., 2008) (provided by T. Copf) to *w; UAS-mCD8:GFP/CyO*. For Pdm loss of function experiments the following stocks were used: (1) nub^{1}*, FRT40A/Cyo* (Neumann and Cohen, 1998) (provided by Stephen Cohen) (2) *Df (2L) ED773/CyO* (Grosskortenhaus et al., 2006) obtained from BDSC (3) $pdm2^{E46}$*/Cyo* (Yeo et al., 1995) obtained from BDSC (4) *8-113-Gal4* (Hughes and Thomas, 2007) (provided by Cynthia Hughes) (5) *w;* nub^{R5}*, FRT 40A/Cyo* (Terriente et al., 2008) (provided by F.J. Diaz-Benjumea) (6) *hs-FLP,* $elav^{c155}$*-Gal4, UAS-mCD8:GFP; tub-Gal80, FRT40A/CyO* (Lee and Luo, 1999) (7) *w; FRT40A/Cyo*$^{nuclear\ GFP}$ *males (BDSC)*. To generate clones lacking functional *pdm1* and *pdm2,* stocks 5 and 6

were mated. To generate control clones, stocks 6 and 7 were mated. For behavioral experiments *Nub-Gal4; UAS-mCD8:GFP* virgins were crossed to w^{1118} or *UAS-shibire*^{TS} (Kitamoto, 2001) males.

Chapter 2

Cut mutant and control MARCM clones were generated as described below by crossing females of the genotype *tub-Gal80, hs-FLP, FRT19A; 109(2)80-Gal4, UAS-mCD8:GFP* (Grueber et al., 2003) to males of the genotype *w,* ct^{c145}*, FRT19A/* $y^{+}ct^{+}$ *(Y)* (Grueber et al., 2003) or *yw, FRT 19A (Lee and Luo, 1999)*. For analysis of Pdm expression in Cut mutants we used ct^{db3}*/FM6; E 7-2-36-lacZ* (Grueber et al., 2003). Overexpression experiments used the FLPout method described below and one of the following UAS lines: *UAS-*cut^{5} (Grueber et al., 2003)*, UAS-Pdm1/*Cyo^{YFP} (Neumann and Cohen, 1998)*; UAS-Pdm2/*Cyo^{YFP} (Grosskortenhaus et al., 2006)(C. Doe)*, UAS-Abrupt* (Cook et al., 2004; Li et al., 2004); *UAS-Knot* (Mohler et al., 2000). To assay the effects of Pdm2 misexpression on axon projections, *clh201-Gal4, UAS-mCD8:GFP* virgins were mated to w^{1118} or *UAS-Pdm2* males.

Chapter 3

Mutant analysis for *frazzled*, *CadN*, and *flamingo* were generated by crossing the following stocks (1) *FRTG13, fra3/Cyo; (2) CadNM19, FRT40A/Cyo; (3) FRT42D,* $stan^{3}$*/Cyo* or the appropriate FRT control chromosome to the corresponding MARCM stock, which are described below. For gene profiling of sensory neurons, *w; clh201-Gal4, UAS-mCD8:GFP/Cyo* (Hughes and Thomas, 2007; provided by C. Hughes) were crossed to either w^{1118} (control) or *UAS-pdm2* (Grosskortenhaus et al., 2006) males.

GFP and UAS-transgene expression

To visualize dmd1 and dbd morphology, I used *Nubbin-Gal4* (*Nub-Gal4*)(Calleja et al., 2000), *clh8-Gal4* (Hughes and Thomas, 2007), *8-113-Gal4* (Hughes and Thomas, 2007), or the pan-md driver *109(2)80-Gal4* (Gao et al., 1999) to express membrane tethered GFP from the *UAS-mCD8:GFP* construct (Lee and Luo, 1999). To visualize other md neurons I used the pan-md drivers *109(2)80-Gal4* or *clh201-Gal4* (Hughes and Thomas, 2007). Gal4 and *UAS-mCD8:GFP* constructs were recombined using standard genetic methods. To drive expression of additional transgenes for misexpression studies, virgins of the appropriate Gal4 line recombined with *UAS-mCD8:GFP* were mated to males carrying the desired UAS construct. Crosses were reared at 25°C to ensure robust Gal4-based expression unless otherwise noted.

Generation of MARCM clones

MARCM (Lee and Luo, 1999) clones were generated by allowing appropriately mated females to lay embryos on grape juice agar plates for 3 hours at 25°C. Embryos were then allowed to develop for an additional 3-4 hours at 25°C before providing a heat shock to induce Flp-mediated recombination. Heat shock treatment was given by sealing the agar plate in a water-tight bag and immersing in a 38°C water bath for 30 minutes, followed by 30 minutes at room temperature, followed by an additional 45 minutes at 38°C. Embryos were then returned to 25°C to develop. Third instar larvae were examined for the presence of GFP+ clones under a fluorescent dissecting scope while immersed in PBS. Animals containing clones were removed to a fresh agar plate before being dissected. Genotypes of the animals used for MARCM crosses can be found in the Fly Stocks list for each data chapter.

FLP-out overexpression

To create individually labeled md neuron clones, I used a "FLPout" method to create mosaics of GFP expression. Virgin females of the genotype *hsFLP; 109(2)80-Gal4; UAS<rCD2-stop<mCD8:GFP* (where < indicates a **f**lipase **r**ecognition **t**arget (FRT) sequence) (Wang et al., 2004; Wong et al., 2002) were mated to males containing the UAS construct of interest. Females were allowed to lay embryos on a grape agar plate for 3 hours or overnight. Plates were given a heat shock after ~24 hours of development. Heat shock was applied by immersion in a 38°C water bath for 15-30 minutes depending on the scarcity of GFP+ cells desired.

Dissection of larvae and Immunohistochemistry

Third instar larvae were dissected in PBS in a small sylgard-coated dish. Briefly, animals in PBS were pinned taut at anterior and posterior ends to immobilize them. Using fine dissection scissors (Fine Science Tools) a small, shallow incision was made at the posterior end of the larvae. From this incision, each larvae was then cut up the dorsal or ventral midline (depending on what structures were going to be analyzed). Four additional pins were used to prepare a flat fillet of the larval body wall, with an effort to keep the CNS connected. Up to six animals were dissected per dish. No more than 10 minutes elapsed from first cut to fixation. Filleted larvae were fixed in 4% paraformaldehyde (Electron Microscopy Sciences) in PBS at room temperature for 15-20 minutes with gentle agitation on a rotational platform shaker. Following fixation, animals were rinsed briefly with PBS before the pins were removed.

Fillets were transferred to 5ml round bottom tubes using forceps and rinsed several times in PBST (PBS with 0.3% TritonX) before being incubated with blocking solution (5% normal donkey serum in PBST) for 1 hour at 4°C or 30 minutes at RT. Primary antibodies were diluted in PBST and added for overnight incubation at 4°C with shaking. The following day, animals were washed for ~1.5 hours with 4-6 changes of PBST before adding secondary fluorescent antibodies (Jackson Immunoresearch) diluted 1:100-1:200 in PBST. Animals were incubated in secondary antibodies for either 2 hours at RT or overnight at 4°C. Animals were again washed for ~1.5 hours with 4-6 PBST solution changes. Animals were then mounted on poly-L-Lysine (Sigma) coated coverslips and taken through an ethanol dehydration series (5 minutes each in 30% EtOH in PBS, followed by 50% EtOH in water, then 70%, 95%, 100%, 100% EtOH) and clearing in xylenes (10 minutes each in two 100% xylenes solutions) before permanent mounting in DPX media (Fluka).

Primary antibodies:

Mouse anti-GFP (1:250, Molecular Probes/Invitrogen, Carlsbad, CA)
Chicken anti-GFP (1:1000, Abcam, Cambridge, MA)
Rat anti-mCD8 (1:100, Caltag)
Mouse anti-rCD2 (1:50-1:100 Serotac)
Goat anti-HRP (1:200, Jackson Immunoresearch, West Grove, PA)
Rabbit anti-HRP (1:500, Jackson Immunoresearch)
Mouse anti-Cut (1:20, Developmental Studies Hybridoma Bank (DSHB), Iowa City, IA)
Rat anti-Cut (1:5000, (Grueber et al., 2003))
Rabbit anti-Pdm1 (1:1000, provided by S. Cohen)
Rat anti-Pdm2 (1:10, provided by Chris Doe)
Mouse anti- FasII (1:10 DSHB)
Mouse anti-laminin (1:100, provided by John and Lisa Fessler, UCLA)
Mouse anti-Nc82 (1:10 DSHB)

Secondary antibodies:

Cy2-, FITC-, DyLight 488-, Rhodamine Red-X, Cy5-, and DyLight 649-conjugated secondary antibodies against the appropriate primary species (used at 1:100-1:200; Jackson Immunoresearch) were used for antibody detection.

Electron Microscopy

Mature third instar larvae were dissected in PBS as described above and fixed immediately with 3% glutaraldehyde in 0.1M phosphate buffer (PB). Specimens were fixed for a total of 20 minutes, with 60 seconds of the fixation time in a Pelco 3451 Microwave System. Fixed tissue was washed 3 x 20 minutes in 0.1M PB, post-fixed with 1% osmium tetroxide in 0.1M PB in a microwave for 2 x 40 seconds (each 40 second exposure in fresh osmium), then washed 3 x 10 minutes in 0.1M PB. Tissue was dehydrated in the microwave in ethanol dilutions of 50%, 70%, 95% (1 x 40 seconds each), and 100% (2x 40 seconds). Dehydrated tissue was infiltrated in epon resin and ethanol (1:1) for 15 minutes in the microwave, then in 100% epon resin (2 x 15 minutes each with fresh epon) in the microwave. Specimens were mounted between 2 plastic slides with epon and polymerized overnight at 60˚C. Areas of interest were identified in the epon wafer, placed flat to the bottom of the tip of a Dykstra flat embedding mold, and polymerized in epon for 18-24 hrs at 60˚C. The block was trimmed to include the area of interest and 10 mm serial sections were cut using a diamond Histo-knife with an ultramicrotome. Relevant regions were selected for thin sectioning and remounted on blank epon blocks using a small amount of fresh epon and allowed to polymerize overnight. Thin sections were collected on formvar-coated slot grids and stained with

uranyl acetate and lead citrate. Grids were viewed using a JEOL 1200EX electron microscope and photographed using a digital camera.

Embryo fixation and Immunohistochemistry

Embryos used for immunohistochemistry were gathered from either overnight collections (to get a variety of stages) or from short 2-3 hour collections aged to the desired stage before fixation. Embryos were rinsed from agar collection plates into a mesh cell strainer using a paintbrush and distilled water. Embryos were dechorionated using 100% Clorox bleach for 2 minutes or 50% Clorox bleach for 5 minutes, followed by thorough rinsing with distilled water and Drosophila Embryo Wash (0.7% NaCl; 0.03% Triton X-100). Embryos were transferred to scintillation vials with ~4 mls of 4% paraformaldehyde in PBS and ~4 mls heptanes, and fixed for 20 minutes with agitation. After fixation the paraformaldehyde aqueous layer was removed. ~4 mls of 100% methanol was added and the vial was shaken by hand for ~10-20 seconds to devitellinize the fixed embryos. Appropriately processed embryos from the bottom of the vial were rinsed 3x 5 minutes with fresh methanol and then stored at -20°C, or immediately rehydrated using 2x washes with 50% methanol, 50% PBT followed by 3x 5 minutes with PBT before blocking solution was applied. Staining and mounting procedures were as for larvae.

***In situ* hybridization**

Antisense DIG labeled RNA probes against Pdm1, Pdm2, and array candidate gene mRNA were made via PCR from full length cDNA clones in the BDGP Gold Collection

using the universal primers described below followed by standard in vitro transcription using the appropriate enzyme.

	Forward	**Reverse**	**IVT**
For cDNA in pBS SK vectors	T7 or M13f	T3 or M13b	T7
For cDNA in pOT2 vectors	Sp6 or PM001	T7 or PM002	Sp6
For cDNA in pFLC-1 vectors	T7 or M13f	T3 or M13b	T3
For cDNA in pOT B7 vectors	Sp6 or PM001	T7 or PM002	T7

Primer sequences:

T7: CTA ATA CGA CTC ACT ATA GGG
T3: AAT TAA CCC TCA CTA AAG GG
SP6: CAT ACG ATT TAG GTG ACA CTA TAG
M13f: GTA AAA CGA CGG CCA GT
MI3b: GGA AAC AGC TAT GAC CAT G
PM001: CGT TAG AAC GCG GCT ACA AT
PM002: GCC GAT TCA TTA ATG CAG GT

PCR reactions from bacterial colonies were used as templates for IVT using the appropriate RNA polymerase (T7, T3 Roche; Sp6 Fermentas) and a DIG RNA labeling kit (Roche). Paraformaldehyde fixed (see above) embryos were post-fixed in methanol and 4% formaldehyde, rehydrated, and incubated overnight with freshly made probe for hybridization. Labeling was detected using AP-conjugated anti-DIG antibody (Roche) and developed in NBT/BCIP solution (Roche). Development times ranged from 10 minutes to 2 hours with regular visual inspection of the reaction depending on the probe.

FACS and microarray analysis

Cell harvesting and sorting

In order to collect RNA from *Drosophila* sensory neurons that were overexpressing Pdm2, virgin females of the genotype w^{1118}*; clh201-Gal4; UAS-mCD8:GFP/(Cyo)* were crossed to homozygous males of the genotype w^{1118}*; UAS-pdm2* or males with the genotype w^{1118}*; +*. In order to get a large collection of similarly staged embryos for analysis ~2,500 virgins were used for each condition. These crosses were set-up in collection chambers with agar plates for precisely timed embryo collections. Collections were performed as a one hour "pre-lay" (which was discarded) followed by 2 hour collection periods. Embryos were then aged until 15-17 hours AEL. At this stage embryos were dechorionated using 50% Clorox bleach for 5 minutes. After thorough rinsing with distilled water, embryos were placed into 7ml glass douncers (Wheaton Scientific) with 7ml of ice-cold Drosophila S2 media (Gibco) supplemented with 8% fetal bovine serum (Sigma) (S2-FBS). Using the loose-fitting plunger, embryos were physically dissociated using 10 downward non-twisting strokes. The suspension was transferred to a 15ml Falcon tube and spun at 40g for 5 minutes at 4°C to pellet tissue and debris. The supernatant containing isolated cells was transferred to a fresh tube and spun at 380g for 10 minutes at 4°C to pellet single cells. Cells were resuspended in fresh ice-cold S2-FBS media and passed through a 40µm strainer to ensure that there were no clumps. Cells were maintained on ice for no more than 30 minutes before sorting. Cells were sorted using a FACSAria Cell Sorter (BD) using excitation at 488nm. Collection gates were set manually using control samples made from w^{1118} flies that had no GFP-expressing cells.

RNA isolation and array analysis

Cells were sorted directly into Trizol-LS (Invitrogen). Total RNA was harvested using a Trizol-RNeasy (Qiagen) hybrid protocol and RNase-free techniques and reagents. Trizol portion: Cells were homogenized in Trizol and left at RT for 5 minutes. Chloroform was added at 0.2ml per ml of Trizol. After ~15 seconds of vigorous shaking the sample was left at RT for 2-3 minutes for phases to begin to form. Samples were spun at maximum speed (12,000g) for 15 minutes at 4°C, and the resulting top aqueous phase was transferred to a fresh tube and combined with an equal volume 70% EtOH. RNeasy portion: The resulting sample was loaded onto an RNeasy column, and the Rneasy standard protocol was used from this point on (Qiagen). Samples were treated with on-column DNase digestion. Final elution volume was 15µl.

Total RNA was checked for purity and degradation using Bioanalyzer Pico Chips (Agilent). Linear amplification of mRNA was performed using the Ovation RNA amplification kit (Nugen) following manufacturer instructions. Fragmentation and labeling was performed using the Encore Biotin labeling kit (Nugen). Samples were hybridized to Drosophila genome 2.0 array (Affymetrix) by the staff at the Columbia University Medical Center Genomics Facility. Three biological replicates/condition were analyzed. Raw data was analyzed using the Guided Work Flow in GeneSpring Software (Agilent). Robust Multichip Analysis (RMA) was used to estimate and eliminate "noise" from true signals. Normalization was performed using a baseline transformation to the median of all samples. To identify differentially regulated genes an unpaired t-test, without multi-sample correction was applied using a significance threshold of $p<0.05$.

Analysis of the *nub^{R5}* deletion region

Genomic DNA was prepared from homozygous *nub^{R5}* embryos (purified by selecting against the *CyO$^{nuclear\ gfp}$* under fluorescence) and *w^{1118}* embryos for use as a reference strain using standard gDNA isolation protocols. Primers were designed to genomic DNA surrounding the *pdm1* and *pdm2* loci at regularly spaced intervals of ~10kb. Individual 25µl PCR reactions were setup using GoTaq MasterMix (Promega). Each primer pair was tested with *w^{1118}* gDNA and *nub^{R5}* gDNA. PCR products in *w^{1118}* samples but not *nub^{R5}* samples indicated that the primer pair spanned a region removed in the *nub^{R5}* deletion allele. PCR products from both genotypes signified that the deletion did not spread beyond the location of the primers.

Behavioral analysis

For behavioral analysis *Nub-Gal4; UAS-mCD8:GFP* females were crossed to either *w^{1118}* or *UAS-shi^{TS}* males. *UAS-shi^{TS}* females were crossed to *w^{1118}* for an additional control. Crosses were kept at 25°C until there wandering 3rd instar larvae were observed crawling up the vials. Larvae were removed from the food using a paintbrush, placed briefly in PBS to remove any food residue and screen for GFP expression to confirm genotype. Five larvae at a time per condition were placed on 3% non-nutritive agar plate. After a 60 second acclimation, larval behavior was recorded for 2 minutes using the Multi Worm Tracker (MWT) software program, and data was analyzed using the associated Choreography software program (Wu et al., 2011). Results from each cohort of larvae is analyzed as a population, that is an average of all five larvae used in each session is created, so that each "N" represents the average of 5 individuals. Behavior of

control and experimental larvae was tracked at ~20-25°C and ~37°C. Temperature was controlled by placing the agar dish on a heated plate. For the permissive temperature the heat source was off and the experiments were carried out at room temperature. Agar surface temperature was recorded just prior to the start of each run.

Imaging acquisition and analysis

Confocal images were obtained using a Zeiss 510 Meta confocal microscope using 40X Plan Neofluar 1.3 N.A. and 63X objective lenses. When arbors could not be imaged with in a single frame, tiled images were assembled using Photoshop CS2 (Adobe Systems, San Jose, CA) or aligned manually in Neurolucida (MBF Bioscience). For quantitative analysis of dendrite length and branching flattened confocal projections were traced in Neurolucida. To obtain information about dmd1, tracing and distance measurements were made by tracing in 3-dimensions through confocal stacks in Neurolucida. Orthogonal views of the VNC were obtained by making optical transverse sections of the VNC using LSM 510Meta Software (Zeiss).

Statistics

Statistical tests were performed using R (R Team, 2009). Normality of data sets was assessed using the Shapiro-Wilk normality test. Significance was tested with a Student's t-test (normal data sets) or a Wilcoxon rank-sum test (non-normal data sets). Data is presented as boxplots: the thick line represents the median, while the box delimits the second and third quartiles, the whiskers extend to include data in the 1.5x quartile range, and outliers from this range are represented as open circles.

Chapter 1

Analysis of stretch receptor neuron morphology and its specification by POU domain transcription factors Pdm1 and Pdm2

Abstract

The size, shape, and complexity of dendritic arbors influence the sensory and synaptic inputs that neurons receive and are thus important determinants of neural function and connectivity. Studies of dendrite morphogenesis, therefore, seek to understand the developmental origins of the diverse dendritic morphologies and, when possible, to link neuronal form to neuronal function. In this chapter, I describe the characteristic morphology of the *Drosophila* dmd1 multiple dendrite (md) sensory neuron. Dmd1 projects its dendrites to an internal nerve in an anatomical arrangement that suggests it functions as a stretch receptor, and behavioral studies indicate that a population of neurons including dmd1 is required for proprioceptive feedback during larval crawling. I also describe roles for two POU domain transcription factors, Pdm1 and Pdm2, in stretch receptor morphological development. Pdm1 and Pdm2 are expressed in dmd1 and dbd, another md neuron believed to function as a stretch receptor. Our results suggest that Pdm1 and Pdm2 control the acquisition of important stretch receptor neuron characteristics by limiting epidermal growth and branching while promoting proper targeting of dendrites to non-epidermal substrates.

Introduction

"We shall start with the fundamental unit of the nervous system, the nerve cell…"

-Ramon y Cajal *The Histology of the Nervous System*

In the nervous system, form and function are intimately linked, with the particular morphologies of individual neurons shaping inputs, connectivity, and processing of neural signals. The nervous systems of various species of insect have been models for studying the development and function of nervous systems for nearly a century. The *Drosophila* larva peripheral nervous system (PNS) contains a variety of individually identified neurons with highly stereotyped morphologies, making it an ideal model system for studying the development of specific neuronal morphologies in a genetic organism (Corty et al., 2009). Despite a growing literature on the development of *Drosophila* PNS neurons, there is still relatively little known about their sensory functions or how their distinct, stereotyped morphologies might underlie their functional properties.

Insect body wall sensory neurons can be divided into 3 main categories: the chordotonal (ch) neurons, the external sensory (es) neurons, and the multiple dendrite (md) neurons. The ch and es neurons have single dendrites and function in association with support cells to form sensory organs. The ch organs function as stretch and vibration detectors (Wu et al., 2011), while the majority of es neurons are associated with external sensory bristles and transmit tactile information. The md neurons are a heterogeneous group of neurons that form a meshwork of neural processes beneath the

cuticle. The majority of these neurons have complex **d**endrite **a**rborizations that innervate the epidermis, and are thus termed md-da neurons. In addition there subsets of md neurons that are associated with trachea, nerves, or other connective tissues. The sensory function of the majority of md neurons remains unknown with the exceptions of the class IV md-da neurons that have recently been implicated in nociception (Hwang et al., 2007), and the class I md-da and md neurons with bipolar morphologies (md-bd) that function in sensory feedback during crawling (Hughes and Thomas, 2007).

Studies have increasingly implicated intrinsic transcriptional programs in the control of class-specific dendritic morphology in both vertebrates and *Drosophila* (reviewed in Corty et al., 2009; Parrish et al., 2007). In *Drosophila* md neurons, an emerging theme is that selective expression of different transcription factors in distinct morphological classes underlie the development class-specific arbor features. For example, the BTB zinc finger transcription factor Abrupt is expressed exclusively in class I md-da neurons to limit their branching (Li et al., 2004; Sugimura et al., 2004); whereas the COE transcription factor Knot is expressed exclusively in class IV neurons where it promotes class-IV specific terminal branching patterns (Jinushi-Nakao et al., 2007; Hattori et al., 2007; Crozatier and Vincent, 2008). The homeodomain transcription factor Cut is expressed in several md-da neuron classes, but at distinct levels that specify class-specific complexity and terminal branching (Grueber et al., 2003). These transcription factors cannot explain the full diversity of md neurons. The study of dendrite development of PNS neurons has focused on the md-da neurons, with much less understood about the morphology and development of other md neurons in *Drosophila*. Identifying additional transcription factors that direct morphogenesis of these neurons is

an important goal. One way to identify such factors is to look for transcription factors with restricted expression in subsets of md neurons that share common morphological and/or functional features.

Anatomical and electrophysiological studies in several insect species conducted a half century ago identified a pair of dorsal md sensory neurons in each abdominal segment as putative stretch receptors (Finlayson and Lowenstein, 1958; Osborne, 1962; Osborne and Finlayson, 1962; Lowenstein and Finlayson, 1959). These neurons have dendrites associated with connective tissue and internal structures such as muscles and nerves. Based on the orientation of their dendrites these neurons were named the longitudinal and vertical stretch receptors. The longitudinal stretch receptor has dendrites that span each segment between the intersegmental folds; while the vertical stretch receptor extends processes within a strand of connective tissue to connect to a motor nerve and/or muscles. This results in the two cells being oriented to detect stretch in approximately orthogonal directions, which is thought to provide soft-bodied larvae with important proprioceptive information. The *Drosophila* homolog of the longitudinal stretch receptor has been identified as the dorsal bipolar dendrite neuron, dbd, while a *Drosophila* homolog of the vertical stretch receptor has not yet been described.

In this chapter I present a morphological analysis of the *Drosophila* dorsal multiple dendrite 1 (dmd1) neuron. I have found that this neuron is located on the epidermal surface but its dendrites are associated with an internal nerve. Dmd1 axons project to the dorsal region of the central neuropil—a region associated with proprioceptive afferents in insects (Grueber et al., 2007; Murphey et al., 1989). Based on this morphological profile, I propose that dmd1 is the *Drosophila* homolog of the vertical

stretch receptor described in several other insect species. In the embryonic PNS, the POU domain transcription factors Pdm1 and Pdm2 are co-expressed exclusively in two dmd1 and dbd (Billin et al., 1991; Dick et al., 1991; Lloyd and Sakonju, 1991). Both of these neurons have non-epidermal arborizations and are presumptive stretch receptors. I present data that implicate Pdm1 and Pdm2 transcription factors in controlling the morphological development of these proprioceptive neurons. Finally, I present preliminary evidence that implicates these neurons in proprioceptive feedback used during larval crawling.

Results

The dorsal multiple dendrite neuron dmd1 expresses POU domain transcription factors Pdm1 and Pdm2

The dorsal cluster of *Drosophila* body wall sensory neurons contains a total of 13 neurons: five es neurons, six md-da neurons (representing all four md-da subclasses), an md-bd neuron (dbd), and an additional md neuron termed dmd1 (Figure 1.1A). All neurons in the cluster have been extensively characterized with the exception of the dmd1 neuron, which has been described as projecting its dendrites to either trachea or muscle rather than along the epidermis (Gao et al., 1999; Grueber et al., 2003; Orgogozo and Grueber, 2005).

Though the morphology of this cell has not been well described, there is information about its developmental origin and gene expression. The majority of PNS neurons are derived from lineages that are dependent on expression of the proneural bHLH transcription factors of the Achaete-Scute complex (Dambly-Chaudiere and

Ghysen, 1987) or Atonal (Jarman et al., 1993). Two neurons, however, require instead the proneural gene Amos for their formation (Huang et al., 2000; Grueber et al., 2003). These include the dorsal bipolar neuron (dbd) and a second dorsal md neuron. These *amos*-dependent neurons were subsequently identified as two dorsal PNS neurons that express the POU domain transcription factors Pdm1 (Flybase: *Nubbin*) and Pdm2 (Brewster et al., 2001). Pdm1 and Pdm2 are two closely related type II POU domain transcription factors located adjacent to one another in genome, which have nearly identical expression patterns in developing embryos suggesting functional redundancy (Billin et al., 1991; Dick et al., 1991; Lloyd and Sakonju, 1991).

To begin the study of dmd1 morphology, I studied the wild type expression patterns of *pdm1* and *pdm2* in embryos and third instar larvae. *In situ* hybridization with probes against Pdm1 and Pdm2 in late stage embryos confirmed expression of these genes was confined to two dorsal PNS neurons, as well as the glial cells of the lch5 chordotonal organ consistent with previous reports (Billin et al., 1991; Dick et al., 1991; Lloyd and Sakonju, 1991) (Figure 1.1B-C). Immunohistochemistry in third instar larvae confirmed the specific identity of the Pdm-positive neurons as dbd and dmd1, as the full morphology of md neurons can be observed at this stage allowing for unambiguous identification (Figure 1.1D). Moreover, these experiments revealed that expression of Pdm1 and Pdm2 persists throughout larval stages suggesting that these transcription factors may play important roles throughout the development of these neurons.

Consistent with this expression pattern, we found that the enhancer trap Nubbin-Gal4 (Calleja et al., 2000) drives expression exclusively in dbd and dmd1 in the PNS (Figure 1.2A-B). Nubbin-Gal4 also expresses in numerous CNS neurons, including

motor neurons. We identified several additional Gal4 drivers with restricted PNS expression that includes dmd1. Among these are clh8-Gal4 (dmd1 and all bd-md neurons; Hughes and Thomas, 2007), 8-113-Gal4 (dmd1, dbd, class I neurons; Hughes and Thomas, 2007), and OK333-Gal4 (dmd1 and tracheal dendrite neurons). The precise genomic locations of these enhancer traps have not yet been determined, but could represent genomic loci with developmental or functional roles in PNS neurons including dmd1.

Dmd1 projects dendrites away from the epidermal surface to the intersegmental motor nerve

The morphology of the dmd1 neuron has not been well described in the literature, which has varying reports about dmd1 dendrites projecting internally to trachea, nerve, or muscle. In order to facilitate studies about the development and function of this neuron we analyzed wild type dmd1 morphology in detail. Dmd1 morphology in third instar *Drosophila* larvae was visualized by making single-cell labeled clones with the MARCM (Lee and Luo, 1999) or FLPout techniques or by using the Nubbin-Gal4 driver to express membrane tethered mCD8:GFP throughout the neuron (Figure 1.2A-B). The cell body of dmd1 lies in the dorsal cluster of sensory neurons, most often amongst the three es neurons near the middle of the cluster. It is in the same plane as the cell bodies of the md-da neurons in the cluster, sandwiched between the epidermis and overlying muscles (Figure 1.2C, E, F).

The dendrites of the class I-IV md-da neurons arborize in approximately two-dimensions on and within the epidermis (Kim et al., unpublished; Grueber et al., 2002). In contrast, the dendrites of dmd1 projected off the body wall towards the muscle layer forming a 3-D architecture (Figure 2C-F). Dmd1 had a unipolar dendritic appearance,

with a dendrite or dendrites emerging from the same position on the cell body that traveled together towards the interior of the animal as a single unit, which I refer to as the dendrite stalk.

Membrane labeling of dmd1 with mCD8:GFP or antibodies directed against HRP (which recognizes all neuronal membranes in *Drosophila*), combined with confocal fluorescent microscopy, did not allow us to resolve individual dendrites well enough to determine the precise number of dendrites within the stalk. In some wild type neurons (and more frequently in some mutants) the dendrites of the stalk were less tightly packed, revealing gaps between labeled membranes that suggest the presence of multiple dendrites. Preliminary EM data (see below), and homology to the vertical stretch receptor of other insects supports the conclusion that multiple dendrites travel in the stalk.

The dmd1 dendrite stalk projected to the interior muscle surface to target the second lateral branch point of the intersegmental nerve (ISN), where ISN bifurcates to innervate dorsal muscles 2 and 10 (Figure 1.2 C,E). Targeting to this landmark was consistent despite variation in dmd1 cell body positioning within the dorsal cluster. To reach this target, the dmd1 dendrite stalk passed between a gap between neighboring muscles. Upon reaching its target, dmd1 dendrites ramified at the level of the nerve and muscles. Multiple dendrites were distinguishable at the ISN target (Figure 1.2B'). These dendrites gave dmd1 a tufted appearance at its distal end. These dendrites may represent fanned out stalk dendrites or bifurcations and branches of stalk dendrites. They often appeared to crossover one another or tangle together (Figure 1.2B' arrows). The dendrite stalk prior to ramification is on average 88.2-µm +/- 22.5µm (n=20), while the average z-distance from the dmd1 cell body to the ISN nerve is approximately 56.0µm +/- 23.1 µm.

Note that this is less than average stalk length (assessed by tracing the stalk in 3-D through confocal stacks), indicating that there is excess dendrite length than what is needed to span the distance between the epidermis and ISN nerve. This may allow for changes in the distance between anchor points when the segment is deformed during movement of the animal.

In the majority of observed wild type dmd1 neurons no branches or dendrites extend away from the main 3-D trajectory until the ramification at the ISN. Rarely, in wild type neurons there are small branches that extend away from the main bundle--occasionally in the plane of the epidermis, but also sometimes off of the dendrite stalk. When seen in wild type neurons these extensions are typically just few microns long (data not shown).

In summary, we have characterized novel aspects of sensory neuron morphology for dmd1. Dmd1 morphology is unique in the *Drosophila* PNS with its projection to an internal nerve. Dmd1 show many similarities to descriptions of the vertical stretch receptor—a highly conserved sensory neuron identified in numerous insect species that functions as a stretch receptor (Finlayson and Lowenstein, 1958; Osborne, 1963)—suggesting that dmd1 is the *Drosophila* homolog of this conserved neuron. We next examined in more detail the scaffold upon which dmd1 grows and the molecular basis for this specialized dendrite growth.

Dmd1 dendrites are ensheathed by the neural lamella and associated with a moody-expressing cell

We reasoned the dmd1 stalk, with dendrites spanning a distance of over 50μm between epidermis and muscle, must require a support structure to promote and maintain 3-dimensional growth. Such a structure could serve as a substrate upon which to grow or

as a means to ensheath and bundle the dmd1 dendrites to provide physical support and close association of multiple dendrites. Descriptions of vertical stretch receptors of other insects indicated that their dendrites grow within "connective tissue" (Osborne, 1963; Osborne and Finlayson, 1962), but the exact nature of this substrate remind unclear. We initiated experiments to determine if dmd1 dendrites are encapsulated, and if so, the nature of this tissue.

Connective tissue in insect nervous systems consists of a thick extracellular matrix (ECM) termed the neural lamella that surrounds the central nervous system and major nerves(Ashhurst, 1968; Edwards et al., 1993). This acellular neural lamella forms the outermost layer of ensheathing material around peripheral nerves in embryos and larvae(Stork et al., 2008). To determine if the dmd1 stalk was surrounded by the neural lamella we used an antibody against laminin, a component of ECM. We co-stained for laminin in animals where dmd1 was clearly visualized using *Nub-Gal4* to drive membrane bound GFP. All dmd1 dendrite stalks that were examined showed co-labeling with laminin along the length of the dendrite stalk (Figure 1.3A). The laminin staining appears not to perfectly colocalize with GFP, but rather extends beyond the GFP labeling, suggesting that it forms a layer around the dendrites. These results suggest that neural lamella surrounds dmd1 dendrites.

In *Drosophila,* the neural lamella is just the outermost layer of encasement around the nervous system. Several layers of glial cells lie between neurons and this outer covering to form a blood brain barrier (Stork et al., 2008; Xie and Auld, 2011; Yamamoto et al., 2006). To determine whether glial cells might form part of the dmd1 stalk

substrate, we examined the expression patterns of Gal4 drivers that label specific glial populations involved in neuronal ensheathment.

There are three layers of glial cells that surround peripheral nerves: outermost are perineural glia, followed by subperineural glia, and the innermost wrapping glia (Stork et al., 2008; Xie and Auld, 2001). We began by using *Repo-Gal4* to drive *UAS-mCD8:GFP* in all glia cells. The axons, cell bodies, and proximal dendrites of peripheral md neurons including dmd1 were covered with GFP+ glial membrane, consistent with previous reports (Yamamoto et al., 2006). We did not observe GFP+ glial membrane covering more than just the proximal portion of the dmd1 stalk (Figure 1.3B). Since *Repo-Gal4* should label all glial ensheathment layers (Xie and Auld, 2011), these results indicated that the glial sheath that encases peripheral nerves does not extend the cover the dmd1 dendrite stalk.

We also used the *Moody-Gal4* driver to examine the distribution of the subperineural glia specifically. In approximately one third of the segments examined we found GFP+ membrane that surrounded the entire length of the dmd1 bundle (Figure 1.3C; n=8/23). We also observed several instances of a thin strand of GFP+ membrane that ran the entire length of the stalk (Figure 1.3D; n=5/23). In the remaining segments no GFP+ membrane could be seen associated with the dendrite stalk (n=10/23; data not shown) similar to what was observed in *Repo-Gal4* experiments. These data suggest that a *moody*-expressing cell is likely associated with the dmd1 stalk to provide ensheathment or substrate, but this cell may not be a repo-expressing glial cell. Notably, dmd1's sibling cell temporarily expresses *repo* immediately after it is born (Umesono et al., 2002). The fate of this cell has not been tracked beyond this, but it is tempting to speculate that the

dmd1 sibling might be the moody-expressing cell and serve as a supporting scaffold for dendrite growth of its sibling.

EM data suggests multiple dendrites grow within connective tissue towards the ISN

To better understand the relationship of dmd1 dendrites and their substrate we performed EM analysis on cross sections of the dmd1 stalk to observe its ultrastructure. Few, if any, structures besides the dmd1 dendrites span the space from the epidermal surface to the muscle surface. Presumptive dmd1 dendrite stalks were identified as structures present in this space between the muscles and epidermis (Figure 1.4A). The dmd1 stalk appeared as fairly dense tissue containing less dense round structures of varying diameter (~250nm-750nm) that appear to correspond to individual dmd1 dendrites (Figure 1.4B-D, asterisks). These presumptive dendrites did not appear to be in direct contact with one another, and were relatively loosely packed within the surrounding tissue. Compared with similar micrographs of ensheathed peripheral nerves, dmd1 dendrites did not appear to have multiple concentric layers of glial ensheathment (Figure 1.4B-D; compare to Stork, et al., 2008, Figure 6). However there do seem to be multiple structures (potentially multiple cells) associated with stalk containing the dmd1 dendrites (Figure 1.4B structures 2-4). These images suggest that dmd1 dendrites are ensheathed by a cell as well covered as a layer of ECM as they travel to their ISN target and may be supported by additional cells or connective tissue.

Dmd1 dendrites do not form chemical synapses with motor axons

We wanted to determine the exact nature of the relationship between the dmd1 dendrites and motor neurons in the ISN nerve, as the proximity of dendrites to axons

might allow for synaptic connections. To determine if any synapses are formed between the dmd1 dendrites and ISN motor axons or muscles, we stained *NubGal4; UAS-CD8: GFP* animals with an antibody against the presynaptic active zone protein *bruchpilot* (nc82), which labels all chemical synapses in *Drosophila* (Wagh et al., 2006). Nc82 puncta were observed at adjacent NMJs but we found no colocalization of nc82 puncta with dmd1 dendrites (GFP) (Figure 1.5). Lack of a synaptic connection between dmd1 dendrites and the motor nerve suggests dmd1 functions primarily as a stretch receptor and that tethering of dendrites to the ISN provides a structural basis for stretch sensing.

The dmd1 axon targets dorsal proprioceptive regions of the neuropil

To further test the hypothesis that dmd1 functions as a proprioceptor, we examined dmd1's axonal projection to the CNS. In invertebrate systems, position of termination on the dorso-ventral axis is correlated with sensory function. Dorsal terminations correspond to proprioceptive function whereas ventral terminations correspond to tactile or nociceptive functions (Murphey et al., 1989; Pfluger et al., 1988; Schrader and Merritt, 2000). We used the MARCM technique (Lee and Luo, 1999) to generate individually labeled wild type dmd1 neurons and follow their axons from the periphery into the ventral nerve cord (VNC) in dissected third instar animals. In the VNC, GFP-labeled axons were visualized in relation to stereotyped longitudinal tracts labeled with an antibody against Fasciclin II (FasII), the *Drosophila* NCAM homolog. This labeling allows for detailed description of the relative position of axons and their terminations along with the dorso-ventral axis with respect to the FasII landmarks.

MARCM clones showed that dmd1 axons traveled within the ISN nerve along with other dorsal cluster sensory axons and entered the VNC through the anterior fascicle. Upon entering the neuropil in a relatively dorsal position, the dmd1 axons traveled ventrally and medially towards the ventromedial (VM) Fas-II fascicle (Figure 1.6A2). The axons then made a dorsal turn and bifurcated to send two axonal endings to terminate near the dorsomedial (DM) fascicle, one slightly anterior to the other (Figure 1.6A-B). Neither axonal ending was observed to cross the midline (Figure 1.6A). Like most other md neurons, the axon projection of appeared to be roughly confined to a single segment without passing over anterior or posterior segment borders. Thus, the dmd1 axon projection terminates in the dorsal neuropil consistent with dmd1 acting as a proprioceptor.

Deletion of the Pdm1 and Pdm2 genomic region causes dendrite overgrowth in md neurons

The morphology of dmd1 is unique among md neurons and from distinct from the md-da neurons in particular. Little is known about the genetic or molecular programs that specify the morphogenesis of non-da md neurons. Expression of Pdm1 and Pdm2 is limited to dmd1 and dbd neurons, both of which share many morphological features that distinguish them from other md neurons including limited dendrite growth and branching as well as non-epidermal dendrite substrates (this study; Schrader and Merritt, 2007) as well as suspected function as stretch receptors. To determine if there is an endogenous role for these genes in the morphogenesis of dmd1 and dbd, we analyzed dmd1 and dbd neurons lacking functional *pdm1* and/or *pdm2*.

We first tested whether mutations in *pdm1* affected dendrite development using the hypomorphic *pdm1* allele nub^1 (Ng et al., 1995). dmd1 and dbd neurons in homozygous mutant nub^1 animals and nub^1 MARCM clones of dbd or dmd1 did not show any obvious morphological defects (data not shown). Previous studies of *pdm1* and *pdm2* function in the *Drosophila* CNS have demonstrated that these genes act redundantly where they are co-expressed, such that both genes must be compromised in order to cause a phenotype (Yeo et al., 1995). *pdm1* and *pdm2* are similarly co-expressed in the PNS and seem equally capable of suppressing dendritic growth in overexpression assays (Chapter 2), thus it is likely they also perform redundant roles in the PNS.

To test this idea, we placed a large deficiency, *Df(2L) ED773*, which removes both *pdm1* and *pdm2* along with 27 other neighboring loci, *in trans* with a null allele of *pdm2*. This results in an animal that completely lacks any functional Pdm2, and has only one copy of *pdm1*. We analyzed the dendritic phenotypes of dbd and dmd1 in these animals by using the *clh8-Gal4* driver to drive expression of mCD8:GFP in dmd1 and dbd. These animals were able to survive to third instar (and possibly beyond), and there was no clear dendritic phenotype in either dbd or dmd1 (data not shown). These results indicated that if Pdm1 and Pdm2 play roles in the morphological development of dbd and dmd1, they act redundantly in the PNS, as in the CNS. Furthermore, they suggest that even a reduced amount of wild-type Pdm1 protein is sufficient to specify the correct morphology of PNS neurons and prevent lethality. We therefore decided to focus our studies of Pdm function on cases where both genes were compromised.

Because Pdm1 and Pdm2 lie adjacent to each other in the genome (Figure 1.7A), one strategy is to use a genomic deficiency that covers both coding regions. Studies of

Pdm1 and Pdm2 function in the CNS have relied on the large genomic deficiency, *Df (2L) ED773*, which removes ~429kB and 27 genes in addition to *pdm1* and *pdm2* (Figure 1.7A, D)(Grosskortenhaus et al., 2006)(Flybase). We sought to reduce the number of additional deleted genes and identified a genetic deletion of the region near *pdm1* and *pdm2* generated by imprecise excision of a P-element (Terriente et al., 2008). The resulting deletion, named nub^{R5}, was described as an embryonic lethal null allele of *pdm1*, however, two pieces of evidence suggested to us that this allele might actually affect both *pdm1* and *pdm2*. First, the embryonic lethality of the allele suggested that genes in addition to *pdm1* were likely to be affected, as no lethal allele of *pdm1* has previously been described and even null alleles of *pdm2* were also non-lethal, presumably due to redundant functions of *pdm1* and vice versa (Yeo et al., 1995). Second, the original P-element was reported to be in the intervening region between *pdm1* and *pdm2*; thus, it seemed plausible that the imprecise excision could affect both genes.

We mapped the endpoints of the allele using PCR and determined that the 5' end of the deletions lies between the *CG5435* and *SC35* coding regions and the 3' endpoint lies ~2-2.5kb upstream of the *pdm2* coding region. Thus, the *pdm1* coding region is completely deleted and much of the upstream enhancer region of the *pdm2* gene is removed (Figure 1.7A-C). Individual nub^{R5} MARCM clones of dmd1 or dbd stained for Pdm2 protein revealed that nub^{R5} homozygous clones do not express detectable levels of Pdm2 protein indicating that nub^{R5} can be considered a null allele for both Pdm1 and Pdm2 (Figure 1.7C). Overall, the nub^{R5} deletion removes about 224 kb of genomic material and 11 protein coding regions, which is about half the size of Df(2l)ED773 that removes 439kB and 29 genes (Figure 1.7A, B, D).

Individual *nub*^{R5} MARCM clones of dmd1 were characterized by dendritic overgrowth and dendrite targeting defects (Figure 1.8A-C). *nub*^{R5} dmd1 clones varied in their severity however the majority (n=6/8) of clones showed uncharacteristic epidermal dendrite growth and incomplete targeting to the ISN. Most completely lacked the typical three-dimensional dendrite growth characteristic of dmd1 (Figure 1.8B). To analyze dmd1 phenotypes semi-quantitatively, I segregated mutant neurons into three categories and assigned a numerical score: (1) wild type—indistinguishable from wild type morphology with normal targeting and no epidermal growth, (2) mild—targeting still intact with additional branches extending from the main arbor, (3) severe—complete loss of targeting and 3-dimensional growth, dendrites arborizing epidermis (Figure 1.8C). By giving each clone a numerical score I was able to calculate a scoring index that would range from 1 (all cells completely wild type) to 3 (all cells showing the most severe defects in growth and targeting). Wild type *FRT40A* dmd1 clones had an average score of 1.18 (n=11), while *nub*^{R5}*, FRT40A* dmd1 clones had an average score of 2.65 (n=8). Many of the mutant neurons were unrecognizable as dmd1 based on morphology and were instead positively identified by one of two methods. In animals that were co-stained with Pdm2 and HRP antibodies positive identification of dmd1 clones was made by determining that the only other Pdm2-positive nucleus in the cluster was that of dbd, no other dmd1-like neuron was visualized in the HRP staining, and that other dorsal cluster neurons were accounted for in the HRP label. In animals that were co-stained with anti-Cut and anti-HRP, dmd1 was positively identified based on lack of Cut staining along with no dmd1-like neurons in HRP.

Dbd clones were also characterized by dendrite overgrowth. Wild type dbd neurons have one anterior unbranched dendrite and one posterior unbranched dendrite with a thin dendrite linking the two under the cell body (Figure 1.8D) (Schrader and Merritt, 2007). *nub*^{R5} dbd neurons frequently had an additional dorsal oriented dendrite that was extensively branched as well as ectopic branches from each of their two main dendrites (Figure 1.8E-F). In addition, some *nub*^{R5} dbd neurons completely lacked their characteristic bipolar morphology and orientation along the anterior-posterior axis and had to be identified by examining the co-staining of other dorsal cluster neurons with HRP and Cut and/or Pdm2 antibodies. Dbd phenotypes were quantified similarly to dmd1 by ranking of the phenotype in a semi-quantitative scale to yield a scoring index ranging from 1 (completely wild type) to 3 (all severely affected clones). Wild type 40A dbd clones had an average scoring index of 1.00 (n=15), while *nub*^{R5}, 40A dbd clones had an average scoring index of 2.68 (n=34).

These results suggest that *pdm1* and *pdm2* are required for the development of normal stretch receptor dendritic morphology in dmd1 and dbd. However, as noted above *nub*^{R5} MARCM clones lack a number of other genes in addition to Pdm1 and Pdm2, raising the possibility that these phenotypes are due, at least in part, to the loss of one or more of these additional genes. We noted dendritic abnormalities in *nub*^{R5} clones of other md neurons that do not normally express Pdm1 and Pdm2 postmitotically. These phenotypes were variable and mostly consisted of reduced growth, which is distinct from the overgrowth phenotype seen in the dmd1 and dbd clones. One possibility is that Pdm1 or Pdm2 is required early during the development of these other md neurons. However, this is not supported by data from in situ hybridization or antibody staining of

embryos, which do not show expression of Pdm1 or Pdm2 in more than just two PNS neurons (Dick et al., 1991; Umesono et al., 2002) (Figure 1.1). Rather, these findings suggest that another gene(s) in the nub^{R5} deletion might be required for postmitotic dendrite growth of the other md neurons.

Silencing *Nub-Gal4*-expressing neurons disrupts normal larval crawling behavior

The dendritic and axonal morphology of dmd1 suggested that it likely functions as a stretch receptor to provide proprioceptive sensory information to the animal. We tested this hypothesis by silencing dmd1 and dbd neurons to see if this would impact coordinated locomotion. *Drosophila* larvae crawl by a series of coordinated peristaltic waves that progress from posterior to anterior segments. As the peristaltic wave passes through a segment, that segment undergoes a wave of contraction followed by relaxation. Timely progression of these phases, and transmission of the wave to the next anterior segment is important for coordinated movement, and recent studies have demonstrated that md neurons provide feedback necessary for coordinated locomotion in the larvae (Hughes and Thomas, 2007; Song et al., 2007).

To analyze the contribution of dmd1 and dbd stretch receptor function during peristalsis, we transiently silenced these neurons by using the *Nubbin-Gal4* driver to express a temperature-sensitive dominant negative form of the *shibire* gene, which inhibits synaptic transmission at temperatures over 29°C. The crawling behavior of control or $UAS\text{-}shi^{TS}$ -expressing larvae was recorded and analyzed by an automated custom built tracking system (Methods), and average speed was used a measure of coordinated and efficient peristaltic wave progression. $Nub\text{-}Gal4/\ UAS\text{-}shi^{ts}$ larvae

crawled significantly slower (and thus covered a shorter distance) than *Nub-Gal4* alone control larvae at the restrictive temperature, but not at the permissive temperature where neural transmission would not be affected (Figure 1.9A-B). These results are consistent with the dbd and dmd1 stretch receptors providing proprioceptive feedback that helps to coordinate wave propagation and crawling. As *Nub-Gal4* drives in a number of CNS neurons in addition to dmd1 and dbd in the periphery we cannot completely rule out the possibility that the effects we see are caused in part by silencing of these CNS neurons. Additional experiments using more specific drivers or laser ablations of dmd1 or dbd will be needed determine the specific contribution of each of these cells to the locomotor circuitry.

Discussion

In this study we have provided a morphological description of the dmd1 and described a molecular basis for the development of its unique dendritic arbor. Unlike other md neurons that spread their dendrites in a mostly two-dimensional plane to innervate the epidermis, the dmd1 neuron anchors its dendrites on an internal nerve. This morphology can provide a structural basis for sensing stretch during segment contraction. A role as proprioceptor is further supported by dmd1's homology to the vertical stretch receptor of other insects and the dorsal termination of its axon in the ventral nerve cord. The POU-domain transcription factors Pdm1 and Pdm2 are expressed exclusively in the dmd1 and dbd stretch receptors and we now provide evidence that these genes are required for their morphological development. The unique dendritic properties of the dmd1 neuron, now established, make this neuron an interesting model for studying its

morphological development in more detail and identifying the molecules downstream of Pdm1 and Pdm2 regulation that direct dmd1 morphogenesis.

The morphology of dmd1 supports a role as a stretch receptor

The dmd1 neuron differs from other *Drosophila* md neurons both molecularly and morphologically. Unlike the md-da neurons surrounding it, dmd1 does not arborize its dendrites on the epidermal surface. Rather, it extends its dendrites within connective tissue towards the interior of the animal to tether its dendrites to the ISN nerve (Figure 1). Comparative morphological descriptions of various insect nervous systems from the 1950s-60s describe a dorsal neuron with its cell body on the epidermis with dendrites embedded in connective tissue and anchored to either dorsal muscles or nerves which is conserved throughout several insect classes and termed the vertical stretch receptor (Finlayson and Lowenstein, 1958; Osborne, 1963). Based on our morphological description, dmd1 is the *Drosophila* homolog of this highly conserved insect vertical stretch receptor.

Studies of insect stretch receptors describe two dorsal stretch receptors per segment—a vertical stretch receptor and a longitudinal stretch receptor, which as their names suggest are oriented orthogonally (Finlayson and Lowenstein, 1958; Osborne, 1963). These stretch receptors have been assumed to work in tandem to provide comprehensive proprioceptive information by sensing stretch in orthogonal directions. Identification of their *Drosophila* homologs as dmd1 (this study) and dbd (Schrader and Merritt, 2007) has revealed that these cells share unique developmental histories and gene expression. They are the only PNS neurons derived from *amos*-dependent proneural

clusters and arise from simplified cell lineage patterns in which a sensory organ precursor undergoes a single cell division to produce a neuron and accessory cell (Umesono et al., 2002). All other PNS neurons are dependent on the proneural genes *atonal* or *achaete-scute* for their development and arise from more complex lineages involving multiple rounds of cell division. One possibility that this suggests is that the highly conserved dbd and dmd1 stretch receptors represent an ancestral md neuron type that functions to coordinate locomotion. Conceivably other types of receptors may have evolved by suppressing and/or modifying this ground state, a theme we will return to in Chapter 4.

Dmd1 and dbd also share exclusive expression of the Pdm1 and Pdm2 transcription factors, and we have shown that these transcription factors are required for normal stretch receptor morphogenesis (Figure 1.8). Without these transcription factors, these neurons do not develop the characteristic morphological features that underlie their ability to sense stretch in a particular orientation. Pdm1 (Nubbin) has well-conserved functions throughout insect phyla in wing and appendage development. It would be interesting to determine if the longitudinal and vertical stretch receptors of other species also express Pdm1/Pdm2. This could be determined simply by examining antibody staining patterns for Pdm1 in the PNS of multiple species. Expression in other species would support an evolutionarily conserved role for Pdm genes in promoting stretch receptor development.

Potential mechanisms for 3-dimensional growth of dmd1

The unique morphology of the dmd1 neuron makes it a potentially useful model for understanding dendrite-substrate preference and interactions as well as dendrite

targeting. The unique 3-dimensional arrangement of dmd1 dendrites presents a significant developmental challenge for these dendrites that dendrites of other md neurons do not face—namely, how is the gap between the ISN and epidermis spanned during development? There are several possible scenarios based on the data presented in this chapter describing mature dmd1 morphology. In mature third instar larvae, the distance between the dmd1 cell body and ISN nerve is over 50μm, but this distance may be considerably less during embryogenesis when dmd1 dendrites are first growing, in which case initial targeting made across a small gap could be expanded throughout development as the nerve and epidermal layer separate and dendrite length is increased from the dmd1 cell body. A similar possibility is that the dmd1 dendrites initially target a cell, such a glial cell, in the same plane as the cell body, which subsequently migrates away, taking the attached dendrites with it. These scenarios are similar in concept to the development of sensory neuron dendrites in *C. elegans*, with the exception that the dendritic attachment is stationary while the cell body migrates away (Heiman and Shaham, 2009). A distinct possibility is that the connective tissue associated with the dmd1 dendrites precedes or parallels their development such that the dendrites use this tissue as a substrate upon which to grow to their target. In this case the challenge facing the dendrites is one of substrate recognition and preference, rather than unsupported 3-dimensional growth and maintenance across an empty space.

Determining the exact nature of the dmd1 connective tissue and the timing of its formation will be important for distinguishing between these different scenarios. So far our evidence suggests that a *moody*-expressing cell and neural lamella (ECM) provide either a substrate upon which to grow or physical support for dmd1 dendrites by

ensheathment after the dendrites have extended. Live imaging of dmd1 dendrites during embryogenesis and analysis of staged embryos counterstained with markers for the dmd1 substrate and target should also help to narrow the possible ways dmd1 forms its projection and the function of any supporting structures.

Most of the glia involved in ensheathing the peripheral nerves migrate to the periphery from the CNS along the sensory and motor axons as they grow (Sepp et al., 2000). However, one exception to this rule is in the case of dbd, whose sibling cell becomes its specialized glial support cell. The dbd glia is required for dbd dendrite extension and completely ensheathes dbd cell body and dendrites (Schrader and Merritt, 2007; Sepp and Auld, 2003). Dmd1 has an identical lineage pattern as dbd, and its sibling cell at least transiently expresses the glial marker *repo* (Umesono et al., 2002) raising the possibility that the dmd1 sibling cell develops into a support cell for dmd1—quite possibly the moody-expressing that we have observed in association with dmd1 dendrites. Lineage tracing techniques could be used to determine the fate and positioning of the dmd1 sibling, which might provide important insights into how the dmd1 dendrites reach their target.

Pdm1 and Pdm2 act redundantly to specify stretch receptor neuron morphogenesis

Data from loss-of-function studies suggests that Pdm1 and Pdm2 act redundantly during the development of dbd and dmd1, to specify key features of stretch receptor morphology such as limited dendrite growth and branching and proper dendrite targeting. Our data combined with the findings that Pdm1 and Pdm2 also have redundant roles in the CNS (Yeo et al., 1995), suggest that these genes may act redundantly wherever they

are co-expressed. Pdm1 is required and expressed alone in the wing disc (Ng et al., 1995), but it is not clear whether Pdm2 can substitute for Pdm1 during wing development. Determining this might provide insight about whether Pdm1 or Pdm2 have any unique functions.

Because of the functional redundancy of Pdm1 and Pdm2, our loss of function studies rely on the use of relatively large deficiencies to remove the neighboring *pdm1* and *pdm2* loci simultaneously. Analysis of MARCM clones homozygous for this deficiency revealed major dendritic abnormalities in most dbd and dmd1 clones including ectopic branches and loss of dendrite targeting. These are key features that are likely to directly impede the ability of these neurons to function as stretch receptors. Incomplete penetrance of the phenotype in some clones is likely due to perdurance of Pdm1 and Pdm2 protein in the clone due to the fact that Pdm1 and Pdm2 are expressed in dmd1 and dbd precursors. Our MARCM analysis strongly points to a role for Pdm1 and Pdm2 in directing the morphology of dmd1 and dbd, but we cannot completely rule out the possibility that the phenotypes are partially attributable to the loss of other genes in the deletion. Ultimately, obtaining rescue of the dbd and dmd1 phenotypes with Pdm1 or Pdm2 transgenes will be required to demonstrate that these phenotypes are specifically due to loss of these transcription factors. However, there is correlative evidence that supports our conclusion that the phenotypes seen in dmd1 and dbd are due primarily to loss of Pdm1 and Pdm2. First, ectopic expression of Pdm in Cut mutant neurons results in dendritic arbors closely resembling dmd1 and dbd arbors (see Chapter 2). In addition, postmitotic misexpression of Pdm1 or Pdm2 is capable of causing severe dendrite undergrowth in md neurons (see Chapters 2,3), which is consistent with a role for these

genes in limiting dendritic growth. Finally, the abnormalities observed in *nub*^{R5} MARCM clones of other md neurons involved undergrowth--opposite of the overgrowth phenotypes observed in dbd and dmd1, suggesting that phenotypes may be due to loss of distinct genes.

The discovery of the important roles of Pdm1 and Pdm2 in mediating stretch receptor morphogenesis is an important first step in elucidating the cellular and molecular mechanisms that promote 3-dimensional dendrite growth. These Pdm transcription factors likely coordinate the regulation of multiple genes including guidance cue receptors, cell adhesion molecules, and molecules that restrict dendrite growth and branching to promote dmd1 morphogenesis. Identification of these downstream targets using gene-profiling techniques has the potential to provide important insights into the mechanisms of 3-dimensional growth and dendrite targeting of dmd1, as well as general mechanisms of how dendrite growth and branching are regulated. We present the results of such profiling experiments in Chapter 3.

Preliminary data suggest a unique role for dmd1 in providing proprioceptive feedback during crawling

Coordinated movement underlies a wide variety of essential behaviors and requires feedback from the periphery about body position and muscle tension, termed proprioception. In insects the majority of proprioceptive information is thought to come from stretch receptors, and the high level of structural conservation of such stretch receptors between species suggests they play critical roles in coordinating insect movement. Its structural homology to the well described and well conserved vertical stretch receptor coupled with our findings that the dmd1 axon terminates in the dorsal

region of the ventral nerve cord strongly support a role for dmd1 as a proprioceptor. Our own preliminary behavioral data combined with that of other recent behavioral studies specifically suggest that dmd1 provides proprioceptive feedback required for coordinated locomotion (Hughes and Thomas, 2007).

Recent studies have demonstrated that sensory feedback is required for coordinated locomotion, without which larval crawling is laborious and nearly futile (Hughes and Thomas, 2007; Song et al., 2007). Only one study has attempted to pinpoint which sensory neurons are required for this feedback (Hughes and Thomas, 2007). Based on experiments in which different subpopulations of md neurons were silenced, Hughes and Thomas assigned redundant function to the md-bds and class I neurons in providing proprioceptive feedback during crawling. Both the md-bds and class I neurons have dendrites oriented along the anterior-posterior axis of the animal, which the authors suggest allow them to detect segment length (Figure 9C). It should be noted, however, that the authors report the strongest defects in crawling when dmd1 is included in the silenced population. Based on the findings of Hughes and Thomas (2007) coupled with our own preliminary silencing experiments using *Nub-Gal4*, we propose that dmd1 provides additional and unique feedback about segment contraction status. Namely, we propose a model in which the dmd1 neuron is active during segment contraction (Figure 1.8D). Observations of fluorescently labeled dmd1 dendrite stalk elongation during peristalsis (M. Corty, personal observations) and models of vertical stretch receptor tension during peristalsis, the dmd1 dendrites should be at maximal tension during contraction and display increased firing rates compared to when the segment is in a relaxed state (Finlayson and Lowenstein, 1958). Conversely, dbd and class I md-da

dendrites oriented along the A-P axis should be maximally stretched, and hence, most active when the segment is elongated during relaxation (Figure 1.8C, also see Finlayson and Lowenstein, 1958 Figure 4C-D). Thus, dbd (the longitudinal stretch receptor) and dmd1 (the vertical stretch receptor) should provide information about different phases of contraction. One way to test this hypothesis would be to use genetically encoded activity sensors (such as GCaMP (Tian et al., 2009)) to observe the activity patterns of dmd1, dbd, and class I neurons during a segment contraction. Anti-phase increases in activation between dmd1 and dbd/classI neurons would support our model that these cells respond to distinct phases of segment contraction. Recently a technique to record from dbd neurons in semi-intact embryonic preparations has been described (Nair et al., 2010), suggesting that direct electrophysiological testing of our hypotheses may be may be possible. Continued studies of dmd1 anatomy and function should reveal its precise role in proprioceptive feedback to the crawling circuit contributing greatly to our understanding of how this circuit develops and operates, as well as provide direct evidence for the importance of dendritic form to sensory neuron function.

Figure 1.1: Dmd1 and dbd express the POU domain transcription factors Pdm1 and Pdm2

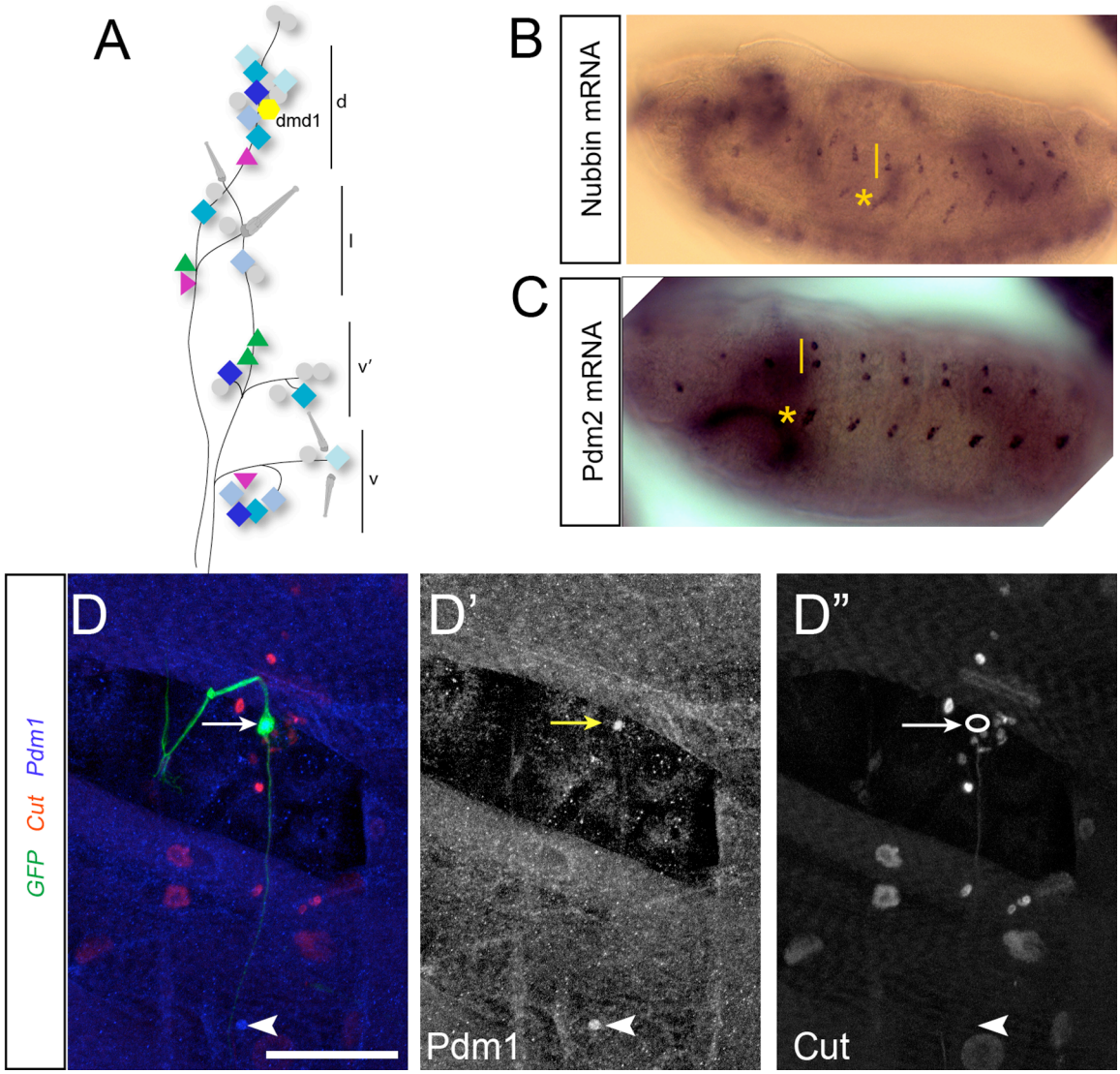

Figure 1.1: Dmd1 and dbd express the POU domain transcription factors Pdm1 and Pdm2

(A) Schematic diagram showing of one hemisegment of the *Drosophila* larval PNS. Dorsal (d), lateral (l), ventral prime, (v'), and ventral (v) clusters are labeled. Es neurons are depicted as gray circles, chordotonal organs as gray triangles. Md neurons are depicted in color. Md-da neurons are represented with diamonds in increasing shades of blue to correspond to subclass (Class I <ClassII <ClassIII <ClassIV). Md-bd neurons are represented as magenta triangles. Md-td neurons are represented with green triangles. The dmd1 neuron is in the dorsal cluster and is depicted in yellow.

(B-C) In situ hybridization shows that *pdm1* and *pdm2* are expressed in 2 dorsal neurons. Probes against *pdm1* **(B)** and *pdm2* **(C)** where hybridized in late stage w^{1118} embryos. Both genes show the same expression pattern: two dorsal PNS neurons (bracket) and glial cells of the lch5 chordotonal organ (asterisk) in each abdominal segment.

(D) Dmd1 expresses Pdm transcription factors throughout larval stages. Dmd1 MARCM clone stained with antibodies against Pdm1 and Cut. Dmd1 expresses Pdm1 but not Cut. Arrow points to cell body and nuclear staining (or absence of staining) in separated channels. Arrowheads indicate location of dbd cell body and show that dbd also express Pdm1 but not Cut continuing through late larval stages. (The ventrally oriented neurite is the dmd1 axon.)

Dorsal is up and anterior to the left in this and all images. Scale bar =50μm.

Figure 1.2: Dmd1 dendrites project off the epidermis to target the ISN nerve

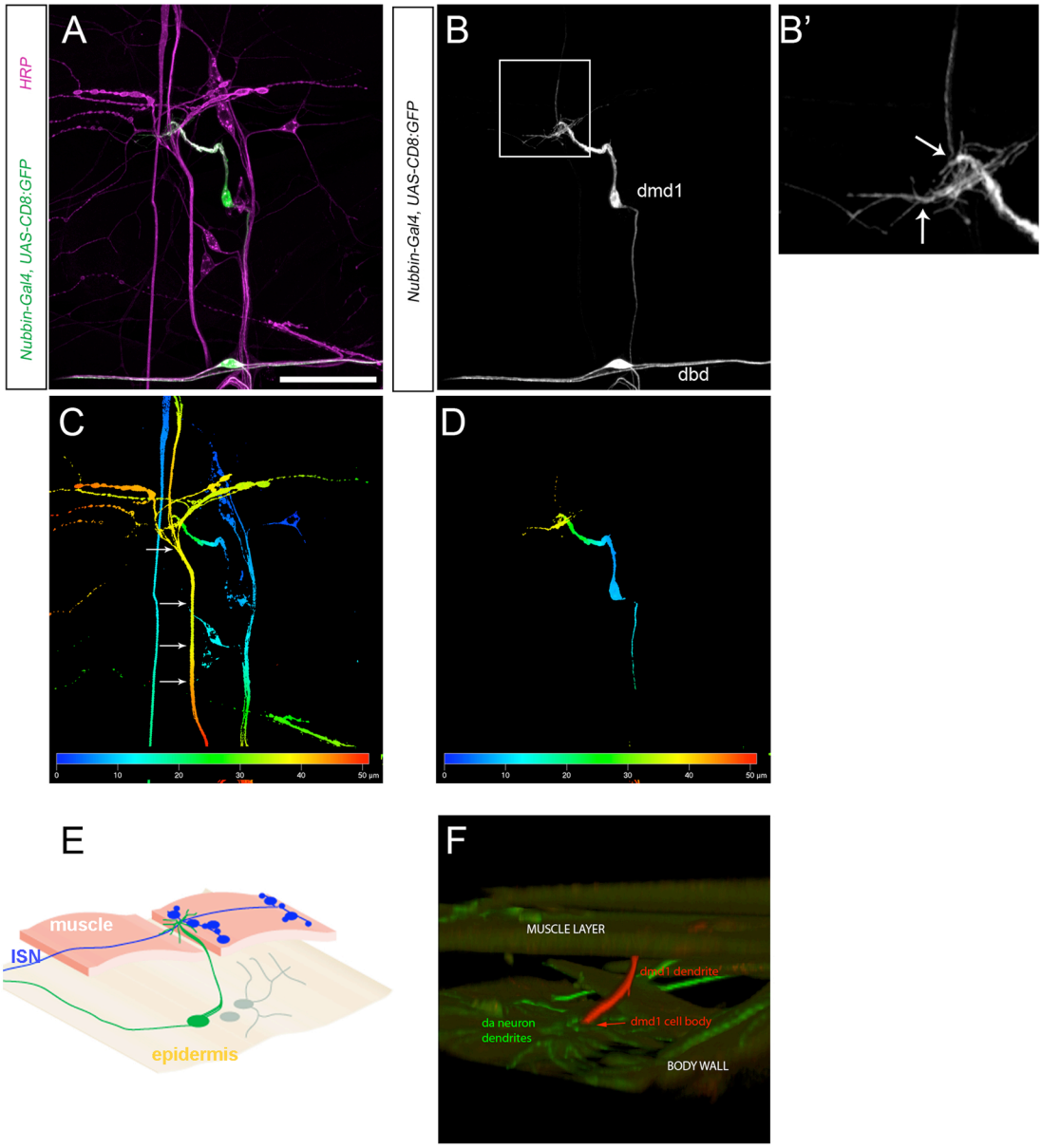

Figure 1.2: Dmd1 dendrites project off the epidermis to target the ISN nerve

(A-D) Dmd1 morphology can be analyzed using the Nub-Gal4 driver to express GFP throughout the cell. Confocal projections of a representative dorsal cluster from a third instar larvae with genotype *Nub-Gal4, UAS-mCD8:GFP/+* stained with anti-GFP (green) and anti-HRP (magenta) to label all neuronal membranes. *Nub-Gal4* drives GFP expression in dmd1 and dbd. The GFP channel is separated in B to show dmd1 morphology. B' shows the boxed area in B at higher magnification to show the distal ramification of dmd1 dendrites at their target. In panels C and D the images have been pseudo-colored according to a depth code to show the 3-D nature of the dmd1 dendrite stalk which spans between 40-50μm in this image to reach its ISN target (arrows indicate ISN).

(E) Schematic diagram showing the 3-dimensional targeting of dmd1 dendrites to the ISN nerve at the muscle layer. Dmd1 (green), muscles (pink), ISN (blue with NMJs depicted as circles on the muscle surface). (Not to scale.)

(F) 3-D rendering generated from confocal stacks that show dmd1 dendrites spanning the distance between the body wall and muscle layer.

Scale bar= 50μm

Figure 1.3: Dmd1 dendrites are ensheathed by the neural lamella and associated with a moody-expressing cell

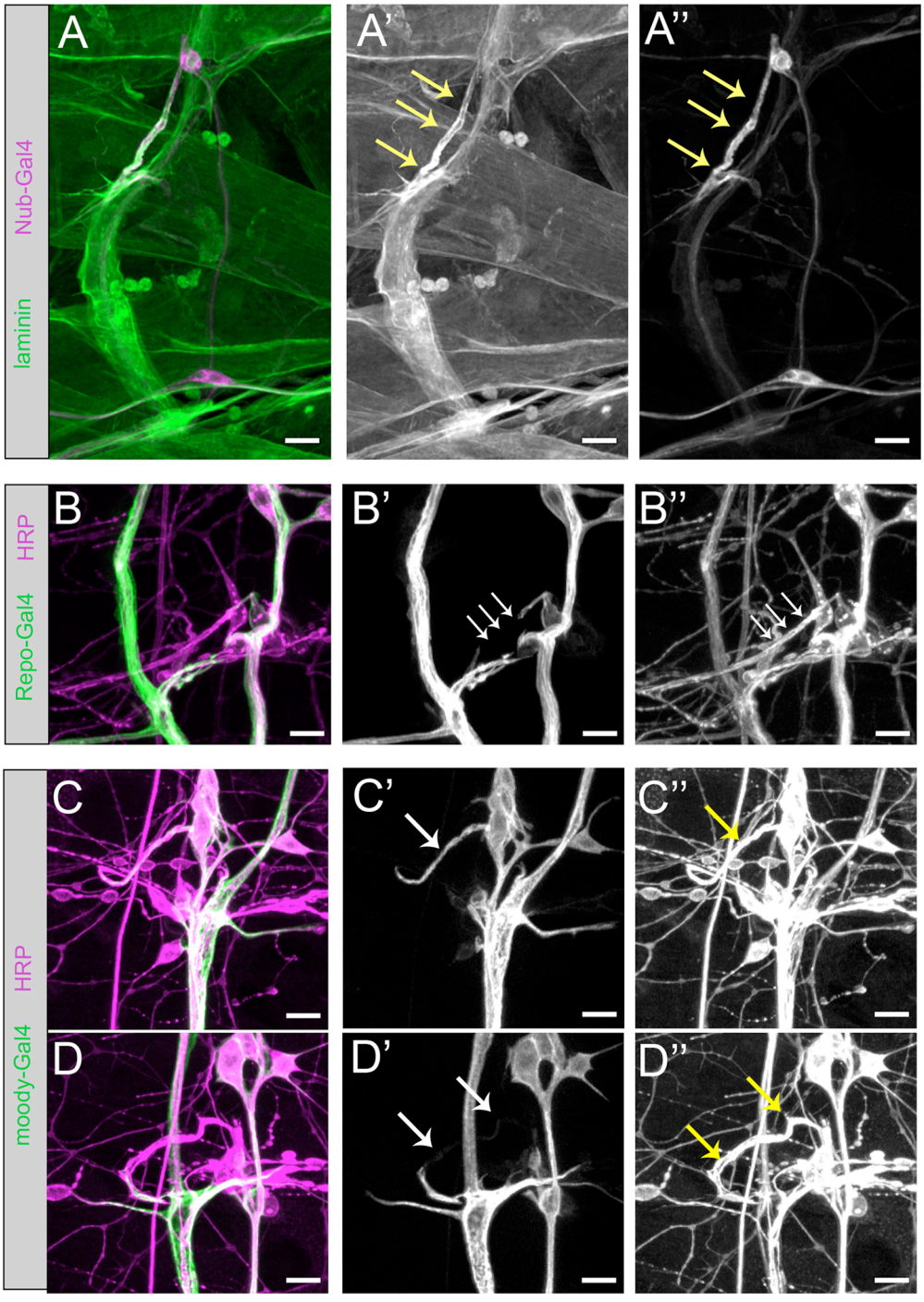

Figure 1.3: Dmd1 dendrites are ensheathed by the neural lamella and associated with a moody-expressing cell

A) The neural lamella surrounds the dmd1 dendrite stalk. *Nub-Gal4, UAS-mCD8:GFP* larvae stained with anti-laminin antibody (magenta) shows co-localization along the dmd1 dendrite stalk. Arrows indicate location of dmd1 dendrite stalk.

B) The dmd1 dendrite stalk is not ensheathed by a *repo-Gal4* expressing glial cell. Glia (green) labeled with *Repo-Gal4/UAS-mCD8:GFP*. Neuronal membrane labeled with HRP (magenta). The abrupt end of the GFP staining at the proximal dmd1 stalk is clearly seen in B'.

C-D) Moody-Gal4 expressing cells are sometimes associated with the dmd1 dendrite stalk. *Moody-Gal4; UAS-mCD8:GFP*. Neuronal membrane labeled with HRP (magenta). In C, GFP driven by *moody-Gal4* is present along the length of the dmd1 stalk (arrow). This complete ensheathment was observed in 8/23 segments. A thin process or no GFP at all was observed in the remaining 15/23 segments as shown in D, only a faint thin GFP process is seen in association with the stalk.

Scale bars= 10µm

Figure 1.4: Ultrastructural morphology of the dmd1 dendrite stalk

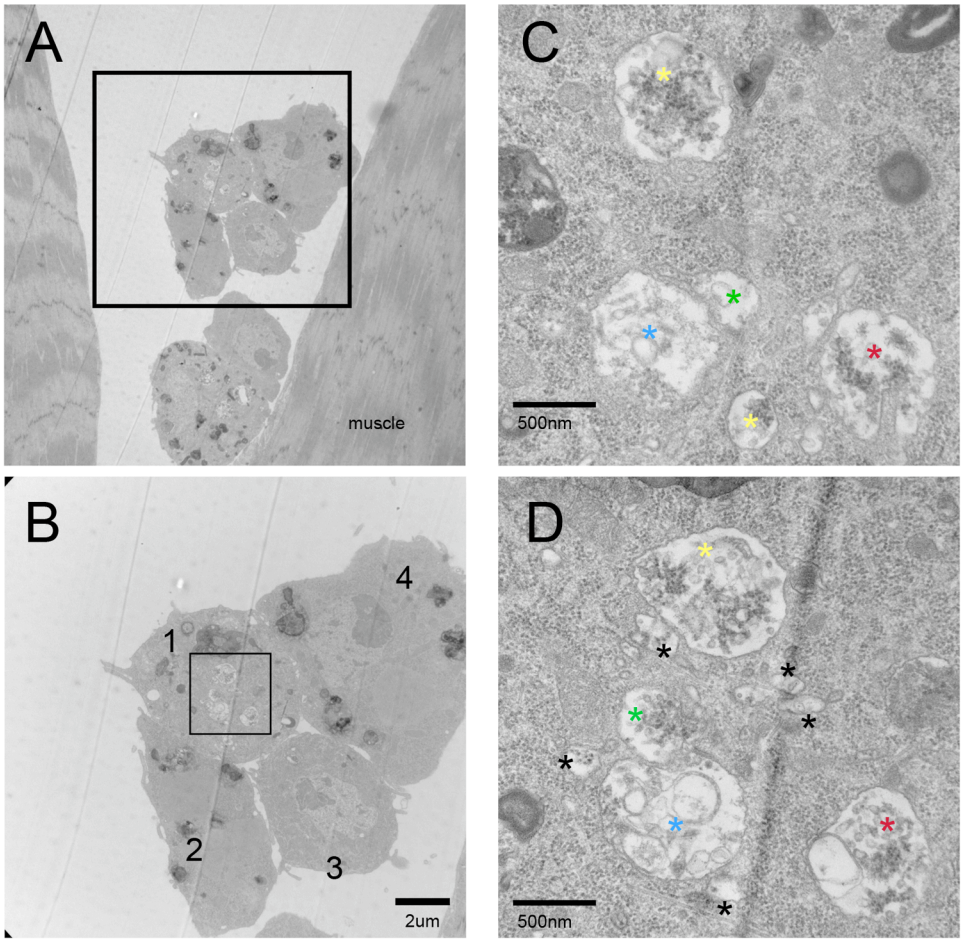

Figure 1.4: Ultrastructural morphology of the dmd1 dendrite stalk

A) Dmd1 dendrite stalk and associated cells at the level of the muscle. The stalk seems to be split into two parts in this plane.

B) Boxed area from **(A)**. Magnified view of presumptive dmd1 stalk. The boxed area in this panel contains presumptive dendrites that are ensheathed by a cell. Rather than multiple layers of ensheathment, there appears to be only one cell (1) that makes contact to ensheath the dendrites, but there also appear to be other cells or tissue (2-4) that are associated with the stalk.

C-D) Magnified view of area boxed in **(B)**. **(C)** and **(D)** show two thin sections from the same region. Presumptive dendrites are marked with asterisks. Asterisks of the same color indicate that the same dendrite is being viewed in both images. Notice that individual dendrites are encompassed by the surrounding cell and do not appear to contact one another directly. Images are not from directly adjacent sections.

Figure 1.5: Dmd1 dendrites do not form synapses with ISN axons

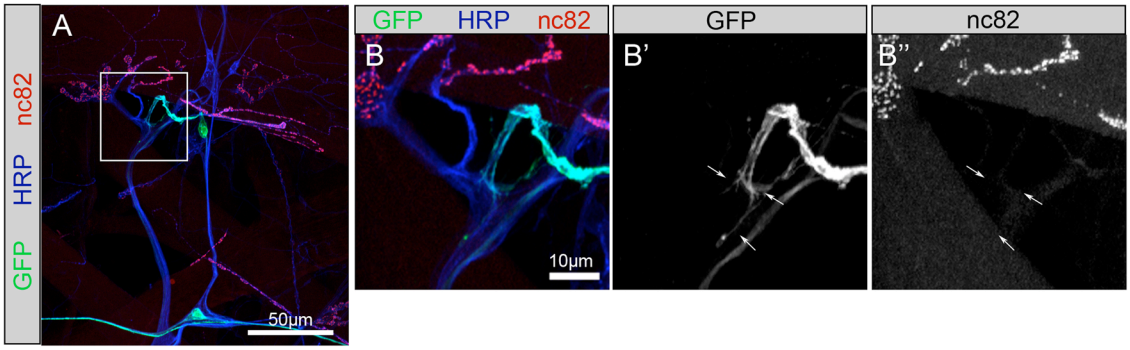

Figure 1.5: Dmd1 dendrites do not form synapses with ISN axons

A) Labeling for synaptic proteins on dmd1 dendrites reveals that they do not form chemical synapses with axons in the ISN nerve. Image of the dorsal cluster region of a third instar larvae reveals the only synapses in the periphery are NMJs. Dorsal cluster from a *Nub-Gal4; UAS-mCD8:GFP* larva stained with anti-GFP (green), anti-HRP (blue) and anti-nc82 (blue), which labels active zones at chemical synapses.

B-B'') Magnified view of boxed area from A showing no co-localization of dmd1 dendrites (GFP) and nc82 puncta (red).

Figure 1.6: Dmd1 axons project to the dorsal neuropil

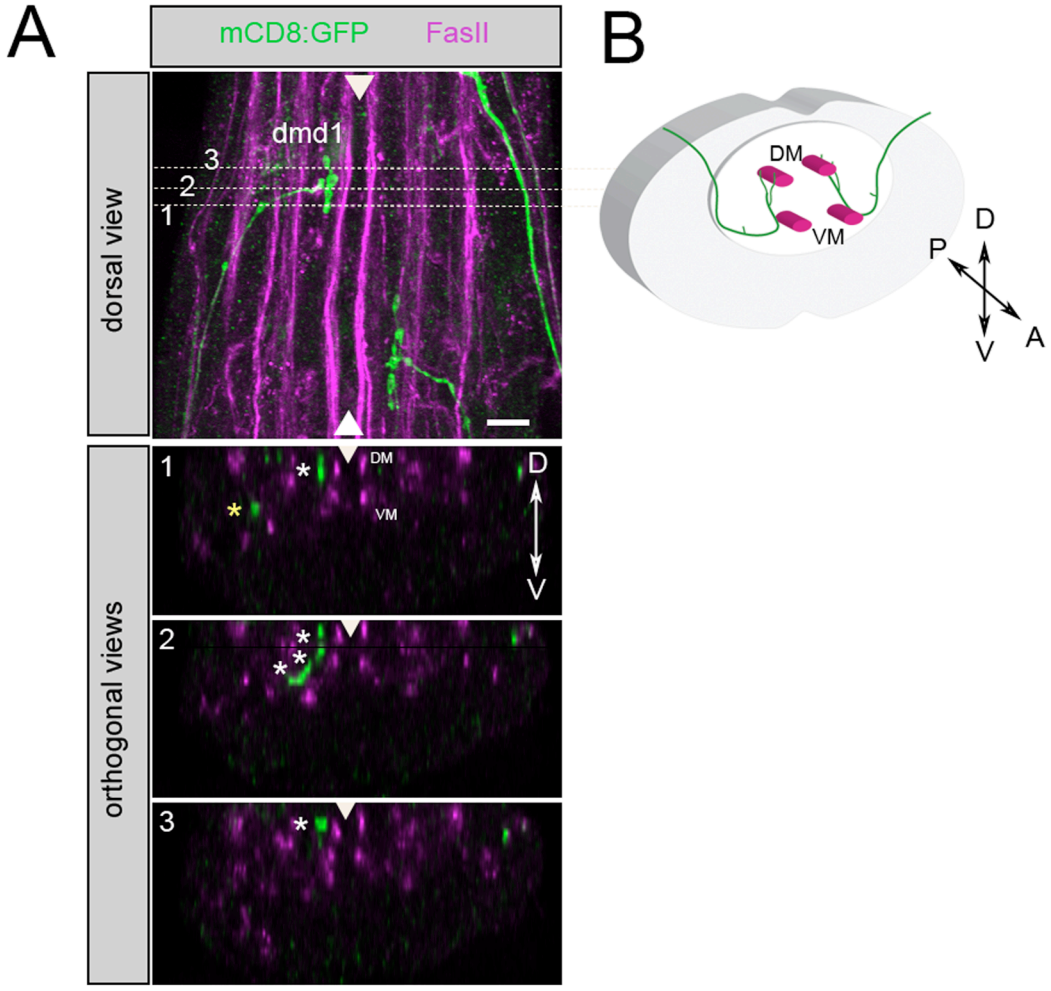

Figure 1.6: Dmd1 axons project to the dorsal neuropil

A) Dmd1 axons project to the dorso-medial fascicle of the VNC. In the top panel the axon of a representative wild type 19A dmd1 MARCM clone is shown entering from the left side of the animal and terminating near the medial most fascicles with a small collateral near the lateral fascicles. Orthogonal views are made from optical slices taken at the position indicated by the dotted lines, and reveal the position of the axon on the dorso-ventral axis. GFP labeled axons (green); Fas2 labeled fascicles (magenta). Arrowheads mark the midline.

1) Posterior orthogonal section shows the ventral position of the lateral collateral (yellow asterisk). The posterior axon termination ends near the DM fascicle (white asterisk).

2) The next orthogonal sections show the trajectory of the dmd1 axon. The axon travels medially in the ventral region of the neuropil before turning dorsally near the midline.

3) The anterior axon termination is also positioned near the DM fascicle (asterisk).

B) Schematic view of dmd1 axon trajectory in the VNC. Dmd1 axons enter through the anterior fascicle and project ventrally and medially within the neuropil before turning dorsally near the VM fascicle. After making the dorsal turn, the dmd1 axon bifurcates. Both branches grow dorsally to terminate near the DM fascicle, with one branch slightly anterior to the other. Dmd1 axons also have a short collateral branch in the ventrolateral region. (Only the VM and DM fascicles are shown for simplicity.)

Scale bar = 10μm

Figure 1.7: Characterization of the *nub*^{R5} deletion

A

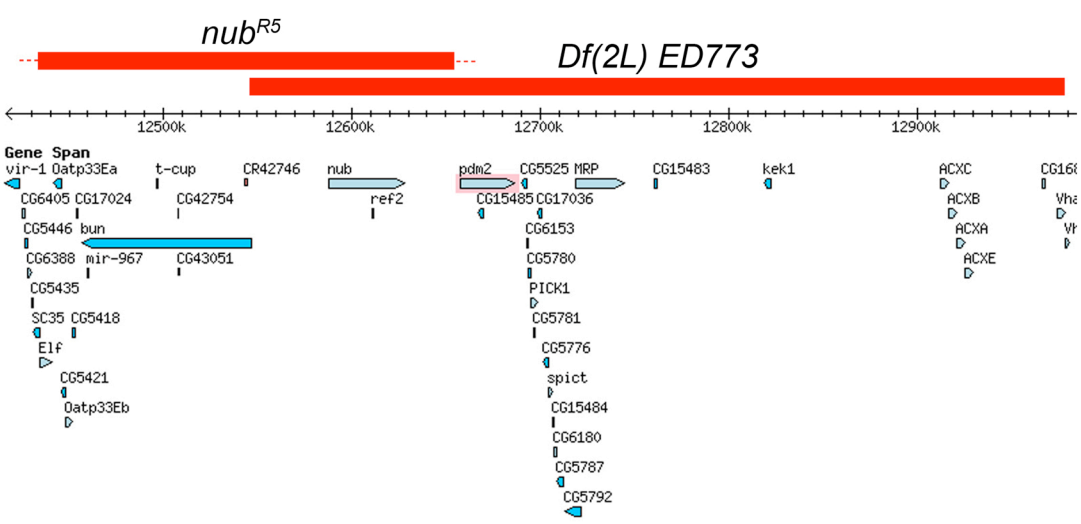

B

Genes deleted by *nub*^{R5}		
SC35	CG5418	bun
Elf	CG17024	nub
Oatp33Ea	t-cup	ref2
CG5421	CG42754	*pdm2*
Oatp33Eb	CG43051	

C

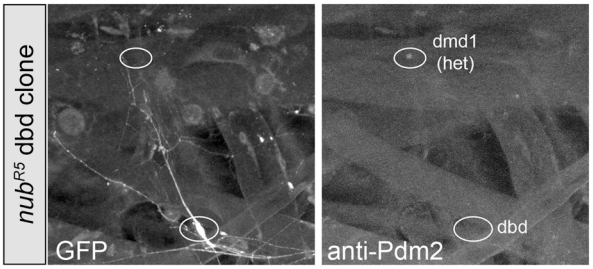

D

Genes deleted by Df(2L) ED773		
bun	CG17036	ACXB
nub	CG5776	ACXA
ref2	spict	ACXE
pdm2	CG6180	CG16800
CG15485	CG5787	Vha68-2
CG5525	CG5792	Vha68-3
CG6153	MRP	CG12404
CG5780	CG15484	Vha68-1
PICK1	kek1	Tor
CG5781	ACXC	

Figure 1.7: Characterization of the *nub*^{R5} deletion

A) Schematic of Pdm1 (Nubbin) and Pdm2 genomic region showing the extent of the *nub*^{R5} and *Df(2L) ED773* genomic deletions (red bars, dashed line indicates the precise ends are not determined). (Obtained from Flybase, August, 2011).

B) List of genes deleted by the *nub*^{R5} deletion as determined by PCR mapping. Gene names in italics indicate that it remains unclear whether the whole gene is affected. Gene names in blue are shared in common with the ED773 deficiency.

C) *nub*^{R5} dbd clone showing no Pdm2 protein. Pdm2 protein is detected in the dmd1 neuron from the same segment. The dmd1 neuron still has one wild type copy of the 2L chromosome, but the dbd neuron is homozygous for the *nub*^{R5} deletion indicating that *nub*^{R5} is protein null for Pdm2.

D) List of genes deleted by the ED773 deficiency as reported by Flybase. Gene names in italics indicate that the gene is partially affected. Gene names in blue are shared in common with the *nub*^{R5} deletion

Figure 1.8: Pdm1 and Pdm2 are required for normal dmd1 and dbd morphogenesis

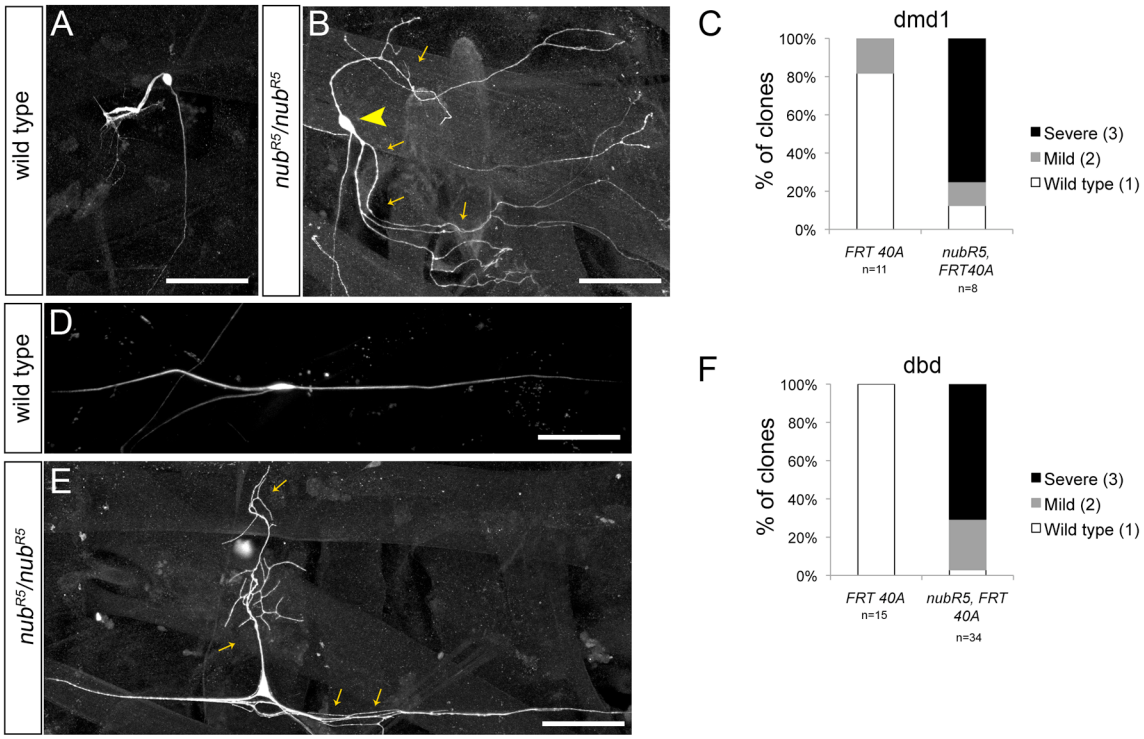

Figure 1.8: Pdm1 and Pdm2 are required for normal dmd1 and dbd morphogenesis

A) Wild type dmd1 neuron projects its dendrites off the epidermis to the ISN nerve.

B) A *nub*^{R5} dmd1 neuron has dendrites that arborize the epidermis and do not grow to their normal ISN target. Example of a severely affected (Score=3) clone. Arrowhead indicates cell body, arrows indicate epidermal dendrite growth.

C) Quantification of *nub*^{R5} dmd1 phenotypes. Clones were scored as (1) Wild type, (2) Mild: targeting intact with ectopic epidermal dendrite growth, or (3) Severe: no targeting, only epidermal dendrite growth.

D) Wild type dbd neuron shows a normal unbranched bipolar morphology with one anterior branch and one posterior branch.

E) A *nub*^{R5} dbd neuron has an ectopic dorsally oriented dendrite that is extensively branched, in addition to branching of its posterior dendrite. Example of a severely affected (Score=3) clone. Arrows indicate abnormal branches.

F) Quantification of *nub*^{R5} dbd phenotypes. Clones were scored as (1) Wild type, (2) Mild: ectopic branching of anterior or posterior dendrites, or (3) Severe: additional primary dendrite (usually with ectopic branching of anterior or posterior dendrites).

Scale bars =50μm

Figure 1.9: Dmd1 provides proprioceptive feedback required for normal locomotion

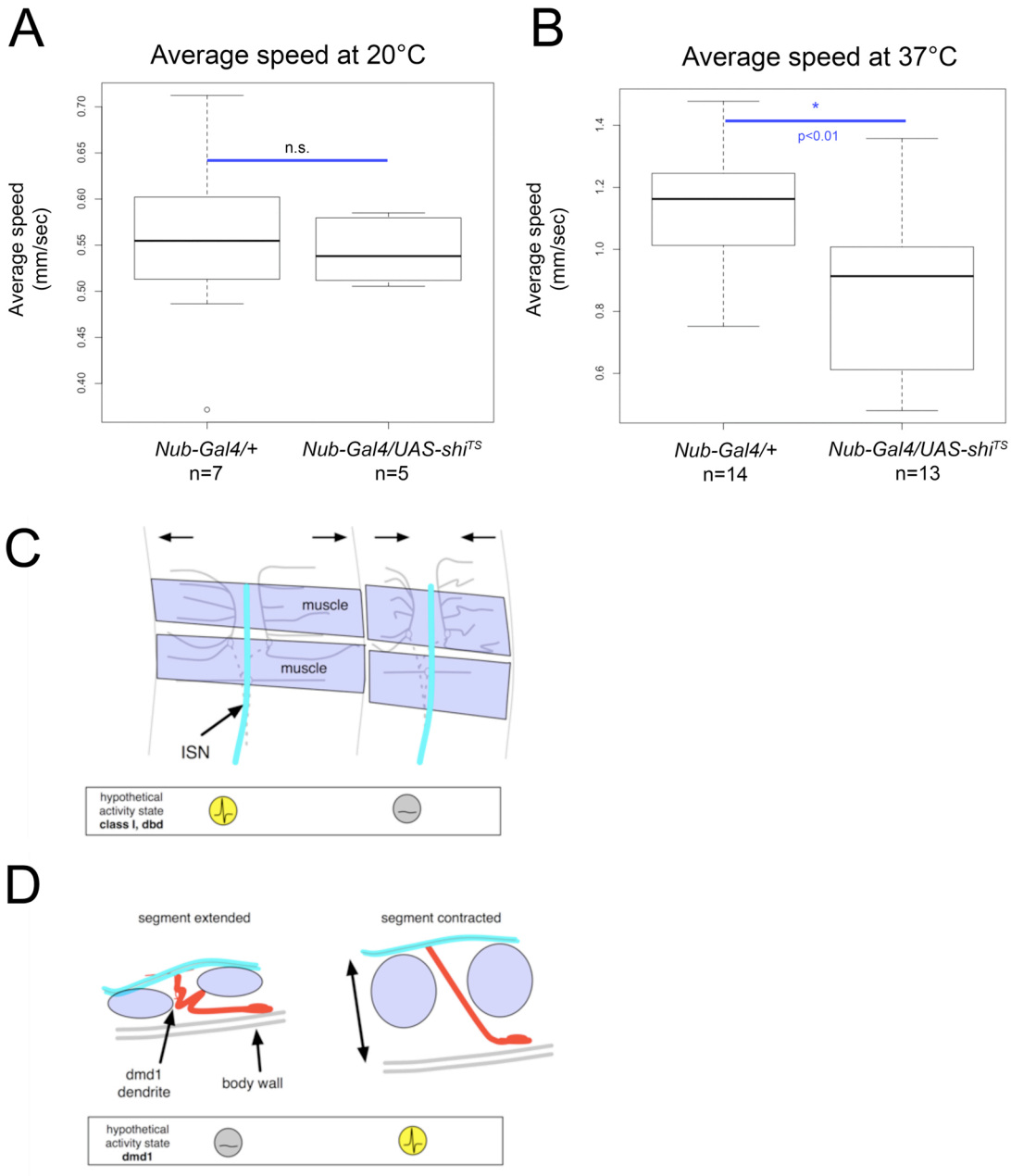

Figure 1.9: Dmd1 provides proprioceptive feedback required for normal locomotion

A) At permissive temperatures there is no difference in the average crawling speed of *Nub-Gal4* driver alone and *Nub-Gal4/UAS-shi^{TS}* larvae. Each "n" represents 5 individual larvae. Average speed from each group of five was averaged to obtain the values presented in the graphs.

B) At restrictive temperatures *Nub-Gal4/UAS-shi^{TS}* larvae crawl more slowly than *Nub-Gal4* driver alone larvae indicating that neurons in the *Nub-Gal4* expression pattern including dmd1 and dbd are important for normal larval locomotion. **(**Note that the scales in the graphs are different because larvae crawl faster at higher temperatures.)

C) Model for the activity of dbd and class I neurons during a peristaltic cycle. These neurons are hypothesized to be most active during segment relaxation, as this will lengthen the dendrites of these cells.

D) Model for the activity of dmd1 during a peristaltic cycle. Dmd1 is hypothesized to be most active during the contraction phase, as this will cause the maximal stretch of its dendrites. Dmd1 (red), Muscles (purple), ISN (turquoise).

Chapter 2

Cut and Pdm transcription factors specify distinct sensory neuron dendrite and axon morphologies

Abstract

Somatosensory neurons are the first component of circuits that deliver mechanosensory information to the brain. It is vital that each sensory neuron detects the appropriate type of stimulus and conveys that information to the appropriate central circuits. Molecular programs that coordinate sensory morphology in the periphery with axon projection patterns centrally are poorly understood. I have used multidendritic (md) sensory neurons of the *Drosophila* PNS to identify genetic and molecular programs that coordinate dendrite and axonal morphogenesis. Neurons with different sensory dendrite morphologies project axons to distinct regions of the central nervous system. Neurons with relatively simple sensory dendrites target axons to dorsal regions of the CNS, suggesting proprioceptive function. By contrast, neurons with more complex morphologies target their axons to ventral, tactile, domains of the CNS. The homeodomain transcription factor Cut is expressed selectively in the latter group of neurons and is absent from proprioceptive neurons. Whereas Cut has previously been shown to promote dendrite branching, the mechanisms of this control, and whether Cut also coordinates axon targeting with branching complexity, was unknown. I show that loss of Cut leads to a transformation from tactile to proprioceptive-like peripheral arbors. In addition, these transformed cells undergo concomitant changes in axon targeting—shifting their axons from ventral (tactile) to dorsal (proprioceptive) regions of the neuropil. I show that transformed neurons acquire expression of the POU domain transcription factors Pdm1 and Pdm2 (Pdm1/2), which are normally restricted to proprioceptive neurons. Gain and loss of function studies of Pdm1/2 are consistent with an instructive role in acquisition of a selective dendritic arbor, and preliminary data indicate that Pdm1/2 may also be instructive in targeting axons to dorsal domains of the CNS. Together these results identify a cascade of transcription factors that coordinately specify proprioceptive dendrite and axon development.

Introduction

Primary sensory neurons deliver information from the periphery to specific circuits in the central nervous system. It is vital that each sensory neuron detects the appropriate type of stimulus and conveys that information to appropriate regions of the sensory neuropil to target second-order neurons. Previous studies in invertebrates, including *Drosophila*, have demonstrated a correlation between peripheral morphology, sensory modality, and axonal projection of sensory neurons (Grueber et al., 2007; Merritt and Whitington, 1995; Murphey et al., 1989; Schrader and Merritt, 2000). Although peripheral morphology and axonal projection are linked, the molecular programs that coordinate sensory morphology in the periphery with axon projection patterns centrally are poorly understood.

Neurons in the *Drosophila* peripheral nervous system (PNS) have been excellent models for studying the genetic and molecular programs that specify distinct dendritic morphologies. As reviewed in the Introduction, the multidendritic (md) sensory neurons are a heterogeneous group of sensory neurons that can be subdivided into several classes. Neurons with complex **d**endritic **a**rborizations that innervate the epidermis are referred to as da neurons. Other md neurons have dendrites that do not innervate the epidermis and are instead associated with trachea, nerves, or muscle. Among these are the bd neurons, which have **b**ipolar **d**endrites and the dmd1 neuron described in the previous chapter. Studies of the md neurons have begun to identify intrinsic developmental programs that generate diverse dendritic morphologies in the nervous system. Numerous transcription factors are involved in the control of specific arbor features of different subclasses of md-da neurons (Grueber et al., 2003; Sugimura et al., 2004, Kim et al., 2006, Jinushi-Nakao

et al., 2007), including the homeodomain transcription factor Cut. Cut is expressed at different levels in distinct morphological classes of md-da neurons. These levels correspond to specific terminal branching patterns that define each class. Manipulating Cut expression levels in these cells leads to bidirectional changes in arbor morphology, providing evidence that Cut regulates class-specific dendritic development in a level-dependent fashion (Gruber et al., 2003). However, how Cut mediates dendritic growth and branching patterns is so far not well understood. Few downstream targets of Cut regulation have been identified, and it is as yet unclear how different levels of Cut influence dendritic development or whether Cut has any level-independent functions in specifying sensory neuron morphology.

Drosophila sensory neurons send their axons to the ventral nerve cord (VNC), which is the *Drosophila* equivalent of the spinal cord. In addition to having distinct peripheral dendritic morphologies that likely underlie their ability to detect distinct sensory stimuli, individual sensory neurons have distinct axonal projections in the VNC (Murphey et al., 1989; Schrader and Merritt, 2000). The region of the neuropil to which each sensory projects is tightly coupled to its peripheral dendrite morphology and to a general function. Ventral termination corresponds to tactile or nociceptive function, and dorsal termination corresponds to proprioceptive function (Grueber et al., 2007; Merritt and Whitington, 1995; Murphey et al., 1989; Schrader and Merritt, 2000). These terminations also correspond to gene expression status. For example, wild type Cut-expressing neurons including class II, III, and IV md-da neurons project their axons to the ventral neuropil of VNC, near the ventro-medial (VM) fascicle. By contrast, md sensory neurons not expressing Cut project dorsally to the dorso-medial (DM) fascicle (Grueber

et al., 2007; Merritt and Whitington, 1995; Schrader and Merritt, 2000; Zlatic et al., 2009). Neurons with dorsal terminations include the dorsal and ventral bipolar neurons, class I da neurons, and dmd1, all of which are implicated in proprioception.

In this chapter I describe work that establishes a level-independent role for Cut in specifying da sensory neuron dendritic features and ventral axon termination in a subset of md-da neurons. When these neurons lack Cut, they adopt a dendritic morphology characteristic of the proprioceptive sensory neuron dmd1, and show a corresponding shift of their axons to dorsal "proprioceptive" regions of the VNC. Cut blocks this alternative morphology, at least in part, by repressing the POU domain transcription factors Pdm1 and Pdm2. Pdm1 and Pdm2 are normally restricted to proprioceptive neurons and contribute to their normal dendritic development, suggesting that Cut vs. Pdm expression coordinately regulates both dendritic and axonal morphology and functions as a binary switch between neuronal morphologies specialized for distinct sensory functions.

Results

Loss of Cut leads to severe stunting of dendrite growth in a defined population of md neurons

Previous studies of the role of the *cut* gene in md sensory neuron dendrite morphogenesis indicated that there might be two distinct loss-of-function phenotypic classes (Grueber et al., 2003). We confirmed this finding using MARCM to study the dendritic phenotypes of md neurons homozygous for a null allele of *cut* (ct^{c145}). Loss of Cut affects all classes of md-da neurons that normally express Cut—the class II, III, and

IV md-da neurons. Class I neurons do not express detectable levels of Cut protein and show no changes in dendrite morphology when *cut* is mutated (Grueber et al., 2003).

In most class II-IV md-da neurons, loss of Cut results in a simplification of dendritic arbors that mainly affects higher order branching patterns, while leaving the underlying scaffold of the arbor intact (Figure 2.1B). A distinct phenotype emerged in a subset of class II and class III neurons of the dorsal and lateral clusters. In these neurons the entire dendritic scaffold was severely reduced, causing a dramatic reduction in the overall field area (Figure 2.1C-D). This phenotype was seen with high penetrance in the dorsal class II (ddaB: 16/17 clones) and dorsal class III neurons (ddaF: 15/15 clones; ddaA: 30/33 clones), and at a lower penetrance in the lateral class III ldaB neuron (7/13 clones). This more drastic phenotype was never observed in any class IV neurons, nor in any other more ventrally located class II or III neurons (Figure 2.1A).

The majority of these clones had a unipolar dendritic morphology with a tufted arborization a short distance away from the cell body (Figure 1C'-D'). The dendrites in this tufted arborization were frequently clumped together and often appeared to cross or tangle with one another. Dendrites were so densely packed and tangled in confocal images that it was not possible to quantify the exact number or length of the dendrites. Some clones also displayed a bipolar dendrite morphology with two main dendrites extending from the cell body, occasionally with some tufting at the end of one dendrite (not shown). These arborizations of mutant neurons bore little resemblance to their own wild type dendritic morphologies and were highly reminiscent of dmd1, which has a unipolar morphology with a distal arborization (Chapter 1), or dbd, which has a simple bipolar morphology. Because of the apparent transition towards a stretch receptor-like

dendrite morphology, I refer to the second category of severely affected *cut* mutant neurons as transformed neurons.

Transformed *cut* mutant neurons exhibit aberrant dendrite targeting

To examine the transformation in more detail, we counterstained MARCM clones with antibodies to label other surrounding structures, and we observed changes in dendrite targeting and/or substrate preference. Dendrites of wild-type Cut-expressing md neurons spread their dendrites across the epidermal surface sometimes becoming enclosed within epidermal cells (Kim et al., unpublished). This is in contrast to the dendrites of the stretch receptor neurons, which grow along and within glia and other connective tissue making no direct contact with the epidermal surface (Chapter 1; Schrader and Merritt, 2007). The dendrites of transformed ddaA, ddaB, and ddaF *cut* mutant neurons, so severely reduced, no longer arborize large patches of epidermis and the compacted arborizations of these neurons, suggested that they may even be targeting specific regions of the epidermis or other nearby structures. By counterstaining MARCM clones with HRP to label all the surrounding neurons and sensory structures, we found that many transformed dendrites abnormally targeted other sensory structures or remained confined to surfaces covered by the glial sheath, suggesting the epidermis is no longer a preferred substrate. Overall more than half of all transformed neurons targeted their dendrites to ectopic surfaces/structures.

Targeting to chordotonal organs

More than half of transformed ddaF neurons inappropriately targeted their dendrites to the nearby lch1 chordotonal organ, which runs parallel and anterior to the

dorsal cluster (Figure 2.2A). Of the clones that were counterstained with HRP to label all sensory structures including lch1, 6 out of 11 transformed ddaF cells targeted lch1 with dendrites either stopping at or growing along the chordotonal organ. Transformed ddaA and ddaB dendrites also targeted lch1, but much more rarely (ddaA n=1/26; ddaB n=1/9).

Targeting to the dmd1 dendrite stalk

Notably, a subset of transformed neurons from all classes had dendrites that were observed to grow along the dmd1 dendrite stalk away from the epidermis towards the ISN nerve (ddaA 4/26; ddaB 4/9; ddaF 3/11; Figure 2.2B). This trajectory was never observed in wild type md neurons other than dmd1. This mainly occurred when the transformed neuron cell body was closely positioned to the dmd1 neuron and its substrate.

Confinement of dendrites to the glial sheath

Finally, several ddaA clones confined their dendrites primarily to the glial sheath covering the dbd neuron, its dendrites, and the ventrally extending axons of the dorsal cluster neurons (Figure 2.2C; ddaA n=5/26). Again this was most frequent when ddaA was positioned near the dbd cell body, and notably the transformed ddaA neurons took on a morphology similar to that of the dbd neuron, albeit with a different orientation of the two main dendrites. Taken together these data demonstrate that loss of Cut results in severe dendritic undergrowth as well as changes in patterning caused by targeting of dendrites to abnormal substrates. These substrates are typical of proprioceptive stretch receptor neurons. Combined with the overall resemblance to proprioceptive arbor morphology, these results are consistent with switches to proprioceptive arbor identity.

POU domain transcription factors Pdm1 and Pdm2 are misregulated in transformed neurons

We next examined how Cut promotes the morphogenesis of the da versus dmd1 arbors. Cut functions as a transcription factor so it is likely that the effects of Cut on dendrite morphogenesis are mediated by changes in gene expression downstream of Cut. A previous study of Cut in the *Drosophila* PNS indicated that the POU domain transcription factor Pdm1 (Flybase: *nubbin*) was misregulated in *cut* mutant embryos (Brewster et al., 2001).

As described in the previous chapter Pdm1 and Pdm2 (Pdm1/2) are co-expressed with the in dmd1 and dbd and act redundantly during dmd1/dbd morphogenesis, specifying features that set them apart from the md-da neurons including limited or no epidermal growth and targeting/confinement to other substrates. Using antibodies against Pdm1 and Pdm2, I confirmed the previous finding that expression of Pdm1 and Pdm2 were expanded in *cut* mutant embryos (Figure 3.3A-B: *cut*/+ = 2 cells/dorsal cluster, *cut/cut* = average of 4.5 cells/dorsal cluster; n=17 segments examined). Expansion of Pdm expression was not seen ventrally, and the number and position of additional Pdm+ nuclei in the dorsal and lateral clusters of *cut* mutant embryos were consistent with the number and position of the transformed md neurons ddaA, ddaB, ddaF, and ldaB. To confirm that Pdm1 and Pdm2 were misregulated specifically in transformed neurons, I co-stained *cut* mutant MARCM clones (Lee and Luo, 1999) with either anti-Pdm1 or anti-Pdm2 antibodies. Ectopic Pdm expression was detected in clones that had undergone dendritic transformation (Figure 2.3C-D ddaA n=9/10, ddaB n=13/13, ddaF n=8/8, ldaB n=7/7), but not in non-transformed mutant clones such as the dorsal class IV neuron (ddaC n=0/28) or ventral clones (n=0/8). As noted above only about 50% of

ldaB clones showed the transformed phenotype, while the remaining clones had intact dendrite scaffolds lacking higher order branches. Importantly, ectopic Pdm expression was observed in transformed ldaB clones, (n=7/7) but not when the clones had an intact scaffold with loss of terminal branching (Figure 3; n=2/2). These data strongly indicate misregulation of Pdm is specifically coupled to the transformed dendrite phenotype.

These data suggested that Cut is required to repress expression of Pdm1 and Pdm2 in a subset of da neurons. To test whether Cut is sufficient to repress Pdm1 and Pdm2 expression we misexpressed Cut using the post-mitotic pan-md *109(2)80-Gal4* driver and assayed the effect on Pdm expression in dmd1 and dbd using antibodies against the Pdm proteins. In third instar larvae, Pdm protein was not detected in either dbd or dmd1 when these cells were forced to express Cut (Figure 2.3E). Together these data demonstrate that Cut is both necessary and sufficient to repress Pdm1 and Pdm2 in a subset of md neurons.

Other class-specific transcription factors cannot restrict Pdm1 and Pdm2 expression

Our data demonstrated that Cut was required to repress Pdm1 and Pdm2 in dorsal class II and III da neurons; however *cut* mutant dorsal class IV neurons did not misexpress Pdm1 or Pdm2, nor did wild type dorsal class I neurons, which always lack Cut expression. In addition, Pdm1 and Pdm2 were not misexpressed in any ventral *cut* mutant da neurons. Together these data suggest that there are additional regional and class-specific factors that must be affecting Pdm expression status. We investigated the ability of known class IV and class I specific transcription factors to repress Pdm1/2 expression by misexpressing them in dmd1 and dbd using the Gal4-UAS system.

Knot is a COE transcription factor that is expressed exclusively in class IV neurons and is required for the development of their class-specific arbor features (Crozatier and Vincent, 2008; Jinushi-Nakao et al., 2007; Hattori et al., 2007). Overexpression of *UAS-knot* using a pan-md driver was not capable of eliminating endogenous Pdm expression in dmd1 or dbd as evidenced by antibody staining for Pdm1 protein (data not shown).

Abrupt is a BTB zinc finger transcription factor that is expressed exclusively in class I neurons where is it required to limit dendrite growth and branching (Li et al., 2004; Sugimura et al., 2004). Overexpression of *UAS-abrupt* using a pan-md driver was also not capable of eliminating endogenous Pdm expression in dmd1 or dbd as evidenced by antibody staining for Pdm1 protein (data not shown). Together these results suggest that class I and class IV neurons must either express additional factor(s) that serve to repress Pdm expression or lack factors that positively regulate Pdm genes.

Pdm1/2 and Cut are expressed in mutually exclusive patterns, suggesting that there might be mutual regulation. To test this, we looked for ectopic Cut expression in dmd1 and dbd nub^{R5} clones, which lack Pdm1 or Pdm2 expression. We found no evidence for Cut expression in these neurons (data not shown) suggesting that the regulatory relationship between Cut and Pdm1/2 is one directional.

Pdm1/2 misexpression suppresses dendritic growth

Because Pdm1/2 expression was tied to dendritic transformation in *cut* mutant clones, we wondered if Pdm1/2 expression might underlie that phenotype. One of the key abnormalities in transformed *cut* mutant neurons was the severe stunting of overall

arbor growth, and we wondered if this was caused by the misregulation of Pdm1/2 or by other still unknown targets of Cut regulation. To test the hypothesis that Pdm1/2 expression in mutant neurons suppressed dendrite growth, we misexpressed either Pdm1 or Pdm2 in otherwise wild type neurons using the post-mitotic pan-md Gal4 driver, *109(2)80-Gal4*. We achieved single cell resolution of dendritic arbors using the FLP-out technique.

Misexpression of either UAS-Pdm1 or UAS-Pdm2 caused a dramatic reduction in dendrite growth in all class II, III, and IV neurons (Figure 2.4 A-B). Quantitative analysis revealed significant decreases in total dendrite length in class II (ddaB : WT length 1732.8um +/- 107.3 n=5; UAS-Pdm1 length 758.1um +/-195.2um, n=6, $p< 0.004$; UAS-Pdm2 length 330.2um +/-140.7um, n=6, $p<0.004$, Wilcoxon rank-sum test) and class III neurons (ddaA: WT length 3988.6um =/- 459.3um n=4; UAS-Pdm1 length 618.775um =/- 236.2um n=4 $p<0.0001$; UAS-pdm2 length 198.3um +/- 51.0um n=4 $p<0.0004$ Student's t-test) (Figure 2.4C-D). There was also a significant reduction in the number of nodes for both class II (ddaB: WT 46.60±12.93 nodes, n=5; UAS-Pdm1 16.67±5.99 nodes, n=6, $p<0.0043$; Pdm2 15.67±11.20 nodes, n=6, $p<0.017$, Wilcoxon rank-sum test) and class III neurons (ddaA: WT 479.5±129.8 nodes, n=4; UAS-Pdm1 19.25±17.1 nodes, n=4, $p<0.005$; UAS-Pdm2 13.5±4.8 nodes, n=4, $p<0.006$, Student's t-test). However when we quantified the number of nodes per unit length we did not find significant reductions in class II neurons (ddaB: WT 0.0267± 0.0063 nodes/µm; Pdm1 0.0238± 0.0116 nodes/µm p=0.67; Pdm2 0.0659± 0.0715 nodes/µm p=0.67; Wilcoxon rank-sum test).

UAS-Pdm1 expression in class III neurons showed a significant reduction in branching even when length was controlled for with UAS-Pdm2 expression showing a similar but not statistically significant trend (ddaA: WT 0.1185± 0.0207 nodes/µm; Pdm1: 0.0316± 0.0234 nodes/µm p=0.0014, Pdm2: 0.0728± 0.0332 nodes/µm p=0.0661, Student's t-test). This difference between class II and class III effects may be a consequence of wild type class III neurons having much higher nodes per unit length compared with class II (Grueber et al., 2002). The robust and consistent reduction in overall dendrite length suggests that the main effect of Pdm misimpression is a growth defect. The effects of Pdm1 and Pdm2 were qualitatively similar, but the effects of Pdm2 over-expression were generally stronger than that of Pdm1. It is unclear whether this indicates that Pdm2 is more capable of suppressing growth or is can be attributed to differences in expression level amongst the UAS constructs.

Roles for Pdm1 and Pdm2 suppressing epidermal dendrite growth are consistent with our findings that these genes are required to limit dendrite growth and branching of dmd1 and dbd (Chapter 1). The roles for Pdm1 and Pdm2 in specifying dmd1 and dbd morphology, together with these overexpression data support our hypothesis that deregulation of Pdm1 and Pdm2 underlies the *cut* transformed neuron dendrite phenotype.

cut mutant md neurons display alterations in axon targeting

We examined the axon projections of Cut mutant neurons (n=80) to determine if dendritic transformation was accompanied by any changes in axon projection. Axon termination within the *Drosophila* VNC can be determined by following individually

labeled axons from the periphery into the nerve cord and viewing the axons in relation to the longitudinal axon tracts labeled with an antibody against the NCAM homolog Fasciclin II (FasII) (Figure 2.5).

Changes in dorso-ventral positioning

The most striking change was a dorsal shift in the axon terminals of dendritically transformed *cut* class II and III mutant neurons. The axons of transformed mutant neurons terminated dorsally, near the DM fascicle rather than their typical position near the VM fascicle (Figure 2.5A-B; ddaA, n=5/5, ddaB, n=2/2, ddaF, n=6/6, ldaB, n=7/7). Dendritic and axonal transformation appeared to be coupled as all of these mutant neurons had transformed dendrites. We analyzed the projections of other md neurons that did not have transformed dendrites and found only 2/32 instances where there appeared to be a dorsal shift in axon termination in non-transformed neurons. Both of these instances were ldaA (lateral class II) neurons; 2/3 ldaA neurons examined had an axon branch projecting dorsally. The axon projections of all other non-transformed *cut* class II, III, and IV neurons we analyzed (n=30) showed no changes in dorso-ventral positioning of their terminations (Figure 2.4C).

The majority of transformed *cut* mutant axons entered the VNC normally and traveled ventrally and medially toward the ventromedial (VM) fascicle where they would normally terminate. Mutant axons of transformed neurons, however, then turned dorsally as they approached the VM fascicle to terminate near the DM fascicle (Figure 2.5D). This route was similar to the routes taken by dmd1 and class I neurons that normally terminate dorsally (as described in Chapter 1). A small number of mutant neurons (n=3/20) took a

more direct dorsal trajectory from entry, similar to that of the wild type trajectory of the dbd neuron (figure 2.5B). All three instances of this type of trajectory were observed in transformed ddaF neurons. We examined a total of six ddaF projections. All six projected dorsally, but half took the dorsal dbd-like route while the other half took the more prevalent dmd1-like route. The different trajectories did not correlate with dendritic resemblance to dmd1 vs. dbd, and may represent a cell type specific feature of ddaF or a function of the timing of clone formation. Overall these data suggest that loss of Cut can affect axonal projections as well as dendrite development. That such changes in dorso-ventral positioning are limited only to dendritically transformed *cut* mutant neurons suggests that this dorsal shift may be mediated by Pdm1 and Pdm2 expression that is a result of loss of Cut. Dorsal axon termination is associated with proprioceptive sensory neurons, indicating that loss of Cut and the accompanying Pdm misregulation in a subset of neurons shifts them towards proprioceptive dendrite and axon morphologies.

Changes in midline crossing

Analysis of *cut* mutant neuron axons also revealed changes in midline crossing of class IV neurons. Both the dorsal class IV (ddaC) and ventral class IV (vdaB) normally have collaterals that cross the midline (Grueber et al., 2007)(Figure 2.5C). These midline collaterals were either reduced or completely absent in most *cut* mutant ddaC (n=14/16) and vdaB (n= 2/4) neurons.

Aside from ddaC and vdaB, the axons of class II-IV neurons do not cross the midline, though they all terminate medially. Fine distinctions in medial lateral positions of class II-IV have been described in relation to one another. The class IV neurons are

the most medial, with class III and then class II having slightly more lateral terminations (Grueber et al., 2007). It was difficult to make these distinctions unless there were multiple axons within the same segment to compare. In the few cases we saw, we could not make out a clear change in relative positioning of the different classes. This is consistent with the observation that this relative positioning does not correspond well to endogenous Cut expression levels of class II-IV neurons. Performing MARCM experiments in a ppkEGFP background to label class IV axons and establish an additional reference point for comparison may aid in determining this conclusively (Grueber et al., 2007). Thus, even though Pdm1 and Pdm2 are not misregulated in class IV neurons, loss of Cut on its own can impact sensory neuron axon development, specifically the ability of class IV axons to cross the midline.

Pdm2 misexpression alters axon termination patterns in the VNC

Changes in dorso-ventral axon targeting of *cut* mutant md neurons were limited to those neurons showing the transformed dendrite phenotype, and thus to those cells in which Pdm1 and Pdm2 are misregulated. Both of the sensory neurons that normally express Pdm1/2 (dmd1 and dbd) target their axons to the dorsal neuropil (Chapter 1, Figure1.6; Schrader and Merritt, 2000), suggesting that Pdm1/2 might play a role in specifying dorsal axon termination. We tested the role of Pdm1/2 in axonal targeting by determining whether misexpression of Pdm1/2 was sufficient to cause changes in axon terminations of sensory neurons.

We misexpressed Pdm2 using the *clh201-Gal4* driver, which expresses in all md and es sensory neurons and a few neurons in the VNC. This expression pattern allows

for an aggregate view of sensory axon projections to the VNC. We compared sensory axon positioning in third instar larvae expressing mCD8:GFP alone to those expressing mCD8:GFP and UAS-Pdm2. This analysis revealed several changes in the axon termination pattern. The sensory neuron scaffold in *clh201-Gal4, UAS-mCD8:GFP* animals appeared as a ladder-like structure, consisting of longitudinals on either side of the midline connected by branches crossing the midline. In *clh201-Gal4, UAS-mCD8:GFP/UAS-Pdm2* animals midline crossing was absent (Figure 2.6, Compare A and B, top panels). The longitudinals of UAS-Pdm2 expressing animals were also thinner, suggesting a reduction in collateral branching on either side of the midline where sensory neurons terminate (Figure 2.6A and B.) We examined the nerve cords in cross section at equivalent anterior/posterior positions by analyzing optical cross sections that contain the characteristic dorsal trajectory of the dbd axons in each segment. This examination revealed a reduction in ventral GFP staining near the VM fascicles (Figure 2.6 bottom panels, compare boxed areas in A and B; n=4 nerve cords/condition), suggesting that there is a reduction in ventral terminations of sensory neurons. These data suggest that Pdm2 misexpression is sufficient to cause changes in axon patterning including inhibiting midline crossing and inhibiting ventral terminations. Together with the findings on *cut* mutant neuron projections, these data suggest that Cut acts through Pdm repression to specify axon termination domain as well as dendrite morphology of a subset of sensory neurons.

Discussion

Previous work had pointed to an important role for the homeodomain transcription factor Cut in level-dependent regulation of class-specific dendritic arbor

morphology, but the mechanism(s) by which Cut controlled dendrite morphogenesis remained unknown. Work described in this chapter establishes a key function for Cut in suppressing the acquisition of proprioceptive dendrite morphology in a subset of md neurons. Moreover, we show that Cut also mediates a switch between ventral and dorsal axon termination of these neurons—a feature that corresponds to sensory modality. We identify Pdm1 and Pdm2 as downstream targets of Cut regulation that are likely to mediate these changes. Together these results identify a transcriptional code that coordinately specifies modality-specific dendrite morphology and axon targeting in a subset of md neurons.

Cut is required to repress proprioceptive dendrite morphology in md neurons

The homeodomain transcription factor Cut is expressed at distinct levels in different classes of md-da neurons. Manipulation of Cut levels in these neurons can lead to bi-directional changes in dendrite morphology demonstrating that Cut regulates dendrite morphogenesis and promotes the development of diverse class-specific features via graded expression (Grueber et al., 2003). We now show that Cut expression is specifically required in dorsal class II and class III md-da neurons to prevent them from acquiring a dendritic morphology similar to that of the proprioceptive stretch receptor neurons dmd1 and dbd. In these neurons, loss of Cut causes dramatic changes in overall arbor structure characterized by severely reduced outgrowth and field size with aberrant targeting to non-epidermal substrates (Figures 1 & 2). Our findings that both high-expressing class III (ddaA, ddaF, and ldaB) and low-expressing class II (ddaB) neurons require Cut to suppress this alternate dendrite morphology, establishes a separate level-

independent role for Cut in controlling md-da neuron morphogenesis. We propose that Cut has dual function to promote diverse dendritic arbors. First, Cut expression represses genes that promote stretch receptor-like dendrite development, establishing a basic epidermal innervating md-da morphology. Then, the specific levels of Cut in a given neuron determine class-specific terminal dendrite morphology, thus diversifying the neurons that innervate the larval epidermis—presumably with consequences for diversification of sensory function amongst the different classes of Cut-expressing sensory neurons.

Cut promotes the development of a cutaneous arborization by repressing Pdm1 and Pdm2

Cut promotes an epidermal innervation by negatively regulating Pdm1 and Pdm2 expression. Loss and gain of function studies provide clear evidence that Cut is both necessary and sufficient to repress the expression of both Pdm1 and Pdm2 (Figure 3). This repression is robust as even low endogenous Cut expression (i.e. as in ddaB) is sufficient to completely repress Pdm1/2 expression and ensure normal class II morphogenesis. Cut has been known to function as a transcriptional repressor in other contexts (Nepveu, 2001), though we have not yet established that this repression is accomplished via direct regulation of the Pdm1 and Pdm2 promoters by Cut. Chromatin immunoprecipitation assays would be needed to determine if Cut binds directly to the Pdm1 and Pdm2 promoter regions to regulate their expression.

The tight correlation between ectopic Pdm1 and Pdm2 expression and the acquisition of the transformed phenotype suggests that unregulated expression of the Pdm

genes underlies the morphological switch towards a proprioceptive arbor in these cells. Pdm1 and Pdm2 are normally expressed in dmd1 and dbd, and the phenotypes of transformed *cut* mutants bear high resemblance to their wild type morphologies. Our findings that Pdm1 and Pdm2 are required in dmd1 and dbd for their characteristic morphologies (Chapter 1) also support this conclusion. Moreover, we show that Pdm1 and Pdm2 can strongly suppress dendrite outgrowth in md-da neurons, and severe reduction in overall arbor growth is a prominent feature of transformed neurons. Taken together we believe these data strongly support a role for Pdm1 and Pdm2 in mediating the transformation of dorsal *cut* mutant neurons. Analysis of dorsal md-da neurons that are mutant for *cut*, *pdm1* and *pdm2* will allow a definitive conclusion. If Pdm1 and Pdm2 are responsible for the transformation, then dorsal clones of such "triple mutants," should not show a transformation of their dendrites (or axons), but rather show a reduction in terminal branching that is similar to what is seen in ventral *cut* clones. An intermediate phenotype would suggest that additional factors are involved in the transformation, and examination of any differences between $cut^{-/-}$ alone and $cut^{-/-}$; $pdm1^{-/-}$, $pdm2^{-/-}$ phenotypes would pinpoint the specific contributions of Pdm misregulation to the transformation.

Pdm1 and Pdm2 are among the first targets of Cut that affect neuronal morphogenesis to be described. A recent study found that Cut positively regulates *turtle,* an Ig superfamily protein (Sulkowski et al., 2011); however, it remains unclear how endogenous regulation of *turtle* by Cut might contribute to class-specific morphogenesis *in vivo* since Cut is not required for *turtle* expression (Long et al., 2009; Sulkowski et al., 2011). Ectopic expression of Cut is capable of increasing *turtle* expression levels (Sulkowski et al., 2011) so that *turtle* might be a level-dependent target of Cut.

Dendrite morphogenesis of md-da neurons is shaped by positional cues and additional class-specific factors

Experiments described in this chapter provide evidence that morphology of md neurons is controlled by combinatorial expression of transcription factors that is in part determined by body wall position. Dendritic transformation upon loss of Cut is limited to a small subset of Cut-expressing cells, which is defined by two features—body wall position and da neuron class. In both wild type animals and in *cut* mutant animals, Pdm1 and Pdm2 expression is limited to neurons in the dorsal and lateral clusters. Moreover, in *cut* mutants, the likelihood of Pdm misregulation is strongest in the most dorsally located neuron (ddaF) with decreased penetrance in the lateral-most affected cell, ldaB. This suggests that body wall position influences Pdm1 and Pdm2 expression, and sensory neuron identity and morphogenesis in general. Cell body position as a determinant of neuronal fate is key concept in developmental biology, but it has not been studied in regards to the neurons in the *Drosophila* PNS and might represent a fruitful area for future investigation. The molecular mechanisms that restrict Pdm1/2 expression to dorsal PNS neuron are unknown. Transcription factors involved in the general dorsal-ventral axis specification of the embryo and ectoderm represent good candidates.

Position alone, however, cannot fully explain the restriction of ectopic Pdm1 and Pdm2 expression to the transformed neurons. ddaC, the dorsal class IV neuron expresses an intermediate level of Cut as compared to the class II and class III neurons, but complete loss of Cut never causes a dendritic transformation nor misregulation of Pdm1 or Pdm2 in this cell. Similarly class I neurons are always Cut-negative, but do not

express Pdm1 or Pdm2. This would suggest additional class or neuron-specific factors must be capable of regulating Pdm expression in sensory neurons. Overexpression of known class IV- (Knot) or class I- (Abrupt) specific transcription factors indicate that neither is sufficient to repress Pdm1 and Pdm2 in dbd or dmd1. Identification of additional class-specific transcription factors in class I and IV neurons may uncover additional positive or negative regulators of Pdm1 and Pdm2 that explain their limited expression pattern.

Transformed *cut* neurons show changes in axon projections that correspond to their altered dendrite features

Cut regulation of Pdm1/2 expression controls a switch between dendrite morphologies characteristic of da sensory neurons and those of proprioceptive neurons. Since the position of axon termination is correlated with sensory modality and peripheral morphology (Grueber et al., 2007; Merritt and Whitington, 1995; Murphey et al., 1989; Schrader and Merritt, 2000), we wondered whether these same genes might also control modality specific axonal targeting and thus help to coordinate dendrite and axon development.

Single cell analysis of *cut* mutant da neuron axons revealed that loss of Cut can affect the dorso-ventral positioning of axons, but only of those neurons with transformed dendritic arbors. Transformed cut mutant neurons send their axons to the dorsal neuropil, a region normally innervated by only proprioceptive afferents. The restriction of axonal changes to transformed neurons suggests that misexpression of Pdm1 and Pdm2, rather than loss of Cut, is playing the instructive role.

Previously, the role of Cut in specifying axon projections had only been studied in the context of es organ transformations caused by loss of Cut (Bodmer et al., 1987; Merritt et al., 1993). Cut mutant es neurons that transformed to a ch morphology in the periphery, showed incomplete transformation of axon projections centrally, suggesting that the role of Cut in determining central axon projections was limited (Merritt et al.). This is consistent with our data in which loss of Cut alone does not seem to affect the axon projections of many of the neurons it is normally expressed in. That Pdm expression may be instructive is supported by the findings that Pdm-expressing neurons have dorsal axon termination (Chapter 1; Schrader and Merritt, 2000) and that forced expression of Pdm2 in all sensory neurons can cause alterations in dorso-ventral axon patterning (Figure 2.6). In these experiments there is still evidence of axons projecting ventrally, suggesting that Pdm2 may not be sufficient to specify dorsal termination in all sensory neurons, or may have a limited role in doing this when Cut is still present. It also remains to be determined if Pdm1 and Pdm2 are required for the dorsal projections of dmd1 and dbd. If so, this would provide strong additional support for our hypothesis that Pdm1/2 play an instructive role in the dorsal termination of *cut* mutant neurons. Single cell analysis of the effects of Pdm1/2 gain and loss of function will allow definitive conclusions about the instructive roles of Pdm1 and Pdm2 in axon targeting.

Given the coordinate regulation of dendrite and axon morphology seen in Cut mutant neurons, one question that arises is whether loss of Cut and acquisition of Pdm1/2 expression constitutes a change in overall cell fate or causes more specific perturbations of neuronal morphology. A lack of independent molecular markers of cell fate in the class II, III, and dmd1/dbd neurons has hindered attempts to directly answer this question

experimentally, but these two possibilities need not be mutually exclusive. Both Cut and Pdm1/2 have well-established roles as cell fate determinants in other *Drosophila* neurons. Cut acts a switch between es and ch organ identity in the PNS (Bodmer et al., 1987; Merritt, 1993). In the CNS, Pdm1/2 act as temporal identity factors that specify fate of neurons in several lineages (Grosskortenhaus et al., 2006; Yeo et al., 1995). On the other hand, Cut also has an established role as a post-mitotic regulator of dendritic development, which is supported by its ability to alter dendrite morphology in postmitotic neurons (Grueber et al., 2003). Taken together, our results indicate that these genes might have dual roles. Cut and Pdm1/2 are expressed in their respective populations beginning in neuronal precursors, consistent with a cell fate role. However, the expression of these genes is maintained and required in post-mitotic neurons for normal morphology (evidenced by our analysis of mutant MARCM clones). Moreover, expression of these genes in postmitotic neurons is capable of significantly altering morphology in predictable ways suggesting that these transcription factors at least have the ability to control dendrite and axon morphogenesis separately from broader fate decisions. Dual early and late roles for transcription factors in specifying aspects of cell fate separate from control of morphological features has been described for other transcription factors including Dlx1/2, which can control cell fate specification of GABAergic interneurons separately from neuronal migration and morphogenesis (Anderson et al., 1997; Cobos et al., 2007; Cobos et al., 2006), and Ngn2, which has early roles in specifying cell fate that are separable from a later role in directing that acquisition of a unipolar pyramidal neuron morphology (Hand et al., 2005; Schuurmans et al., 2004). In the case of Ngn2, these separate functions require different

posttranslational modifications (Hand et al., 2005); in the case of Dlx1/2 changing expression levels over the course of development may play a role (Cobos et al., 2007; Cobos et al., 2006).

CONCLUSIONS

Nervous system function is dependent upon functional circuits, which requires each neuron within the circuit to develop the proper dendritic and axonal morphology. This is particularly true of primary sensory neurons with free nerve endings, as is the case in *Drosophila* md neurons, since the dendritic morphology of these neurons is likely to directly impart sensory input. Here, we have described an example of coordinated control of dendritic and axonal morphology of sensory neurons by Cut and Pdm transcription factors. In *cut* mutant neurons a switch from a tactile dendritic morphology towards a proprioceptive morphology is coupled to a corresponding shift in by its axon to terminate in a proprioceptive brain region. To date there have been only a few other examples of transcription factors that regulate both dendritic patterning and axonal morphology of the same neuron (Komiyama et al., 2003; Spletter et al., 2007), and in these cases it has not been clear that dendrite and axon changes have any correspondence, rather in these cases the axon perturbations are very limited leaving the majority of the arbor in its stereotyped position and pattern.

Our identification of a program in *Drosophila* sensory neurons that serves to match dendrite morphology with axon targeting suggests that may a useful mechanism to ensure that inputs and outputs are well matched, and leads to several additional questions. One possibility that we have not ruled out is that changes in either the dendrites or the axons are translated into corresponding changes in other end of the neuron by changes in

activity patterns. In the case of *cut* mutants, this possibility could be tested by examining the mutant dendrite and axon phenotypes in embryos to see if one precedes the other. Another question is how, on a molecular level, is coordinated control of axons and dendrites achieved? A major milestone in neural development is the breaking of symmetry and the specification of an axon as distinct from dendrites (Tahirovic and Bradke, 2009). Dendrites and axons develop at offset time points and in distinct environments that can be separated by several microns to almost a meter in some animals. Dendrites and axons also have distinct cytoskeletal organizations and cell biological properties(Satoh et al., 2008; Stone et al., 2008; Ye et al., 2007). Moreover, mature dendritic morphology in one neuron may consist of hundreds of branches while the axon of the same cell might be unbranched. Coordinated regulation might be achieved by using the same molecule(s) in both dendrites and axons. Another possibility is that there are separate dendrite and axon programs but their regulation by the same transcription factor ensures coordination of the final outcomes. The identification of downstream targets of Cut and Pdm transcription factors and determination of their roles in either axon or dendrite development (or both) will shed light on these questions.

Figure 2.1: Loss of Cut leads to severe stunting of dendrite growth in a defined population of md neurons

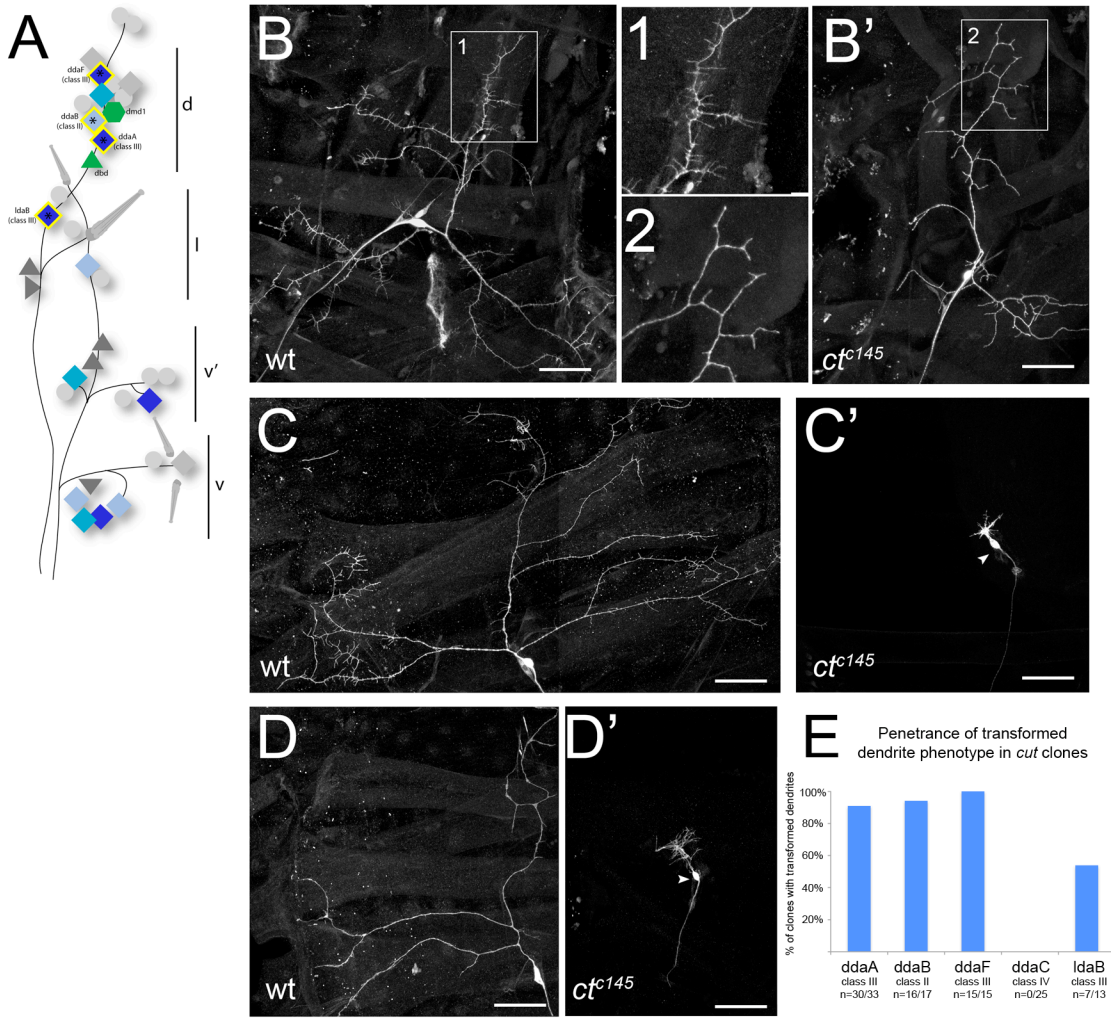

Figure 2.1: Loss of Cut leads to severe stunting of dendrite growth in a defined population of md neurons

(A) Schematic of PNS organization. Wild type Cut expression level is indicated by color—dark blue diamonds represent high Cut class III neurons, turquoise diamonds represent medium Cut class IV neurons, pale blue diamonds indicate low Cut class II cells. Green cells represent Pdm-expressing neurons. Cells outlined in yellow display severe morphological defects in *cut* mutants. Note that no cells ventral to the lateral cluster of any class are affected.

(B) In most cells, loss of cut results in specific alterations to terminal branching patterns. Wild type **(B)** and cut^{c145} **(B')** v'pda (ventral' class III) MARCM clones. Insets (1) and (2) provide a magnified view of single branches. The overall arbor scaffold is maintained in the mutant, but terminal branching is affected.

(C) Example of the transformed dendrite phenotype in a dorsal class III neuron. Wild type **(C)** and cut^{c145} **(C')** ddaF MARCM clones. Note the dramatic reduction in arbor growth between the wild type neuron and the mutant. This mutant ddaF neuron has just a short main dendrite with a small arborization at the distal tip.

(D) Example of the transformed dendrite phenotype in a dorsal class II neuron. Wild type **(D)** and cut^{c145} **(D')** ddaB (class II) neuron. Again, note the dramatic reduction in arbor growth between the wild type neuron and the mutant.

(E) Quantification of the penetrance for the transformed dendrite phenotype. This phenotype is highly penetrant in dorsal class II and III neurons and moderately penetrant in the lateral class III neuron, ldaB. The transformed dendrite phenotype is never seen in the dorsal class IV neuron, nor in any ventral class II or III neurons (not shown).

Arrowheads indicate cell bodies. Scale bars -50μm.

Figure 2.2: Transformed cut mutant clones show aberrant targeting of dendrites

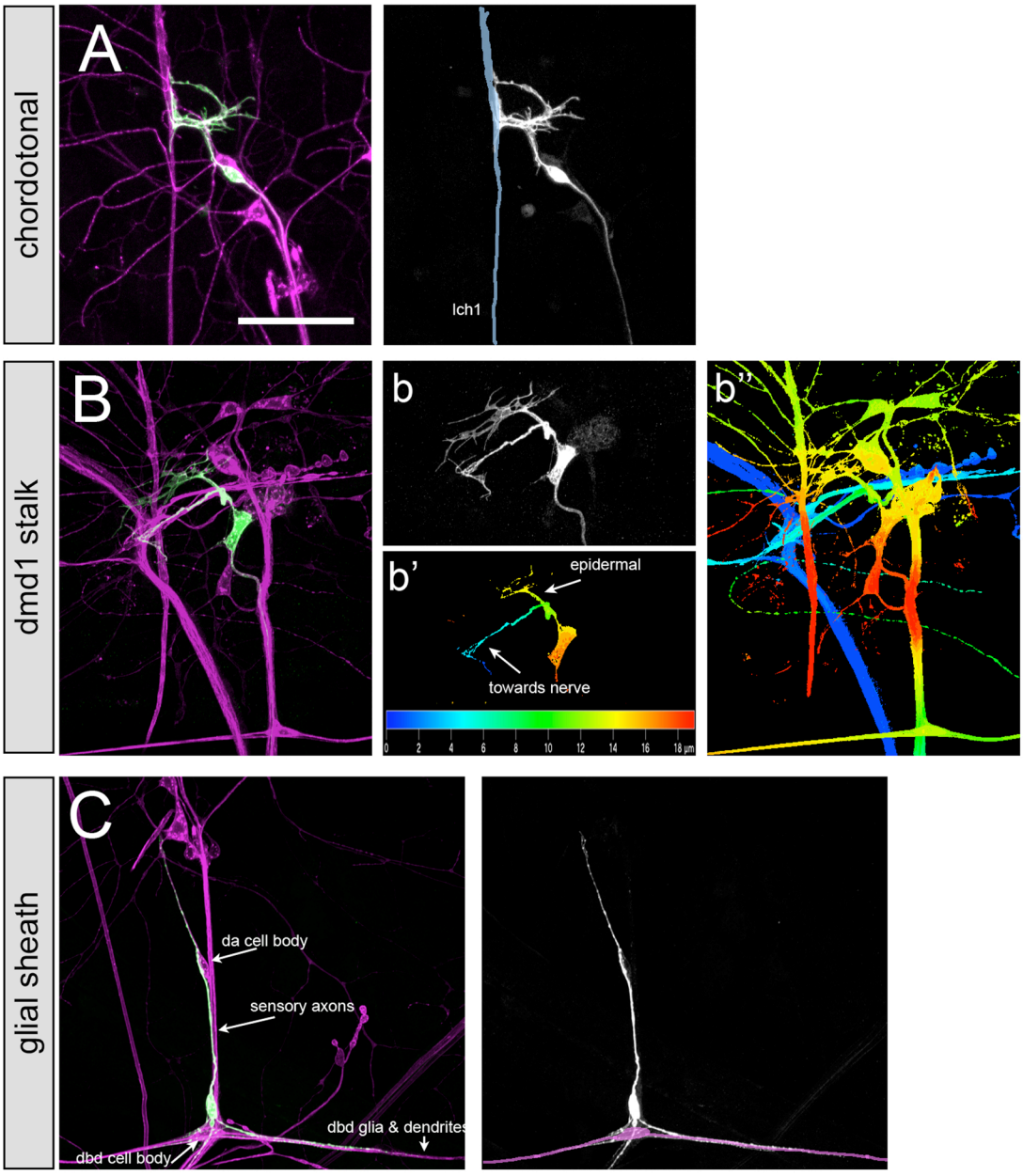

Figure 2.2: Transformed cut mutant clones show aberrant targeting of dendrites

(A) A subset of transformed neurons targeted the lch1 chordotonal organ. Left panel: Anti-HRP labeling of all neuronal membranes (magenta) with a ddaF clone labeled with GFP (green) shows the dendrites of ddaF targeting the lch1 chordotonal that lies just anterior to the dorsal cluster of sensory neurons. Right panel: trace of lch1 is superimposed on ddaF clone. 6/11 ddaF clones targeted lch1, while 1/26 ddaA clones and 1/9 ddaB clones targeted lch1.

(B) Another subset of transformed neurons displayed non-epidermal dendrite growth along the dmd1 stalk towards the ISN for some dendrites. Anti-HRP labeling of all neuronal membranes (magenta) with a ddaB clone. (b) Shows a major bifurcation of dendrites just dorsal to the cell body, in (b') that has been pseudo colored according to depth, it can be seen that the ventral branch grows away from the epidermal plane towards the "blue" level containing the ISN. (b'') shows the HRP channel is pseudo color to demonstrate the plane of the ISN nerve. Growth along the dmd1 stalk was observed in 4/26 ddaA clones, 4/9 ddaB clones, and 3/11 ddaF clones.

(C) A subset of transformed neurons confines its dendrites to the glial sheath surrounding sensory neuron cell bodies and axons. This ddaA mutant clone develops a bipolar like morphology sending one branch dorsally along the axons from nearby neurons. The posterior oriented branch grows along the dbd ensheathment. (Magenta trace in the right panel indicates the location of dbd.) Confinement to this sheath was observed primarily in ddaA clones with a penetrance of 5/26 clones.

Figure 2.3: Cut is required to repress the expression of Pdm1 and Pdm2 in transformed neurons.

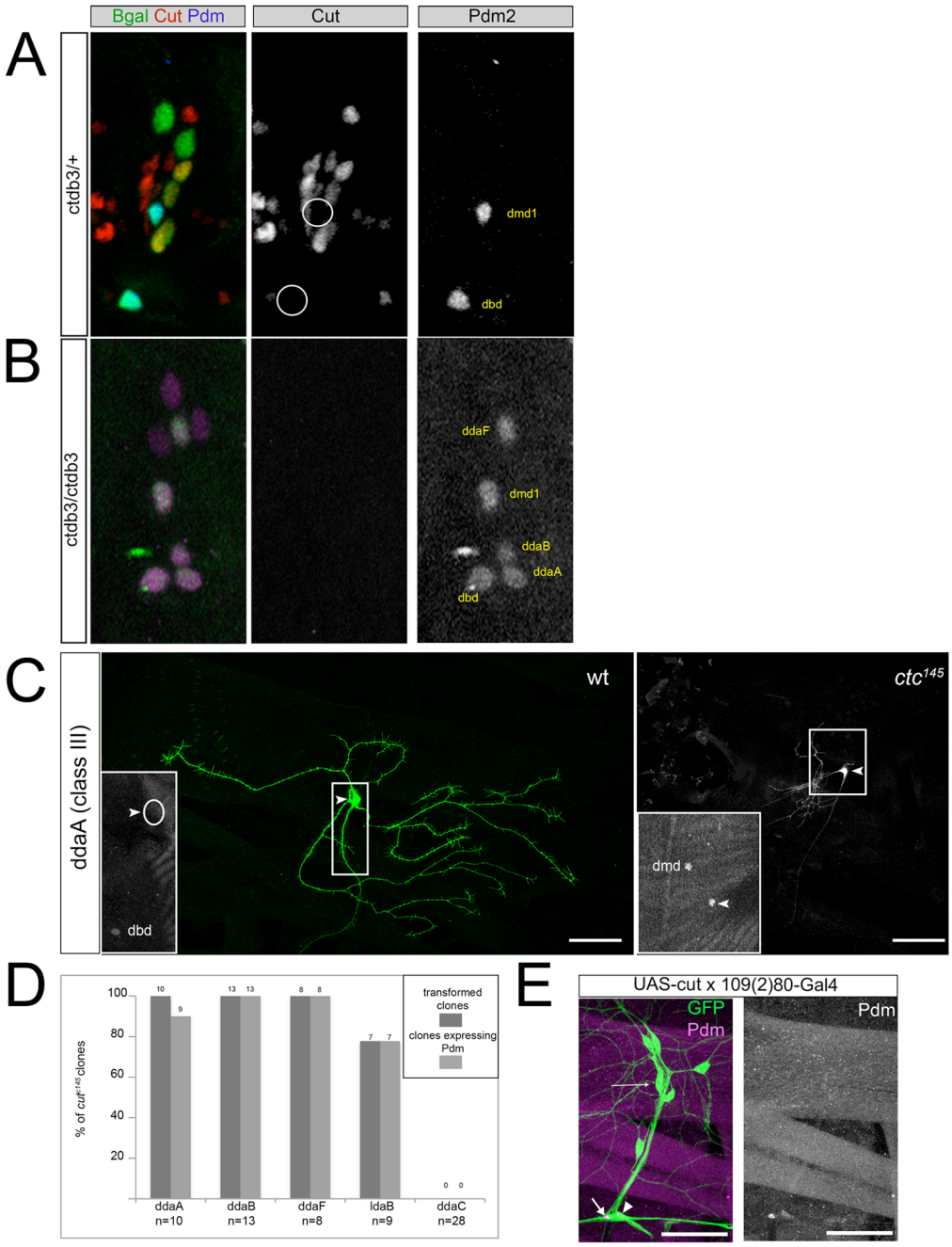

Figure 2.3: Cut is required to repress the expression of Pdm1 and Pdm2 in transformed neurons.

(A) Staining of embryonic dorsal cluster sensory neurons shows wild type Pdm2 expression in 2 dorsal cells. In cut^{+} embryos, Pdm2 (right panel) is expressed in just two dorsal neurons, dmd1 and dbd. These cells do not normally express Cut (middle panel). Md neurons are labeled with Bgal from the enhancer trap line E7-2-36.

(B) Staining of embryonic dorsal cluster sensory neurons of cut^{db3} mutant embryos shows expansion of Pdm2 expression. In cut^{-} embryos, Pdm2 expression in the dorsal cluster is expanded to an average of 4.5 neurons per dorsal cluster. (The predicted identities of these cells are indicated in the right panel.)

(C) Transformed neurons misexpress Pdm1 and Pdm2 transcription factors. A wild type ddaA clone in the left panel does not express Pdm2 (inset), but a cut mutant ddaA neurons does. Arrowheads indicate cell bodies of clones.

(D) Correlation of the transformed dendrite and Pdm misexpression phenotypes. When a cell is transformed by Cut mutation it almost always gains ectopic Pdm expression. Neurons that have not been transformed never ectopically express the protein. (This graph represents pooled data from clones stained with antibodies against Pdm1 or Pdm2.)

(E) Cut expression is sufficient to repress Pdm1 and Pdm2 expression in dmd1 and dbd. Expression of Cut in dmd1 and dbd using the pan-md driver *109(2)80-Gal4* eliminates Pdm staining of dmd1 and dbd nuclei using antibodies against Pdm1 (shown) or Pdm2 (data not shown). Note the absence of staining in the right hand panel. The remaining Pdm+ nucleus is that of the dbd glial cell. (Marked with a thick arrow in the left panel.)

Scale bars =50 μm

Figure 2.4: Overexpression of Pdm1 or Pdm2 inhibits dendrite growth in md-da neurons

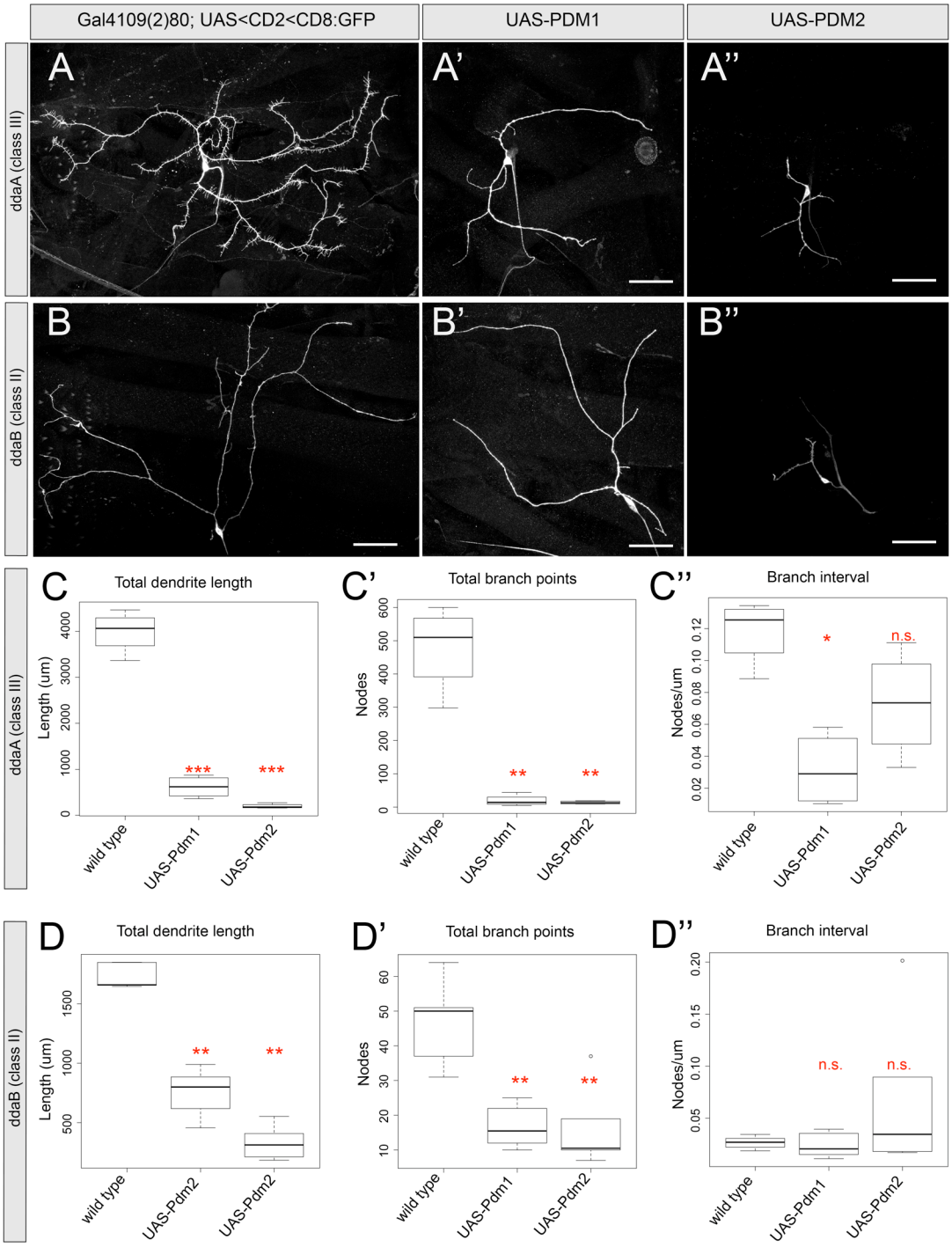

Figure 2.4: Overexpression of Pdm1 or Pdm2 inhibits dendrite growth in md-da neurons

A) Class III da neurons show dramatic reductions in dendrite growth when forced to express Pdm1 (A') or Pdm2 (A'').

B) Class II da neurons also show dramatic reductions in dendrite growth when forced to express Pdm1 (B') or Pdm2 (B'').

C) Quantification of overexpression phenotypes for class III neuron ddaA. (C) Total dendrite length is highly significantly reduced compared to wild type. (C') Total branch number also shows a significant reduction when Pdm1 or Pdm2 is overexpressed. (C'') The reduction in nodes per unit length is significant for UAS-Pdm1, but not for UAS-Pdm2 overexpression.

D) Quantification of overexpression phenotypes for class II neuron ddaB. (C) Total dendrite length is significantly reduced compared to wild type. (D') Total branch number also shows a significant reduction when Pdm1 or Pdm2 is overexpressed. (D'') However there is no reduction in nodes per unit length, suggesting that the primary effect of Pdm overexpression is to limit dendrite growth.

* = $p < 0.05$; ** = $p<0.01$; *** = $p < 0.001$

Figure 2.5: Transformed cut mutant neurons show dorsal termination of their axons.

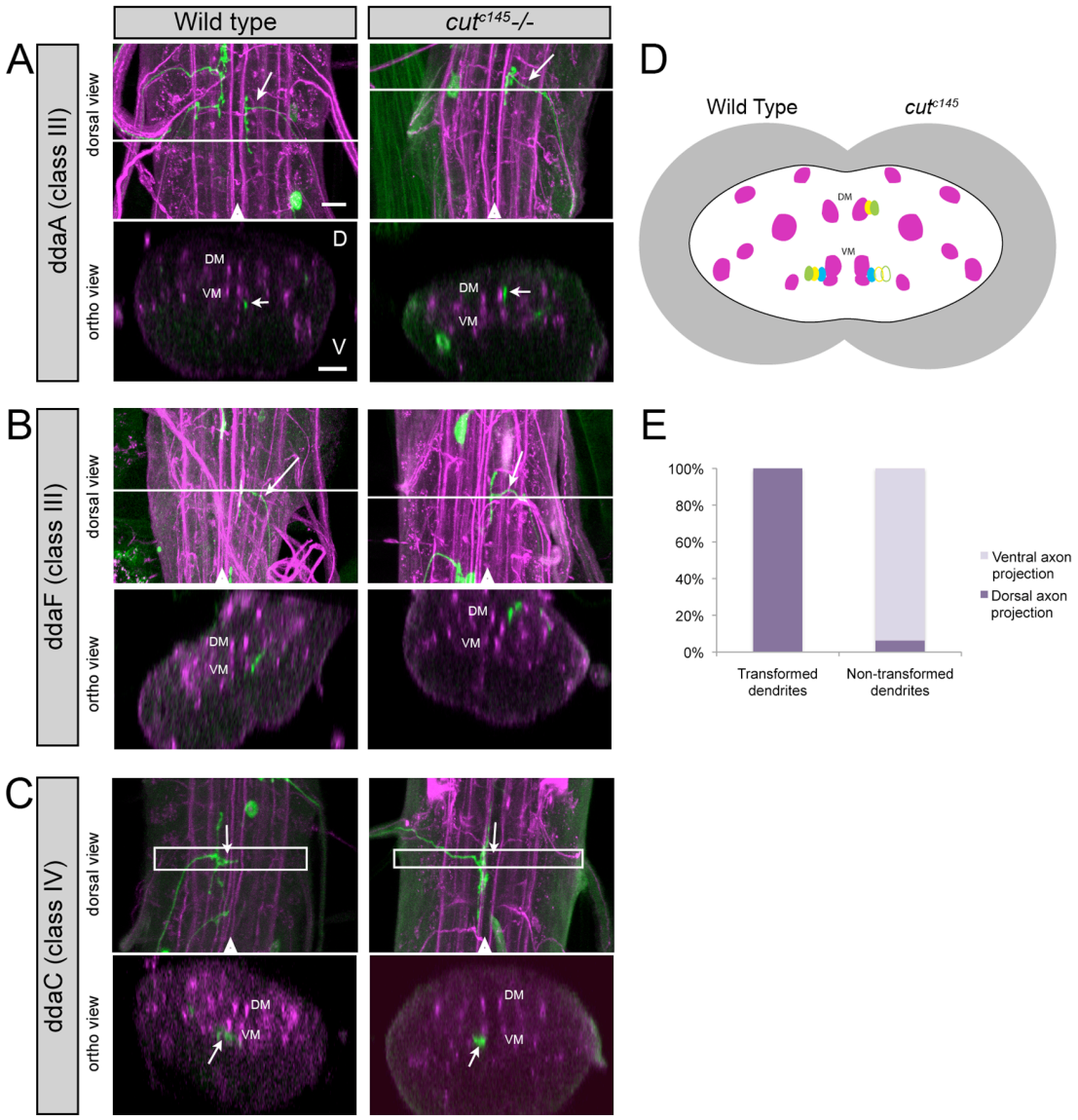

Figure 2.5: Transformed *cut* mutant neurons show dorsal termination of their axons.

(A) WT ddaA neurons typically project their axons to the VM fascicle (left panel, ortho view). Cut mutant ddaA axons terminate near the DM fascicle, arrow right panel ortho view.

(B) Transition to a dorsal termination alters overall trajectory of some cut mutant neurons. In this example the ortho views have been selected to show the trajectory of the axon as it approaches the midline. Wild type class II-IV neurons including ddaF have a ventral entry route. Most *cut* mutant neurons follow a similar path, turning dorsal upon reach the ventral midline, however a few mutant neurons entered along a consistently dorsal trajectory (left panel ortho view).

(C) DV positioning of non-transformed *cut* mutants is not affected, but midline crossing of class IV neurons is absent in *cut* mutant clones. In the dorsal view of the wild type ddaC axon an arrow marks the midline collateral. There is no similar collateral seen in the *cut* ddaC axon (arrow, dorsal view, left panel) the ortho views show that DV positioning of ddaC neurons is not changed. (ddaC neurons do not undergo dendritic transformations.)

(D) Schematic of the VNC showing the wild type (left side) and *cut* mutant (right side) location of dorsal cluster axons. Transformed class II (yellow) and transformed class (III) now terminate near the DM fascicle. (Wild type termination indicated with empty circles.)

(E) Summary of axon phenotypes. 100% (20/20) of *cut* clones with transformed dendrites displayed an abnormal dorsal termination of their axons, whereas only 6.25% (2/32) *cut* clones without transformed dendrites displayed an abnormal dorsal termination. The remaining non-transformed clones retained their wild type ventral terminations.

For all panels, a dorsal view of the VNC is provided in the top panel. Axons of MARCM clones are green (GFP) and Fas II tracts are magenta. The midline is labeled by a white triangle. A white line across the dorsal projection indicates the plane of the orthogonal view shown below. An arrow in the ortho views indicates the location of the relevant axon in the D-V axis.

Figure 2.6: Misexpression of Pdm2 in all sensory neurons causes alterations in sensory axon patterning in the VNC.

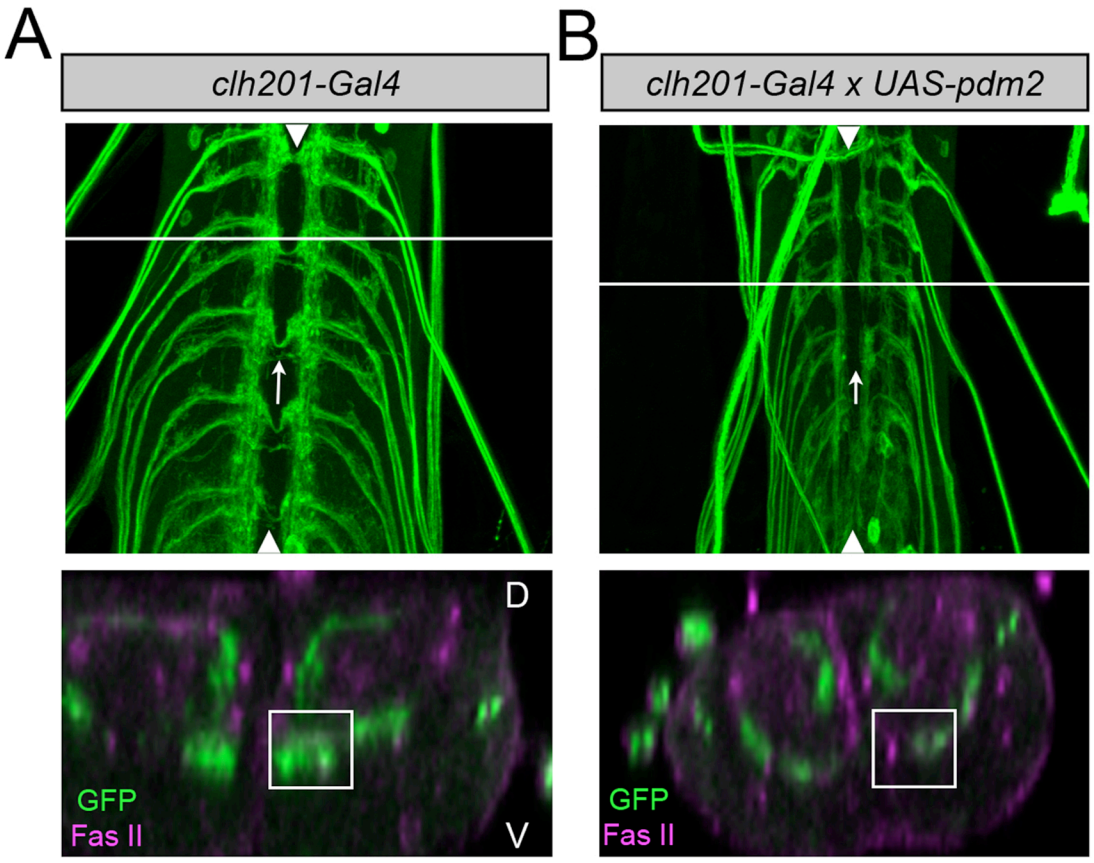

Figure 2.6: Misexpression of Pdm2 in all sensory neurons causes alterations in sensory axon patterning in the VNC.

(A) Sensory neuron axon projection pattern of wild type animals expressing GFP in all sensory neurons under the control of the *clh201-Gal4* driver. Arrow in the dorsal view points out the midline collaterals. The ortho view shows both dorsal and ventral terminations with abundant GFP labeling of the VM fascicle area at the level of the incoming dbd axon (which is recognized by virtue of the fact it is the only axon with a dorsal to dorsal trajectory.)

(B) Sensory neuron axon projection pattern of wild type animals expressing GFP and UAS-Pdm2 in all sensory neurons under the control of the *clh201-Gal4* driver. In the dorsal view several differences are seen. Midline crossing is reduced to being almost absent (arrow), and the medial fascicles are thinner. The ortho view shows evidence of both dorsal and ventral projections, but GFP is reduced in the VM quadrants marked by a box placed with its upper left hand corner at the VM fascicle. (Compare boxed areas in the ortho views of **A** and **B**). (Ortho view of *UAS-pdm2* condition also taken at the plane of an incoming dbd axon. This dorsal trajectory is seen in ortho view and was a criterion for scoring at the same position between conditions.)

Chapter 3

Molecular regulators of proprioceptive neuron morphogenesis

Abstract

Roles for intrinsic transcriptional programs in regulating dendritic and axonal development are well established in both vertebrate and invertebrate systems. *Drosophila* sensory neurons, in particular, have been a useful model system for identifying transcription factors that direct class-specific morphological features of neurons. Despite the identification of a wide variety transcription factors with specific influences on morphological development, the downstream targets that they regulate remain largely unknown; thus, it remains unclear how different transcriptional programs result in distinct morphologies. We have identified the Pdm1 and Pdm2 transcription factors as important regulators of proprioceptive neuron morphogenesis. We sought to identify genes that are regulated by Pdm1 and Pdm2 and that underlie the development of proprioceptive morphologies using two approaches. First, in a candidate-based approach we identified the Netrin receptor Frazzled and the cadherin family members N-cadherin and Flamingo as mediators of dmd1 dendrite morphogenesis. Second, we developed a strategy to isolate and profile *Drosophila* sensory neurons to identify targets of Pdm2 regulation. This strategy has resulted in the identification of more than 600 genes with altered expression levels after Pdm2 misexpression, which are being tested for contributions to neuronal morphogenesis. Our overexpression based profiling method has potential to be easily applied to other transcription factors that affect md neuron morphogenesis.

Introduction

Work described in previous chapters establishes roles for Pdm1/2 in regulating dendrite growth and axon targeting of proprioceptive sensory neurons. Similar roles in regulating class-specific dendrite development of sensory neurons have been reported for a handful of other transcription factors in *Drosophila* (Grueber et al., 2003; Jinushi-Nakao et al., 2007; Kim et al., 2006; Sugimura et al., 2004); however the target genes they regulate to affect dendrite growth and patterning are rarely identified, with only two such targets described to date (Jinushi-Nakao et al., 2007; Sulkowski et al., 2011).

I sought to identify the molecular regulators of proprioceptive neuron morphogenesis, particularly those that are downstream targets of Pdm1/2 regulation. In this chapter I first describe a candidate-based approach to identify guidance pathways and cell adhesion molecules that might be involved with the three dimensional growth and targeting of dmd1 dendrites. Through this approach I have identified Frazzled, the attractive Netrin receptor, as well as two members of the cadherin superfamily of cell adhesion molecules—the classical cadherin N-cadherin and the atypical cadherin Flamingo (Flybase: *Starry Night*)—as regulators of dendritic morphology. My data suggest that multiple partially redundant mechanisms direct the three-dimensional growth and targeting of dmd1 dendrites. Second, to identify novel regulators of morphogenesis and focus on genes regulated by Pdm1/2, I developed a gene-profiling approach for *Drosophila* md sensory neurons and used this approach to examine genes regulated by Pdm2 misexpression. This approach has identified ~300 candidate genes whose expression levels are altered at least 1.5-fold by Pdm2 misexpression. Among the regulated genes are several known to play roles in neuronal morphogenesis, as well as

genes that may be involved in neuronal function. The microarray analysis also identified numerous genes for which a role in neural development or function has not yet been established. Preliminary testing of a subset of candidate genes in also described.

Results

Frazzled-Netrin signaling contributes to dmd1 targeting fidelity

As described in Chapter 1, dmd1 dendrites consistently grow away from the epidermis to the second dorsal branch point of the ISN nerve, suggesting that there may be guidance mechanisms that underlie this targeting fidelity. Ligand-receptor pairs once primarily known for their roles in axon guidance have been increasingly implicated in dendrite growth and targeting as well (Furrer et al., 2003; Matthews and Grueber, 2011; Ou et al., 2008). The secreted axon guidance molecule Netrin is expressed in the dorsal muscle targets of ISN motor neurons, and attractive Netrin signaling is required for appropriate targeting of these axons to muscles (Kolodziej et al., 1996; Mitchell et al., 1996). Dmd1 dendrites target ISN precisely where these motor neurons are making Netrin-Frazzled based guidance decisions, prompting us to investigate whether Netrin-Frazzled attractive signaling might also contribute to dmd1 dendrite targeting to this location. To test this hypothesis we examined dmd1 neurons homozygous for null mutations of the *frazzled* (*fra*) gene, which encodes an attractive Netrin receptor (Kolodziej et al., 1996) using the MARCM method (Lee and Luo, 1999). We found that fra^3 dmd1 MARCM clones had partially penetrant defects in targeting and 3-dimensional dendrite growth, (n=5/9 clones with defects; Figure 1). Of the affected clones, some

failed to target ISN at all (n=2/9), while others targeted some dendrites to ISN, but had additional branches that grew away from the main stalk on the epidermis (n=3/9; Figure 3.1B, arrow). The remaining 4 clones had an essentially wild type appearance.

Frazzled acts primarily as an attractive receptor for secreted Netrin molecules during axon and dendritic guidance (Kolodziej et al., 1996). We examined dmd1 morphology in Netrin mutants to determine if Frazzled was acting with Netrin to mediate three-dimensional growth and targeting in dmd1 dendrites. Dmd1 morphology was observed in third instar animals lacking both *Drosophila* Netrin genes, *netrinA* and *netrinB* (Brankatschk and Dickson, 2006). Similar to the results from the *fra* clones, most dmd1 neurons targeted at least some dendrites to the ISN in *netAB* mutant animals (n=7). In these experiments, dmd1 was not individually labeled. The level of resolution afforded by HRP labeling limited our ability to visualize ectopic epidermal branching due to co-labeling of all other md sensory dendrites, but evidence of such branching could be discerned in at least a few segments (n=3/7; data not shown) indicating that *netAB* and *fra* phenotypes were comparable in terms of penetrance and severity. These data suggested that Frazzled mediated attractive Netrin signaling may represent one of several partially redundant pathways that contribute to three-dimensional dmd1 dendrite growth and proper dmd1 dendrite targeting.

Dmd1 dendrites require N-cadherin for proper targeting of dendrites off of the epidermis

Like all neurons, the development of dmd1 depends upon interactions between its dendrites and many other cells and structures—epidermal cells, glia cells, ECM, the ISN, muscles, etc. Cell surface molecules including cell adhesion molecules mediate such

interactions between cells and are thus potential regulators of dmd1 morphogenesis and targeting. We began our investigation of cell surface molecules by studying the role of the classical cadherin, N-cadherin (Flybase: *CadN*) in dmd1 development. N-cadherin is a conserved homophilic cell adhesion molecule with multiple roles in neuronal development, including several well-described roles in axon and dendrite development in flies and vertebrates (Iwai et al., 1997; Nern et al., 2008; Takeichi, 2007; Zhu and Luo, 2004). $CadN^{M19}$ MARCM clones of dmd1 showed partially penetrant defects in targeting, stalk cohesion, and ectopic epidermal dendrite growth. The majority of examined clones had at least some dendrites that appropriately targeted the ISN, but also had dendrites that grew on the epidermis or otherwise away from the main dendrite stalk (n=7/12); while smaller number of clones (n=3/12) completely failed to target the ISN, and did not have a cohesive dendrite stalk (Figure 3.2). These results suggest a role for N-cadherin in promoting dendrite-dendrite or dendrite-substrate interactions that are important for three-dimensional growth and targeting. A simple interpretation of the loss of function phenotype is that without N-cadherin, adhesive interactions are weakened allowing some branches to grow away from the main stalk and onto the epidermis.

The atypical cadherin Flamingo limits dendrite growth and promotes targeting in dmd1 dendrites

The incomplete penetrance of N-cadherin phenotypes suggested there might be additional adhesion molecules regulating interactions between dmd1 dendrites and their substrate and target. The atypical cadherin flamingo (*fmi* ;Flybase: Starry night) has roles in both axonal and dendritic development in a number of systems(Chen and Clandinin, 2008; Gao et al., 2000; Kimura et al., 2006; Reuter et al., 2003; Steimel et al., 2010;

Steinel and Whitington, 2009; Sweeney et al., 2002). Flamingo is expressed in md sensory neurons where it has been shown to play a role in restricting class IV md dendrite growth and promoting the outgrowth of dorsal sensory neuron axons (Gao et al., 2000; Grueber et al., 2007; Steinel and Whitington, 2009). We asked whether fmi might play a role in dmd1 neurons by examining *fmi* mutant dmd1 neurons using the MARCM method (Lee and Luo, 1999). All fmi^{3} clones were able to send some dendrites to the ISN, however I observed a range of abnormalities suggesting a role for *fmi* in dmd1 morphogenesis. These abnormalities fell into three categories, with some neurons showing combinations of defects. The majority of dmd1 *fmi* clones showed substantial epidermal dendrite growth, most often emerging from a proximal region of the stalk (n=6/13; Figure 3.3D), which was similar to what was seen in both *cadN* and some *fra* clones, or directly from the cell body. In a subset of clones the dendrite stalk appeared abnormally thin (n=2/13; Figure 3.3E) or less cohesive with individual dendrites readily distinguishable (n=3/13; Figure 3.3C). In addition, several of the *fmi* dmd1 clones (n=7/13) also showed increased dendrite growth at the ISN target, as compared to wild type (Figure 3.3C-E). Together these data are consistent with cell autonomous roles for fmi in limiting dendrite growth while promoting targeting and cohesion of dendrites in dmd1.

Misexpression of Pdm2 in sensory neurons causes reduced dendrite growth at embryonic stages

I next focused specifically on identifying genes regulated by Pdm1/2 that affect morphogenesis. To identify the genes likely to be regulated by Pdm2, I developed a protocol for FACS isolation and microarray gene profiling of *Drosophila* sensory

neurons misexpressing Pdm2. I reasoned that this approach might identify important regulators of dendrite outgrowth that are modulated by the Pdm1/2 transcription factors (Chapter 2).

To purify sensory neurons, I took advantage of the GAL4-UAS based expression system to drive GFP in embryonic sensory neurons. Whole animals could then be dissociated and Fluorescent Activated Cell Sorting (FACS) could be used to obtain pools of purified GFP+ neurons to profile (Figure 3.4E). This approach also allows for misexpression of a transgene, such as Pdm2, in addition to GFP to generate different populations for gene expression comparisons.

The pan-sensory *clh201-Gal4* driver (Hughes and Thomas, 2007) was selected for these experiments due to strong, early expression in PNS neurons with minimal expression in other tissues including the CNS and glia (Figure 3.4C). I verified that this Gal4 driver would produce similar phenotypes to what we had seen in earlier misexpression experiments using the more broadly expressing *109(2)80-Gal4* driver described in Chapter 2. Using *clh201-Gal4* to drive *UAS-Pdm2* expression resulted in severely reduced dendritic arbors (Figure 3.4C-D), similar to the dramatic undergrowth seen using the *109(2)80-Gal4* driver used in earlier experiments. The reduction in dendritic growth using *clh201-Gal4* appeared to be stronger than with *109(2)80-Gal4*; and two clear differences between the drivers are worth noting. First, although still remaining severely stunted overall, dendrites from all classes in the experiments using *clh201-Gal4* had numerous short branches that were not as prevalent in the *109(2)80* FLPout experiments (Figure 3.4D, arrows). In addition, class I neurons were not stunted by *UAS-Pdm2* expression with *109(2)80-Gal4*, actually showing a slight overgrowth

(data not shown). In contrast, class I arbors were clearly reduced in the *clh201-Gal4* experiments, showing the same numerous short branches as the other classes (Figure 3.4D). It is likely these differences are due to differences in the onset of expression or strength of the drivers.

To determine which stage of neurons could be used for profiling experiments, I determined the timing of the onset of the Pdm2 misexpression phenotype by examining dendrite growth in live embryos. Compared to controls expressing only GFP, embryos misexpressing Pdm2 already showed clear reductions of dendrite outgrowth by 15-17 hours AEL (Figure 3.4A-B). These results indicated that sensory neurons harvested at this stage should already have changes in their gene expression profiles caused by Pdm2 misexpression that are affecting dendrite outgrow. In addition, these results also rule out the possibility that the reduced dendrites observed when Pdm1 or Pdm2 is misexpressed is due a dendrite maintenance defect and support our previous conclusions that Pdm1/2 misexpression causes a growth defect.

Drosophila embryonic sensory neurons can be purified via FACS

I wanted to obtain purified populations of sensory neurons for profiling to ensure that the different conditions we were comparing differed only in ectopic Pdm2 expression, as well as to identify the targets of Pdm2 most relevant to neuronal morphogenesis. *Clh201-Gal4, UAS-mCD8:GFP* virgins were mated to either w^{1118} or *UAS-Pdm2* males to produce embryos that expressed either GFP alone or GFP and Pdm2 in sensory neurons. Embryos from 2 hour laying windows were harvested at ~15-17 AEL and mechanically dissociated. The resulting cells were sorted using FACS to purify

GFP-expressing sensory neurons. GFP+ cells typically made up about ~2% of the suspension yielding purified 50,000-100,000 neurons per sample from which to harvest RNA.

Our recovery of total RNA was in the range of 30-50ng per sample, necessitating amplification. Linear amplification of mRNA and conversion to cDNA was performed using commercial kits (NuGene) to yield 4-5μg labeled cDNA for hybridization onto Drosophila 2.0 microarrays (Affymetrix) (Figure 3.4E).

Changes in gene expression between wild type and Pdm1-expressing sensory neurons

To identify candidates downstream of Pdm2, labeled cDNA made from three biological replicates of each condition was hybridized to Drosophila 2.0 whole genome microarrays (Affymetrix). Raw data was analyzed using GeneSpring 2.0 software (Agilent). Pooled analysis of the six arrays identified 658 probe sets that showed significantly different expression levels between conditions ($p<0.05$ unpaired t-test without multi-sample correction). Of these, ~300 showed fold changes greater than 1.5, and 157 showed at least a 2-fold change in expression between conditions.

As predicted, *pdm2* was highly upregulated (14.2-fold) in neurons from *clh201-Gal4, UAS-mCD8:GFP/UAS-pdm2* embryos when compared to control neurons. This large fold change likely arises from the small percentage of neurons in the control group that express the gene compared to 100% of the neurons in the misexpression condition, along with robust expression induced by the artificial Gal4-UAS system.

A wide variety of molecules were amongst the regulated genes including regulators of the actin and microtubule cytoskeletons, transcription factors, and

components of signaling pathways (Table 1). Among these are a number of genes with known roles in neuronal morphogenesis including tumbleweed/RacGAP50C (Gao et al., 1999; Goldstein et al., 2005), longitudinals lacking (Spletter et al., 2007); and fzy/cdc20 (Kim et al., 2009).

In addition to identifying numerous genes that might play a role in morphogenesis, these profiling experiments also revealed regulation of several genes that might contribute to neuronal or sensory function including ion channels, hormone receptors, and G-protein coupled receptors by Pdm2 (Table 1). These results point to a role for Pdm transcription factors in coordinating neuronal morphology with other aspects of neuronal identity and function. The gene with the highest fold-change was *ppk20*, a degenerin/epithelial sodium channel in the pickpocket family, which was 117-fold up-regulated when Pdm2 was misexpressed. The function of this channel has not been studied but family members have been implicated in processes such as nociception (ppk; Zhong et al., 2010), crawling (Ainsley et al., 2003), water sensation (ppk28; Chen et al., 2010); salt taste (ppk11 and ppk19; Liu et al., 2003b) and water regulation (ppk4 and ppk11; Liu et al., 2003a). In situ hybridization for *ppk20* in wild type embryos indicated that it is expressed in cells of either the terminal organ or dorsal organ which contain the larval gustatory and olfactory neurons, respectively (data not shown), but no apparent labeling of any body wall PNS neurons. *Nub-Gal4* drives expression in ~2-4 sensory neurons in the larval head, pointing to Pdm2 as a specific and positive regulator for ppk20 in larval gustatory or olfactory neurons.

GO analysis indicated that genes involved in cell cycle regulation and mitosis were highly represented amongst the regulated genes. Genes in this category were almost

invariably upregulated (Table 1). Despite this strong upregulation of cell cycle regulators, we saw no evidence for increased or absent neurons in embryos or third instar animals overexpressing Pdm2, suggesting that these genes may have additional roles in post-mitotic neurons. Indeed, expression of cell cycle genes has been reported in vertebrate post-mitotic neurons, and several recent studies have uncovered novel roles these genes in controlling neuronal morphogenesis (Huang et al., 2005; Kim et al., 2009; Stegmuller et al., 2006). Study of this group of regulated genes could expand our understanding of the how genes that regulate cell proliferation are "reused" during neuronal morphogenesis.

Overall, the majority of regulated genes have no known roles in morphogenesis, with nearly half of the probe sets with a 1.5-fold or greater change representing annotated genes of unknown function. Study of these genes may lead to the identification of novel regulators of dendrite and axon morphogenesis.

Screening of candidate genes for roles in dendrite morphogenesis

Based on the Pdm1/2 overexpression phenotypes, we can make predictions about how candidate genes might function in proprioceptive neuron morphogenesis and/or general dendrite growth. Genes upregulated by Pdm2 are expected to promote proprioceptive neuron features and/or limit dendrite growth. Genes downregulated by Pdm2 are expected to promote epidermal arborization and/or increase dendrite growth. Using primarily loss-of-function experiments, I have performed initial screening of several regulated genes identified by the arrays. So far I have tested 24 candidates for dendrite phenotypes with either UAS-RNAi constructs to knockdown gene expression (Dietzl et al., 2007, Vienna Drosophila RNAi Center; Transgenic RNAi Project) or

mutant analysis using MARCM (Lee and Luo, 1999). Five candidates have been tested using overexpression-based assays. Thus far, I have screened only for dendrite phenotypes. The results of this analysis are listed in Table 1.

Discussion

In this chapter we have described both candidate-based and unbiased approaches to discover the molecular mediators of proprioceptive neuron morphogenesis. Our candidate-based approach has implicated Frazzled signaling and cell adhesion molecules in shaping the dendritic arbor of the dmd1 stretch receptor neuron. The precise mechanisms by which these molecules shape dendrite and axon morphology in general are still not understood, and our studies of dmd1 provide new insights. By developing a strategy to profile md sensory neurons, we have identified hundreds of genes that are likely to be regulated by Pdm2 and may play important roles in neuronal morphogenesis and/or function. Moreover, having a fairly comprehensive list of Pdm's downstream targets will hopefully allow us to identify multiple genes that each control specific aspects of dmd1 morphology and study how they act in conjunction with one another to shape the final arbor. Our over-expression based approach has the advantage of allowing for the discovery of novel regulators of dendritic growth that operate across classes, as misexpression of Pdm2 in other neuron types leads to a dramatic and robust reduction in overall dendrite growth.

Frazzled signaling contributes to dmd1 dendrite targeting

Growing axons and dendrites navigate their surroundings using combinations of guidance cues, receptors, and cell surface molecules. The secreted ligand Netrin and its

receptor Frazzled/DCC/Unc-40 are known to mediate attraction of axons and dendrites in many systems (Brierley et al., 2009; Furrer et al., 2003; Kolodziej et al., 1996; Matthews et al., 2011; Mauss et al., 2009; Mitchell et al, 1996). We found that *fra* mutant dmd1 neurons often fail to completely target the second ISN branch point with some dendrites growing instead on the epidermis. Similarly, we found some evidence of incomplete targeting of dmd1 dendrites in *netAB* mutant animals. The source of Netrins is likely to be dorsal muscle 2, which expresses both NetA and NetB during embryogenesis to attract axons from the ISN to branch away from the nerve to form synapses on this muscle (Kolodziej et al., 1996; Mitchell et al., 1996). Taken together these data suggest that attractive Netrin signaling between dmd1 dendrites and ISN target muscles may be contributing to the directed growth of dmd1 dendrites to their ISN target, but this attractive signaling is likely functioning in concert with other molecules that act in a partially redundant fashion. Our data raise the intriguing possibility that dmd1 dendrites and ISN axons might be guided to a common location by means of the same attractants/repellants. Errors in motor axon targeting of dorsal muscles in *net* and *fra* mutants also showed partially penetrant phenotypes, later shown to be due to partially redundant functions of SemaphorinII and FasII in axonal targeting to these muscles (Winberg et al., 1998). SemaII, FasII and other cell adhesion and targeting molecules that have been implicated in motor axon targeting of dorsal muscles represent good candidates for further study of dmd1 dendrite targeting.

N-cadherin is required for dmd1 dendrite development

Dmd1 neurons lacking N-cadherin have defects in targeting and aberrant epidermal dendrite growth. These data are consistent with a model in which N-cadherin

mediates adhesive interactions between dmd1 sister dendrites or between dmd1 dendrites and their connective tissue substrate. When N-cadherin is removed from the neuron these interactions would be weakened, allowing for some dendrites to grow away from the stalk and onto epidermis.

Our results are bear some resemblance to those that seen in *Ncad*$^{-/-}$ olfactory projection neuron (PN) dendrites. These PN dendrites can target correctly but fail to refine their dendritic projections and restrict their dendrites to one glomerulus so that some of their dendrites target inappropriate glomeruli (Zhu and Luo, 2004). In PNs this defect is not due to a lack of interactions between dendrites and their targets, because N-cadherin is not required in target cells. Conversely, wild type PNs adjacent to *Ncad*$^{-/-}$ PNs show similar defects in refinement suggesting that interactions with neighboring dendrites are mediated by N-cad to refine dendrite projections (Zhu and Luo, 2004). If N-cad functions similarly in dmd1 dendrites, interactions between dmd1 sister dendrites might be important to prohibit ectopic epidermal growth and support cohesion of the dendrite stalk.

It remains equally possible that N-cad mediates interactions between dmd1 dendrites and its substrate. For this to be true, N-cadherin should be expressed in the dmd1 substrate. N-cadherin expression in the periphery has not been extensively studied, but in embryos, N-cadherin is expressed in mesoderm as well as neurons (Iwai et al., 1997). The connective tissue substrate of dmd1 may be derived from mesodermal origins (Edwards et al., 1993), so this expression pattern would be consistent with expression in both dmd1 and its substrate during development. The most straightforward way of distinguishing between these possibilities would be to compare loss of N-cad in dmd1 to

loss of N-cad in the substrate. If loss of N-cad in the substrate fails to reproduce the phenotype it would suggest that N-cad primarily mediates dendrite-dendrite interactions. Determining the precise identity of the dmd1 substrate and support cells will be critical to performing such experiments.

Preliminary experiments to overexpress N-cadherin in md neurons did not cause ectopic targeting of dendrites to the dmd1 substrate nor fasciculation of sister dendrites (data not shown), suggesting that expression of N-cadherin in neurons is not sufficient to dictate substrate preference or dendrite-dendrite adhesion in other md neurons. This may be due to lack of specific isoforms required to mediate adhesion to the dmd1 substrate.

In addition to acting as a homophilic adhesion molecule, N-cadherin also functions as a signaling molecule. Analysis of the expression pattern have N-cadherin isoforms, as well as alpha and beta catenin (which mediate signaling downstream of N-cadherin) and D-Lar (which modulates N-cadherin signaling (Clandinin et al., 2001; Dunah et al., 2005; Kypta et al., 1996)) will help to elucidate the precise molecular function of N-cadherin in dmd1 morphogenesis.

Flamingo is required to suppress dendrite growth and ensure targeting of all dmd1 dendrites

The atypical cadherin flamingo has a complex molecular structure consisting of both extracellular cadherin domains that allow it to participate in homophilic binding, as well as a 7-pass transmembrane domain and C-terminal tail capable of mediating signaling (Usui et al., 1999). Depending on the context, flamingo can function strictly as an adhesion molecule, or as a mediator of signaling downstream of either homophilic

interactions or as a receptor for an unknown ligand. Likewise, the functions of flamingo in different cell types are diverse. In the nervous system Flamingo is capable of regulating both dendrite and axon growth and targeting (Chen and Clandinin, 2008; Gao et al., 2000; Hakeda-Suzuki et al., 2011; Steimel et al., 2010; Steinel and Whitington, 2009; Sweeney et al., 2002).

We found that Flamingo is required for normal dendrite morphogenesis of dmd1 neurons. Dmd1 neurons lacking Flamingo show aberrant epidermal dendrite growth and reduced cohesion of their dendrite stalk—sometimes managing to send only one dendrite to the ISN target. In addition these mutant neurons were overgrown at their target. These data suggest that flamingo plays one or more important cell autonomous roles during dmd1 morphogenesis; the simplest model being that homophilic interactions between dmd1 dendrites between dendrites and their connective tissue substrate are needed to ensure three-dimensional growth and targeting. A similar role was recently described for the *C. elegans* flamingo homolog, FMI-1, in mediating guidance of follower axons. In *C. elegans* a number of axons are guided to their targets by following the route of a pioneer axon, a process that is dependent upon the extracellular homophilic binding domains of FMI-1 (Steimel et al., 2010). Such a model fits our findings well—though some dendrites continue to target properly, many sister dendrites do not associate with the stalk. This suggests that dmd1 targeting might be accomplished via a pioneer dendrite that is then used as a substrate for additional dendrites to follow. This model could presumably be tested with time-lapse imaging of developing dmd1 neurons.

Flamingo can also function as a signaling molecule independent of its ability to mediate adhesion (e.g. the pioneer axons of (Steimel et al., 2010; Steinel and Whitington,

2009) Thus, an alternative hypothesis is that Flamingo functions as a receptor to mediate signaling interactions between dmd1 dendrites and their substrate or target. To test these alternatives it will be important to determine what flamingo domains are required for proper growth and targeting, which can be determined using rescue constructs lacking either the extracellular cadherin or intracellular signaling domains. Live-imaging of dmd1 development to determine the behavior of nascent dendrites might also provide insight—for example in determining whether there is a pioneer dendrite and if initial outgrowth of dendrites is directed toward the muscle later or rather is pruned back from an initial innervation of the epidermis.

Model for the combinatorial effects of guidance signaling and preferential adhesion in shaping the dmd1 arbor

All of the candidates discussed thus far had related, but specific effects on dmd1 dendrite morphology suggesting they may play partially redundant roles during dmd1 dendrite development. One common defect was the presence of epidermal dendrite growth. This suggests a model in which dmd1 dendrite stalk cohesion and non-epidermal growth is likely the result of a strong preference for a connective tissue substrate over the epidermis. In this model, in wild type dmd1 neurons multiple cues and cell surface molecules including those I have identified support attraction and/or adhesion to connective tissue or the ISN target that outweigh the relative balance of stabilizing or attractive factors found in the epidermis/epidermal ECM. Thus the dendrites choose to grow along the connective tissue towards a Netrin source. When one of the stabilizing or attractive forces is lost, the balance is perturbed and some dendrites find the epidermis a

more or equally attractive substrate and grow there instead. For example, dendrites may still show an adhesive preference to connective tissue, but lacking a strong attraction away from the epidermis, some dendrites never contact the connective tissue and instead innervate the epidermis. This model implies that dmd1 (and likely dbd) neurons express different levels or types of cell surface adhesion molecules and receptors as compared to neurons whose dendrites innervate the epidermis.

Identification of genes regulated by Pdm2 in Drosophila sensory neurons

Gene expression profiling of purified neurons has allowed for the identification of transcription factor targets important for neuronal morphogenesis in many studies of vertebrate neurons (e.g. Cobos et al., 2007; Lai et al., 2011; Simon-Areces et al., 2011). Profiling of *Drosophila* sensory neurons to identify targets of transcription factors implicated in neuronal morphogenesis has not been described in the literature. Correspondingly, only one target of a transcription factor known to regulate class-specific dendrite morphology had been identified (Jinushi-Nakao et al., 2007) when we undertook this approach. Our gene-profiling approach has generated a list of nearly 300 candidate genes regulated by Pdm2 that can be tested for effects on class-specific neuronal morphogenesis and function, as well as for basic control of dendrite outgrowth.

The identified regulated genes include known regulators of morphogenesis as well as many genes with no known function in neuronal development. One intriguing finding is the high representation of genes involved in cell cycle regulation and mitosis that were upregulated by Pdm2, seemingly without consequences for cell proliferation. It has been known for some time that several such genes are expressed in postmitotic neurons, and in

recent years there have been findings that these genes have roles in neural development aside from regulation of proliferation (Becker and Bonni, 2005; Huang et al., 2005; Kim et al., 2009). The md neurons will be a useful system in which to evaluate the effects of these genes on neuronal morphogenesis using mosaic techniques such as MARCM to bypass defects in proliferation and focus solely on the post mitotic roles of such genes during morphogenesis.

None of the three genes implicated in mediating preference for non-epidermal growth (*fra*, *CadN*, and *fmi*) were identified in the microarray analysis. Although this may indicate that these genes are not regulated by Pdm2, omission of these molecules may indicate a false-negative resulting from profiling a mixed neuron population overexpressing of Pdm2 rather than comparing wt dmd1 neurons to *pdm-* dmd1 neurons. Flamingo is expressed in all PNS neurons at embryonic stages (Gao et al., 2000), and recent studies in our lab indicate that frazzled is expressed by at least some class III md neurons (Matthews and Grueber, 2011). Heterogeneity in expression levels among included neuronal subtypes may mask changes in levels when looked at across a broad population of cells. We know this to be true for at least one other gene. Misexpression of Pdm1 or Pdm2 can robustly repress expression of the *ppk* locus (M. Corty, personal observation), but *ppk* did not show significant differences in expression in the array. We attribute this to the fact that *ppk* is only being regulated in class IV neurons and therefore might be at such low expression levels in both conditions as to escape detection of a significant difference in levels.) Assaying expression levels of *fra*, *Ncad*, and *fmi* via qPCR or antibody staining in Pdm loss and gain of function conditions will be needed to

determine whether these genes are in fact downstream targets of Pdm regulation in dmd1 and/or dbd neurons.

In addition to identifying candidate regulators of morphogenesis, our profiling experiments revealed that several genes likely to shape the functional properties of neurons are regulated by Pdm2. In addition to the positively regulated ppk20 channel described above, Pdm2 negatively regulates the TrpA1 cation channel implicated in temperature sensation (4.2-fold downregulated) and the Gr28b G-protein coupled receptor implicated in light sensation in class IV neurons (4.3-fold downregulated). In addition, we have previously determined that Pdm1 and Pdm2 can act as potent negative regulators of ppk expression in class IV md neurons (Chapter 2). These findings suggest that an important function of Pdm1 and Pdm2 in proprioceptive neurons is to ensure proper sensory function by limiting the expression of channels or receptors that mediate different sensory modalities. The identification of multiple class-IV specific genes that are repressed by Pdm1/2 is intriguing, but the biological relevance of class IV feature suppression remains unclear. Examining Pdm1/2 mutant dmd1 and dbd for class IV specific markers would indicate an endogenous role for these transcription factors to suppress class IV features in dmd1 and dbd. Of particular interest would be determining whether the class IV specific transcription factor Knot is regulated by Pdm. (We have already determined that Knot cannot suppress Pdm expression (Chapter 2).) Knot regulates many features of class-IV neurons including positively regulating the ppk locus (Jinushi-Nakao et al., 2007), and thus could represent a direct target of Pdm-regulation that leads to the suppression of ppk expression. It is not yet understood how Knot expression is restricted to class IV neurons, so such findings could extend our

understanding of how interactions between transcription factors establish and maintain class-specific expression in md neurons.

Our results establish a method to identify downstream target genes of transcription factors that regulate neuronal morphogenesis in *Drosophila* sensory neurons. Over-expression based comparative profiling of sensory neurons can be easily applied to other transcription factors known to regulate md neuron morphogenesis such as Cut and Knot which cause specific and consistent overexpression effects in other md neurons (Grueber et al., 2003; Jinushi-Nakao et al., 2007). Furthermore, FACS-based isolation and sorting could also be used to obtain purified populations of md neuron subclasses, using appropriate Gal4 driver lines to facilitate comparisons of gene expression between distinct morphological classes.

Our profiling experiments have provided a set of genes to investigate the molecular basis of proprioceptive neuron development, under the control of Pdm1/2 transcription factors. Future experiments include continued evaluation of candidates for roles in neural development and function, as well as further validation of candidate expression patterns. These gene-profiling results form the basis for a comprehensive study of the genes and molecules that interact to produce a specific neuronal morphology. The rich candidate pool identified indicates that there may several novel regulators of dendrite and axon growth and patterning that will enhance our understanding of how these fundamental processes are controlled during neural development. Several of the genes identified in the array, as well as Pdm1 and Pdm2, have vertebrate homologs, some of which are implicated in neurodegenerative diseases (e.g. such as Npc2f). Thus, findings from studies described in this chapter will hopefully identify molecules and

mechanisms that control morphogenesis in a variety of systems and inform our understanding of both development and disease.

Figure 3.1: Frazzled mutant dmd1 clones show defects in targeting

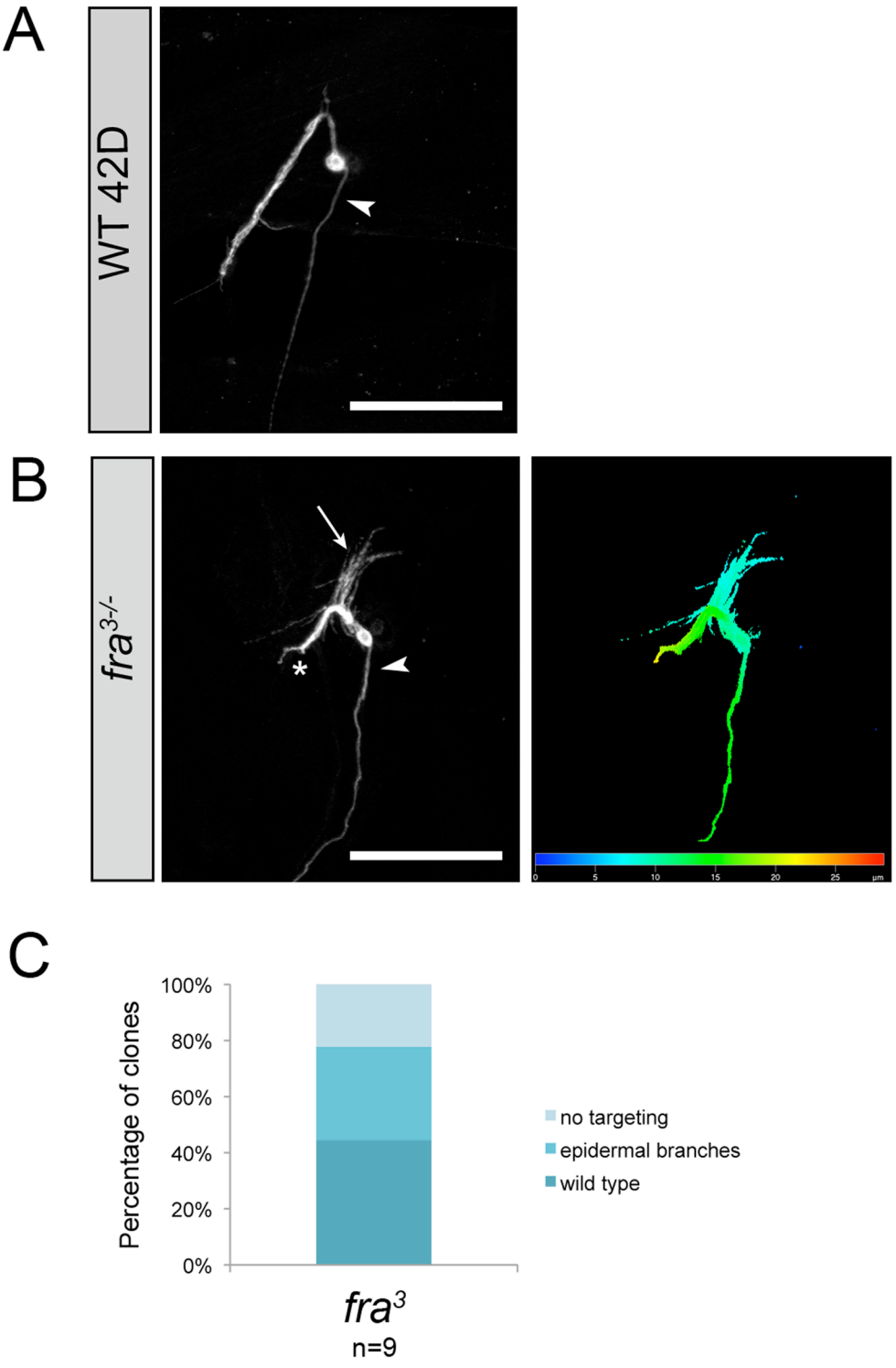

Figure 3.1: Frazzled mutant dmd1 clones show defects in targeting

(A) A wild type dmd1 *FRT42D* clone has a cohesive dendrite stalk that projects away from the epidermis to target the ISN nerve (not shown). Arrowhead marks the axon.

(B) Example of a fra^3 dmd1 clone that show a targeting defect. In this example the dendrite stalk was split into two parts. Part of the stalk remained cohesive and grew off the epidermis towards the ISN (asterisk). Dendrites that have split from the main stalk grow in the epidermal plane are more loosely associated with another (arrow). The right panel shows the same neuron that has been pseudo-colored according to a depth code to illustrate the difference is three-dimension growth between the two parts of the stalk.

(C) Quantification of the penetrance of *fra* phenotypes. About half (n=5/9) fra dmd1 clones showed targeting defects, which were either mild (some dendrites reached ISN target, while some targeted the epidermis, n=3/9) or severe (no targeting of any dendrites to the ISN n=2/9).

Figure 3.2: Dmd1 requires N-cadherin for normal dendrite targeting

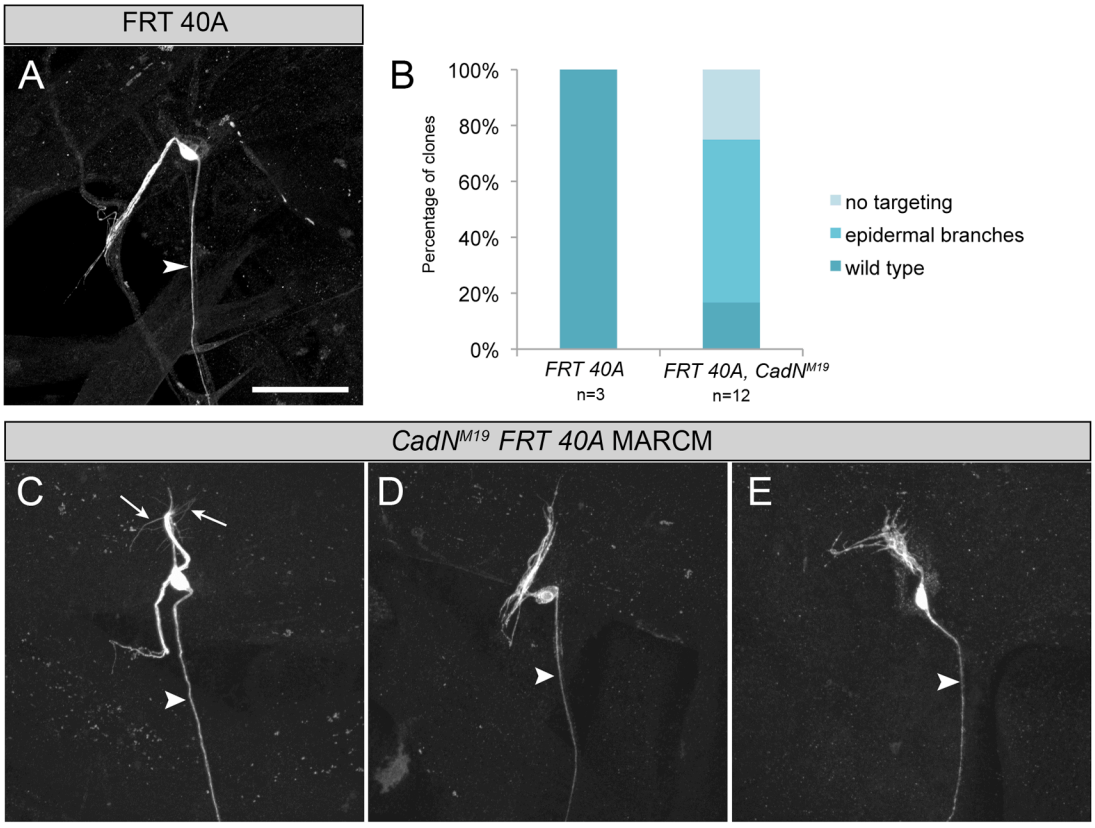

Figure 3.2: Dmd1 requires N-cadherin for normal dendrite targeting

A) A wild type dmd1 clone has a cohesive dendrite stalk that projects away from the epidermis.

B) Quantification of $CadN^{M19}$ phenotypes.

C) One example of a $CadN^{M19}$ /$CadN^{M19}$ clone projects a dendrite stalk away from the epidermis, but has ectopic epidermal branches projecting off the main stalk (arrows).

D) Another example of a $CadN^{M19}$ /$CadN^{M19}$ mutant clone fails to project its dendrite away from the epidermis.

E) A third $CadN^{M19}$ /$CadN^{M19}$ mutant clone fails to project its dendrites away from the epidermis. The remaining dendrites form a loose tangle.

Axons indicated with arrowheads. Scale bar= 50μm

Figure 3.3: Flamingo limits dendrite growth while promoting stalk cohesion and targeting in dmd1

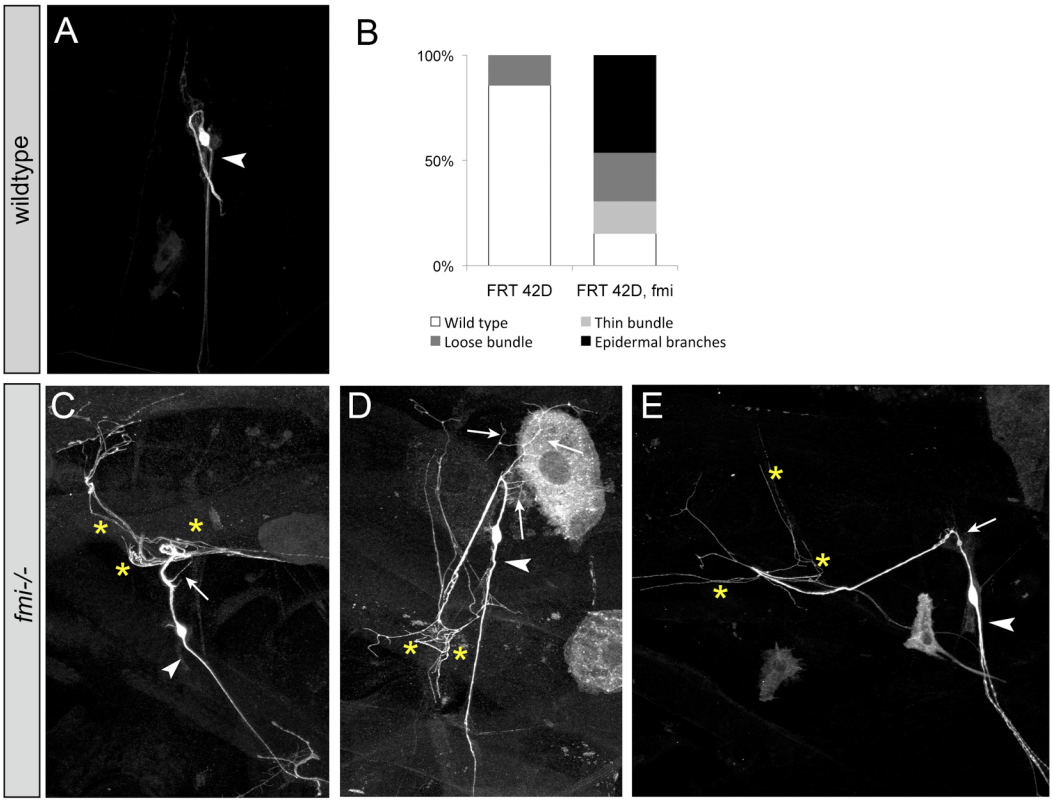

Figure 3.3: Flamingo limits dendrite growth while promoting stalk cohesion and targeting in dmd1

(A) A wild type dmd1 clone has a cohesive dendrite stalk that projects away from the epidermis.

(B) Quantification of fmi phenotypes. Data represented categorically.

(C-E) Examples of *fmi* mutant (*stan*^{3}) dmd1 clones. The clone shown in (c) has individual dendrites that grow away from the main stalk prior to reaching the ISN target (arrow) along with excessive growth at the target (asterisks). The clone shown in (D) has substantial epidermal growth (arrows, partially obscured by epidermal clone) as well as excessive growth at the target. (It also shows a thin stalk, but was categorized at having epidermal growth as its primary defect.) The clone depicted in (E) has a thin stalk (possibly a single dendrite, arrow) as well as excessive branching at the target.

Arrowheads indicate axons. Scale bar= 50μm

Figure 3.4: Misexpression of Pdm2 causes reduced dendrite growth beginning in embryogenesis

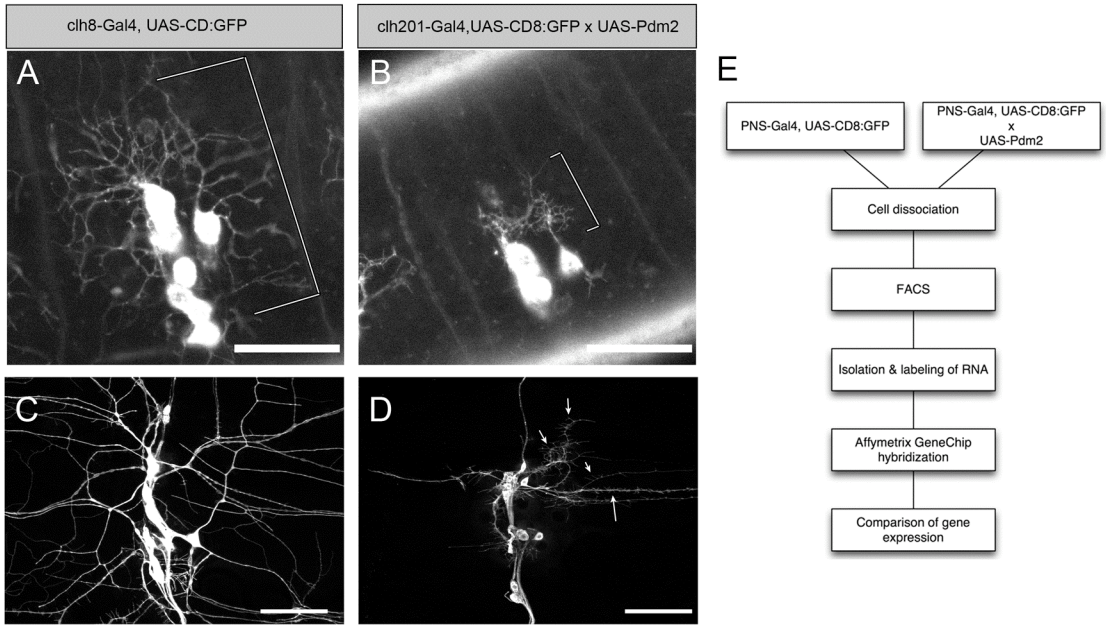

Figure 3.4: **Misexpression of Pdm2 causes reduced dendrite growth beginning in embryogenesis**

(A-B) Dorsal views of live 15-17 hour AEL embryos expressing *mCD8:GFP* in sensory neurons under the control of the *clh201-Gal4* driver. **(A)** Wild type dendrites have initiated outgrowth and have almost filled the hemisegment at this stage. Compare to **(B).** Sensory neurons misexpressing *UAS-Pdm2* at the same stage show severely reduced outgrowth.

(C-D) Dorsal clusters of 3rd instar larvae expressing *mCD8:GFP* alone **(C)** or *mCD8:GFP* and *UAS-Pdm2* under the control of the *clh201-Gal4* driver. Compared to the wild type outgrowth of neurons in **(C)**, neurons forced to express Pdm2 have severely reduced dendrite outgrowth and display numerous short terminal branches (arrows).

(E) Flow chart depicting the gene-profiling strategy.

Scale bars = 50μm

Table 1: List of candidate genes identified by microarray

Table 1: Candidate genes regulated by Pdm2 misexpression					
		Preliminary testing			
Gene	**Fold Change**	**MARCM**	**RNAi**	**UAS**	**Notes**
UAS-driven gene					
pdm2	14.0				
Cytoskeletal regulation					
Sop2	3.2	x			ch organ phenotype
dah	3.0				
tum	2.9	x	x		no dmd1 pheno; already reported for other classes
Rgk2	2.8				
scra	2.4				
cdc2	2.2		x	x	
Ranbp9	2.1				
RanGAP	1.8	x	x		
RhoGAP1A	-1.7	x			
Transcription factors					
senseless	-3.3				
lola D/E	2.2				
lola G/R	1.6				
lola L	1.2	x	x		phenotypes in da neurons
fd96cb	-3.3		x		
CTCF	-6.4	x			
vismay	2.5		x		

Table 1: List of candidate genes identified by microarray (cont.)

Cell cycle/Mitosis							
fzy	3.5						
Orc1	2.5						
bora	3.9						
CycB3	3.8				x		
Mis12	3.2						
polo	3.1	x			xCA	OE of CA trend towards undergrowth class I	
pimples	2.9	x					
CycA	2.9		x		x	dmd1RNAi --overgrowth? Low penetrance	
SMC2	2.5	x				Strong, but low pentrace dmd1 pheno; not reproduced with independent alleles	
Nek2	2.3						
gnu	2.3						
thr	1.8	x					
Ion channels/receptors							
ppk20	117.0						
Gr28b	-4.4						
TrpA1	-4.2						
Obp99b	3.0						
Cng	-3.0		x				
Best3	2.9						
Fsh	2.1		x				
Oamb	-2.1						

Table 1: List of candidate genes identified by microarray (cont.)

Cell surface						
mthl8	-4.2					GPCR
dpr16	-2.1					Ig superfamily
beatIIa	-2.0			x		Ig superfamily
CG10738	-2.4			x		receptor guanylyl cyclase
mol	1.8	x		x		
Miscellaneous						
Npc2f	5.1					Niemann Pick Disease related (Neurodegenerative)
Drip	-4.6	x				water transport
Kua	-4.1					ubiquitination?
ths	3.2					FGF8-like
mas	3.1					protease
ncd	2.5					microtubule minus end motor
Ptp61F	2.4			x		phosphotase, retinal axon guidance
pie	2.1	x				
Rpb4	-2.1					RNA polymerase subunit

Table 1: List of candidate genes identified by microarray

(A) Partial list of Pdm2 regulated genes resulting from our microarray analysis. Genes are listed by general functional category. Positive fold change values indicate at upregulation of the gene in Pdm2-misexpression conditions. Negative fold changes indicate downregulation. Gene names in blue indicate that the gene or its homolog has been implicated in dendrite or axon growth in other systems. "Preliminary testing" indicates what types of functional experiments have been performed. The note column contains information about gene function and/or any phenotypes generated in testing.

Conclusions and Future Directions

The nervous system is comprised of a vast number of morphologically diverse cell types that must form precise connections during development to give rise to a functional nervous system. Two related, important goals of developmental neuroscience are to determine (1) how different neurons acquire their specific morphological characteristics and (2) how these features contribute to nervous system wiring and function. To begin to answer these questions I have used the multidendritic (md) sensory neurons of the *Drosophila* PNS to identify genetic and molecular programs that coordinate cell-type specific dendrite and axonal morphogenesis. The md neurons represent a morphologically and functionally heterogeneous population. As primary sensory neurons the dendritic arbors of these neurons should directly impact the type of sensory information they can detect and transmit to the central nervous system. This correlation between anatomy and function is supported by the observation that neurons with different sensory dendrite morphologies project axons to distinct regions of the central nervous system. Neurons with relatively simple sensory dendrites that are associated with connective tissue target axons to dorsal regions of the CNS, suggesting proprioceptive function. By contrast, neurons with more complex morphologies that innervate the epidermis target their axons to ventral, tactile, domains of the CNS. The homeodomain transcription factor Cut is expressed selectively in the latter group of neurons and is absent from proprioceptive neurons. Whereas Cut had previously been shown to promote dendrite branching in a level-dependent manner (Grueber et al., 2003), the mechanisms of this control, and whether Cut also coordinates axon targeting with branching complexity, was unknown.

The work presented in this thesis demonstrates that loss of Cut leads to a transformation from tactile to proprioceptive-like peripheral arbors, establishing a level-independent role for Cut in control dendrite morphogenesis. In addition, I show that these transformed cells undergo concomitant changes in axon targeting—shifting their axons from ventral (tactile) to the dorsal (proprioceptive) regions of the neuropil. I show that transformed neurons acquire expression of the POU domain transcription factors Pdm1 and Pdm2 (Pdm1/2), which are normally restricted to proprioceptive neurons. Gain and loss of function studies of Pdm1/2 are consistent with an instructive role in acquisition of a selective dendritic arbor, and gain of function studies suggest that Pdm1/2 can promote dorsal targeting of sensory axons. Together these results identify transcriptional programs that coordinately specify proprioceptive dendrite and axon development and advance our understanding of how intrinsic transcriptional programs contribute to nervous system development.

Level dependent transcriptional regulation in neural development

Given the enormous diversity of neuronal morphology, level-dependent transcriptional regulation of morphology provides a mechanism of diversification not possible with simple binary ON/OFF (expression or no expression) transcriptional states. In theory, graded transcription factor expression can be read out as all-or-none regulation of target genes at specific thresholds or as graded levels of target gene expression. Our findings suggest that these outcomes are not mutually exclusive, and that using both methods of regulation may increase the potential to diversify neuronal morphology. Work in this thesis establishes Pdm1 and Pdm2 as level-independent targets of Cut. Cut

represses Pdm1/2 regardless of the level of expression in sensory neurons, and I propose that this action specifies a basic cutaneous da neuron dendritic scaffold. The specific level of Cut expressed, can then diversify this basic scaffold to produce several morphologically (and likely functionally distinct) sensory neurons. With this model in mind we can make predictions about how such a dual role might be read out during morphogenesis. Target genes that are directly regulated in a binary manner are likely to have multiple high affinity transcription factor binding sites to ensure consistent regulation of the gene at all expression levels. Increasing transcription factor levels will likely do little to change the expression levels of such genes, but would allow for regulation of additional genes with, for example, fewer or lower affinity binding sites. These level-dependent targets could then be regulated to diversify a basic morphology dictated by the highest affinity targets. This mode of action may represent an efficient hierarchical strategy for diversifying basic sensory neuron morphology since the ground state is stable (Bate, 1998).

The two known targets of Cut regulation in md neurons fit within this model for dendrite diversification. Pdm1/2 is a level independent target that regulates a clear switch in basic sensory neuron features. The Ig superfamily member, *turtle* is likely to be a level dependent target of Cut, because turtle does not require Cut for its expression, but high levels of Cut can increase *turtle* expression levels in da neurons (Sulkowski et al., 2011). Our model would predict that a gene regulated like *turtle* would mainly alter terminal branching, which is indeed the case (Sulkowski et al., 2011). Graded expression of transcription factors as a determinant of projection patterns is an emerging and evolutionarily conserved theme (Chen et al., 2006), so insight gained about how graded

expression of a transcription factor is read out during development will contribute to understanding of the development of many types of neurons.

Coordinated regulation of sensory dendrite patterning and axonal projections

Cell intrinsic programs that coordinate sensory dendrite morphology with axon projections centrally represent one logical strategy to ensure faithful transmission of sensory information to the nervous system. Wild type neurons have characteristic morphologies and axon projections, so the features must be coordinated, yet there are few examples of such programs that have been described and many examples of transcription factors that selectively control one or the other (See Introduction). Why might this be, and what can it teach us about how dendrite vs. axonal morphogenesis is controlled at a molecular level? To answer these questions we first need to better understand how coordinated regulation is executed, our understanding of which can be informed by identifying the downstream target genes that more directly control dendrite and axon morphogenesis.

Our gene expression analysis has identified many candidate genes that are controlled by Pdm2 in sensory neurons and may represent novel regulators of dendrite and/or axon morphology. Functional analysis of these candidates has the potential to identify novel regulators of neuronal morphogenesis and contribute to our general understanding of how dendrite and axon patterning might be coordinated. Identification of target genes that affect both axon projections and dendritic arborization would suggest that coordinate control of dendrite and axon morphology is accomplished by the regulation of molecules with dual roles in dendrite and axon morphology. As discussed in

the Introduction, there are examples of the same guidance molecular having opposite effects on axons and dendrites (eg: Polleux et al., 2000) and the majority of classical axon guidance cues and neural cell adhesion molecules have been shown to play similar roles in dendrites (reviewed in Parrish et al., 2007). On the other hand, if most target genes regulate either dendrite or axon development, it would suggest that coordination is achieved by simultaneous control of parallel pathways—one specifying dendrite, and the other axonal, development. Such a modular organization would seem to offer a slightly more flexible system that could better account for the coordinated control of two complex process—dendrite morphogenesis and axon targeting—each of which require a series of interrelated steps. This model could also explain the numerous examples of genes and transcription factors that seem to have distinct functions in axons and dendrites.

Implications for sensory and circuit function

Despite all that is known about the development and morphologies of *Drosophila* md neurons, we still know very little about their sensory functions, and therefore, very little about how a particular morphology influences function. The dmd1 neuron's unique dendritic morphology as well as the multiple regulatory mechanisms that converge to ensure its proper development suggest that this neuron has a sensory function that provides specific but indispensable information to the animal. Based on its morphology and our preliminary behavioral data, dmd1 most likely functions as stretch receptor that provides information about the contraction phases during larval crawling. As discussed in chapter 1, this hypothesis can be tested using ablation experiments, as well as genetically encoded activity monitoring.

Future directions

Our data so far support a model in which Cut vs. Pdm expression status dictates cutaneous vs. proprioceptive peripheral and central identity. Further support for this model will come from additional loss of function analysis of Pdm1/2 to demonstrate that Pdm1/2 are required for dorsal axon termination. Although numerous experiments support our interpretation that misexpression of Pdm1/2 in *cut* mutant neurons is causal for transformation, studies of *cut; pdm1, pdm2* mutant combinations would help to confirm this conclusion. These experiments will require a two chromosome MARCM strategy, and the reagents needed to perform these experiments are currently being constructed.

In addition to knowledge about the mechanisms and developmental strategies that underlie coordination of axonal and dendrite development, our findings may inform studies of neural development in vertebrate systems. The vertebrate homologs of Cut (mouse Cux1 and Cux2) and Pdm1/2 (mouse Oct-1 and Oct-2) are expressed in the developing brain (Cobos et al., 2006; Cubelos et al., 2010; He et al., 1989). It has been recently shown that Cux1 and Cux2 genes have roles in regulating the dendritic growth and complexity (Cubelos et al., 2010; Li et al., 2010) and synapse formation (Cubelos et al., 2010) in pyramidal neurons. Although the specific effects of Cux expression may vary depending on cell type, a role in modulating dendritic complexity is analogous to that of *Drosophila* Cut. Moreover, there is some evidence that suggests that the effects of Cux genes in positively regulating dendritic complexity might be dosage dependent (Cubelos et al., 2010), mirroring the level-dependent roles of Cut in regulating morphogenesis. Finally, expression of mouse Cux1 or human CDP, can substitute for

Cut in overexpression experiments in the fly (Grueber et al., 2003), suggesting that these homologs may have similar targets that mediate their ability to control dendrite development.

Pdm1 and Pdm2 are members of the class II family of POU domain transcription factors, with Oct-1 and Oct-2 being their most closely related vertebrate homologs (Dick et al., 1991; Ryan and Rosenfeld, 1997). Oct-1 and Oct-2 are expressed in the developing mammalian nervous system as well as in the adult (He et al., 1989), but specific roles for these genes in nervous system development or morphogenesis have not been described. As a family, POU domain containing transcription factors have roles in neural development in worms, flies, and mammals (Xue et al, 1992; Komiyama et al., 2003; Latchman, 1999; Rosenfeld, 1991). The identification of roles for Pdm1 and Pdm2 in neuronal morphogenesis suggests that Oct-1 and Oct-2 may be good candidates for studies of neuronal morphogenesis in mammals. Furthermore, our array analysis has the potential to uncover novel regulators of neuronal morphogenesis that may have conserved roles in vertebrate species.

Conclusion

Nervous system function is dependent upon functional circuits, which require each neuron within the circuit to develop the proper dendritic and axonal morphology in order to ensure proper connections and the faithful transmission of information. Work in this thesis has identified an example of an elegant and effective strategy to wire the brain: cell autonomous transcriptional programs that coordinate dendritic and axon projections of a single neuron. Thus far, the mechanisms of such coordinate regulation remain unknown. Our identification of Pdm-regulated genes is first step in elucidating the

mechanisms of this coordinated control of dendrite and axon morphogenesis. Determining the role of these genes in controlling axon and/or dendrite morphogenesis and the identification of similar examples of coordinated control in other systems will provide important insights into our understanding of the genetic control of circuit formation in the nervous system.

References

Ainsley, J.A., Pettus, J.M., Bosenko, D., Gerstein, C.E., Zinkevich, N., Anderson, M.G., Adams, C.M., Welsh, M.J., and Johnson, W.A. (2003). Enhanced locomotion caused by loss of the Drosophila DEG/ENaC protein Pickpocket1. Curr Biol *13*, 1557-1563.

Anderson, S.A., Eisenstat, D.D., Shi, L., and Rubenstein, J.L. (1997). Interneuron migration from basal forebrain to neocortex: dependence on Dlx genes. Science *278*, 474-476.

Ashhurst, D.E. (1968). Connestive tissue of insects. In Annu Rev Entomol, pp. 45-74.

Bate, M. (1998). Making sense of behavior. Int J Dev Biol *42*, 507-509.

Becker, E.B., and Bonni, A. (2005). Beyond proliferation--cell cycle control of neuronal survival and differentiation in the developing mammalian brain. Semin Cell Dev Biol *16*, 439-448.

Billin, A.N., Cockerill, K.A., and Poole, S.J. (1991). Isolation of a family of Drosophila POU domain genes expressed in early development. Mech Dev *34*, 75-84.

Blochlinger, K., Bodmer, R., Jan, L.Y., and Jan, Y.N. (1990). Patterns of expression of cut, a protein required for external sensory organ development in wild-type and cut mutant Drosophila embryos. Genes Dev *4*, 1322-1331.

Bodmer, R., Barbel, S., Sheperd, S., Jack, J.W., Jan, L.Y., and Jan, Y.N. (1987). Transformation of sensory organs by mutations of the cut locus of D. melanogaster. Cell *51*, 293-307.

Brankatschk, M., and Dickson, B.J. (2006). Netrins guide Drosophila commissural axons at short range. Nat Neurosci *9*, 188-194.

Brewster, R., Hardiman, K., Deo, M., Khan, S., and Bodmer, R. (2001). The selector gene cut represses a neural cell fate that is specified independently of the Achaete-Scute-Complex and atonal. Mech Dev *105*, 57-68.

Brierley, D.J., Blanc, E., Reddy, O.V., Vijayraghavan, K., Williams, D.W. (2009) Dendritic targeting in the leg neuropil of Drosophila: the role of midline signalling molecules in generating a myotopic map. PLoS Biology *7*, e1000199.

Broihier, H.T., Kuzin, A., Zhu, Y., Odenwald, W., and Skeath, J.B. (2004). Drosophila homeodomain protein Nkx6 coordinates motoneuron subtype identity and axonogenesis. Development *131*, 5233-5242.

Calleja, M., Herranz, H., Estella, C., Casal, J., Lawrence, P., Simpson, P., and Morata, G. (2000). Generation of medial and lateral dorsal body domains by the pannier gene of Drosophila. Development *127*, 3971-3980.

Chalfie, M. (2009). Neurosensory mechanotransduction. Nat Rev Mol Cell Biol *10*, 44-52.

Chen, A.I., de Nooij, J.C., and Jessell, T.M. (2006). Graded activity of transcription factor Runx3 specifies the laminar termination pattern of sensory axons in the developing spinal cord. Neuron *49*, 395-408.

Chen, P.L., and Clandinin, T.R. (2008). The cadherin Flamingo mediates level-dependent interactions that guide photoreceptor target choice in Drosophila. Neuron *58*, 26-33.

Chen, Z., Wang, Q., and Wang, Z. (2010). The amiloride-sensitive epithelial Na+ channel PPK28 is essential for drosophila gustatory water reception. J Neurosci *30*, 6247-6252.

Cheng, L., Lemmon, S., and Lemmon, V. (2005). RanBPM is an L1-interacting protein that regulates L1-mediated mitogen-activated protein kinase activation. J Neurochem *94*, 1102-1110.

Clandinin, T.R., Lee, C.H., Herman, T., Lee, R.C., Yang, A.Y., Ovasapyan, S., and Zipursky, S.L. (2001). Drosophila LAR regulates R1-R6 and R7 target specificity in the visual system. Neuron *32*, 237-248.

Cobos, I., Borello, U., and Rubenstein, J.L. (2007). Dlx transcription factors promote migration through repression of axon and dendrite growth. Neuron *54*, 873-888.

Cobos, I., Long, J.E., Thwin, M.T., and Rubenstein, J.L. (2006). Cellular patterns of transcription factor expression in developing cortical interneurons. Cereb Cortex *16 Suppl 1*, i82-88.

Cook, O., Biehs, B., and Bier, E. (2004). brinker and optomotor-blind act coordinately to initiate development of the L5 wing vein primordium in Drosophila. Development *131*, 2113-2124.

Corty, M.M., Matthews, B.J., and Grueber, W.B. (2009). Molecules and mechanisms of dendrite development in Drosophila. Development *136*, 1049-1061.

Couto, A., Alenius, M., and Dickson, B.J. (2005). Molecular, anatomical, and functional organization of the Drosophila olfactory system. Curr Biol *15*, 1535-1547.

Crozatier, M., and Vincent, A. (2008). Control of multidendritic neuron differentiation in Drosophila: the role of Collier. Dev Biol *315*, 232-242.

Cubelos, B., Sebastián-Serrano, A., Beccari, L., Calcagnotto, M.E., Cisneros, E., Kim, S., Dopazo, A., Alvarez-Dolado, M., Redondo, J.M., Bovolenta, P.*, et al.* (2010). Cux1 and

Cux2 regulate dendritic branching, spine morphology, and synapses of the upper layer neurons of the cortex. Neuron *66*, 523-535.

Cubelos, B., Sebastián-Serrano, A., Kim, S., Moreno-Ortiz, C., Redondo, J.M., Walsh, C.A., and Nieto, M. (2008a). Cux-2 controls the proliferation of neuronal intermediate precursors of the cortical subventricular zone. Cereb Cortex *18*, 1758-1770.

Cubelos, B., Sebastián-Serrano, A., Kim, S., Redondo, J.M., Walsh, C., and Nieto, M. (2008b). Cux-1 and Cux-2 control the development of Reelin expressing cortical interneurons. Dev Neurobiol *68*, 917-925.

Dalla Torre di Sanguinetto, S.A., Dasen, J.S., and Arber, S. (2008). Transcriptional mechanisms controlling motor neuron diversity and connectivity. Curr Opin Neurobiol *18*, 36-43.

Dambly-Chaudiere, C. and Ghysen, A. (1987) Independent subpatterns of sense organs require independent genes of the achaete-scute complex in Drosophila larvae. Genes and Development *1*, 297-306.

Dasen, J.S., De Camilli, A., Wang, B., Tucker, P.W., and Jessell, T.M. (2008). Hox repertoires for motor neuron diversity and connectivity gated by a single accessory factor, FoxP1. Cell *134*, 304-316.

Dasen, J.S., Liu, J.P., and Jessell, T.M. (2003). Motor neuron columnar fate imposed by sequential phases of Hox-c activity. Nature *425*, 926-933.

Dasen, J.S., Tice, B.C., Brenner-Morton, S., and Jessell, T.M. (2005). A Hox regulatory network establishes motor neuron pool identity and target-muscle connectivity. Cell *123*, 477-491.

De Marco Garcia, N.V., and Jessell, T.M. (2008). Early motor neuron pool identity and muscle nerve trajectory defined by postmitotic restrictions in Nkx6.1 activity. Neuron *57*, 217-231.

Dick, T., Yang, X.H., Yeo, S.L., and Chia, W. (1991). Two closely linked Drosophila POU domain genes are expressed in neuroblasts and sensory elements. Proc Natl Acad Sci USA *88*, 7645-7649.

Dietzl, G., Chen, D., Schnorrer, F., Su, K.C., Barinova, Y., Fellner, M., Gasser, B., Kinsey, K., Oppel, S., Scheiblauer, S., Cuoto, A., Marra, V., Keleman, K., Dickson, B.J. (2007). A genome-wide transgenic RNAi library for conditional gene inactiviation in Drosophila. Nature *448*, 151-6

Dunah, A.W., Hueske, E., Wyszynski, M., Hoogenraad, C.C., Jaworski, J., Pak, D.T., Simonetta, A., Liu, G., and Sheng, M. (2005). LAR receptor protein tyrosine phosphatases in the development and maintenance of excitatory synapses. Nat Neurosci *8*, 458-467.

Edwards, J.S., Swales, L.S., and Bate, M. (1993). The differentiation between neuroglia and connective tissue sheath in insect ganglia revisited: the neural lamella and perineurial sheath cells are absent in a mesodermless mutant of Drosophila. J Comp Neurol *333*, 301-308.

Emmons, R.B., Duncan, D., Estes, P.A., Kiefel, P., Mosher, J.T., Sonnenfeld, M., Ward, M.P., Duncan, I., and Crews, S.T. (1999). The spineless-aristapedia and tango bHLH-PAS proteins interact to control antennal and tarsal development in Drosophila. Development *126*, 3937-3945.

Finlayson, L.H., and Lowenstein, O. (1958). The structure and function of abdominal stretch receptors in insects. Proc R Soc Lond, B, Biol Sci *148*, 433-449.

Furrer, M.P., Kim, S., Wolf, B., and Chiba, A. (2003). Robo and Frazzled/DCC mediate dendritic guidance at the CNS midline. Nat Neurosci *6*, 223-230.

Furrer, M.P., Vasenkova, I., Kamiyama, D., Rosado, Y., and Chiba, A. (2007). Slit and Robo control the development of dendrites in Drosophila CNS. Development *134*, 3795-3804.

Gao, F.B., Brenman, J.E., Jan, L.Y., and Jan, Y.N. (1999). Genes regulating dendritic outgrowth, branching, and routing in Drosophila. Genes Dev *13*, 2549-2561.

Gao, F.B., Kohwi, M., Brenman, J.E., Jan, L.Y., and Jan, Y.N. (2000). Control of dendritic field formation in Drosophila: the roles of flamingo and competition between homologous neurons. Neuron *28*, 91-101.

Garbe, D.S., and Bashaw, G.J. (2004). Axon guidance at the midline: from mutants to mechanisms. Crit Rev Biochem Mol Biol *39*, 319-341.

Garel, S., Marín, F., Mattéi, M.G., Vesque, C., Vincent, A., and Charnay, P. (1997). Family of Ebf/Olf-1-related genes potentially involved in neuronal differentiation and regional specification in the central nervous system. Developmental dynamics : an official publication of the American Association of Anatomists *210*, 191-205.

Godenschwege, T.A., Simpson, J.H., Shan, X., Bashaw, G.J., Goodman, C.S., and Murphey, R.K. (2002). Ectopic expression in the giant fiber system of Drosophila reveals distinct roles for roundabout (Robo), Robo2, and Robo3 in dendritic guidance and synaptic connectivity. J Neurosci *22*, 3117-3129.

Goeke, S., Greene, E.A., Grant, P.K., Gates, M.A., Crowner, D., Aigaki, T., and Giniger, E. (2003). Alternative splicing of lola generates 19 transcription factors controlling axon guidance in Drosophila. Nat Neurosci *6*, 917-924.

Goldstein, A.Y., Jan, Y.N., and Luo, L. (2005). Function and regulation of Tumbleweed (RacGAP50C) in neuroblast proliferation and neuronal morphogenesis. Proc Natl Acad Sci USA *102*, 3834-3839.

Gong, S., Zheng, C., Doughty, M.L., Losos, K., Didkovsky, N., Schambra, U.B., Nowak, N.J., Joyner, A., Leblanc, G., Hatten, M.E., and Heintz, N. (2003). A gene expression atlas of the central nervous system based on bacterial artificial chromosomes. Nature *425*, 917-925.

Gray, P.A., Fu, H., Luo, P., Zhao, Q., Yu, J., Ferrari, A., Tenzen, T., Yuk, D.I., Tsung, E.F., Cai, Z.*, et al.* (2004). Mouse brain organization revealed through direct genome-scale TF expression analysis. Science *306*, 2255-2257.

Grosskortenhaus, R., Robinson, K.J., and Doe, C.Q. (2006). Pdm and Castor specify late-born motor neuron identity in the NB7-1 lineage. Genes Dev *20*, 2618-2627.

Grueber, W.B., Jan, L.Y., and Jan, Y.N. (2002). Tiling of the Drosophila epidermis by multidendritic sensory neurons. Development *129*, 2867-2878.

Grueber, W.B., Jan, L.Y., and Jan, Y.N. (2003). Different levels of the homeodomain protein cut regulate distinct dendrite branching patterns of Drosophila multidendritic neurons. Cell *112*, 805-818.

Grueber, W.B., and Sagasti, A. (2010). Self-avoidance and tiling: Mechanisms of dendrite and axon spacing. Cold Spring Harb Perspect Biol *2*, a001750.

Grueber, W.B., Ye, B., Yang, C.H., Younger, S., Borden, K., Jan, L.Y., and Jan, Y.N. (2007). Projections of Drosophila multidendritic neurons in the central nervous system: links with peripheral dendrite morphology. Development *134*, 55-64.

Haase, G., Dessaud, E., Garcès, A., de Bovis, B., Birling, M., Filippi, P., Schmalbruch, H., Arber, S., and deLapeyrière, O. (2002). GDNF acts through PEA3 to regulate cell body positioning and muscle innervation of specific motor neuron pools. Neuron *35*, 893-905.

Hakeda-Suzuki, S., Berger-Müller, S., Tomasi, T., Usui, T., Horiuchi, S.Y., Uemura, T., and Suzuki, T. (2011). Golden Goal collaborates with Flamingo in conferring synaptic-layer specificity in the visual system. Nat Neurosci *14*, 314-323.

Hand, R., Bortone, D., Mattar, P., Nguyen, L., Heng, J.I., Guerrier, S., Boutt, E., Peters, E., Barnes, A.P., Parras, C.*, et al.* (2005). Phosphorylation of Neurogenin2 specifies the migration properties and the dendritic morphology of pyramidal neurons in the neocortex. Neuron *48*, 45-62.

Hand, R. and Polleux, F. (2011) Neurogenin2 regulates the initial axon guidance of cortical pyramidal neurons projecting medially to the corpus callosum. Neural Development *6*, 30.

Hardt, O., Scholz, C., Küsters, D., Yanagawa, Y., Pennartz, S., Cremer, H., and Bosio, A. (2008). Gene expression analysis defines differences between region-specific GABAergic neurons. Mol Cell Neurosci *39*, 418-428.

Hattori, Y., Sugimura, K., and Uemura, T. (2007). Selective expression of Knot/Collier, a transcriptional regulator of the EBF/Olf-1 family, endows the Drosophila sensory system with neuronal class-specific elaborated dendritic patterns. Genes Cells *12*, 1011-1022.

Huang, M.L., Hsu, C.H., and Chien, C.T. (2000) The proneural gene amos promotes multiple dendritic neuron formation in the Drosophila peripheral nervous system. Neuron *25*, 57-67.

He, X., Treacy, M.N., Simmons, D.M., Ingraham, H.A., Swanson, L.W., and Rosenfeld, M.G. (1989). Expression of a large family of POU-domain regulatory genes in mammalian brain development. Nature *340*, 35-41.

Heiman, M.G., and Shaham, S. (2009). DEX-1 and DYF-7 establish sensory dendrite length by anchoring dendritic tips during cell migration. Cell *137*, 344-355.

Herrera, E., Brown, L., Aruga, J., Rachel, R.A., Dolen, G., Mikoshiba, K., Brown, S., and Mason, C.A. (2003). Zic2 patterns binocular vision by specifying the uncrossed retinal projection. Cell *114*, 545-557.

Horton, A.C., Racz, B., Monson, E.E., Lin, A.L., Weinberg, R.J., Ehlers, M.D. (2005). Polarized secretory trafficking directs cargo for asymmetric dendrite growth and morphogenesis. Neuron *48*, 757-71.

Huang, Z., Zang, K., and Reichardt, L.F. (2005). The origin recognition core complex regulates dendrite and spine development in postmitotic neurons. J Cell Biol *170*, 527-535.

Huber, A.B., Kolodkin, A.L., Ginty, D.D., and Cloutier, J.F. (2003). Signaling at the growth cone: ligand-receptor complexes and the control of axon growth and guidance. Annu Rev Neurosci *26*, 509-563.

Hughes, C.L., and Thomas, J.B. (2007). A sensory feedback circuit coordinates muscle activity in Drosophila. Mol Cell Neurosci *35*, 383-396.

Hwang, R.Y., Zhong, L., Xu, Y., Johnson, T., Zhang, F., Deisseroth, K., and Tracey, W.D. (2007). Nociceptive neurons protect Drosophila larvae from parasitoid wasps. Curr Biol *17*, 2105-2116.

Iwai, Y., Usui, T., Hirano, S., Steward, R., Takeichi, M., and Uemura, T. (1997). Axon patterning requires DN-cadherin, a novel neuronal adhesion receptor, in the Drosophila embryonic CNS. Neuron *19*, 77-89.

Jan, Y.N., and Jan, L.Y. (2010). Branching out: mechanisms of dendritic arborization. Nat Rev Neurosci *11*, 316-328.

Jarman, A.P., Grau, Y., Jan, L.Y., and Jan, Y.N. (1993). atonal is a proneural gene that directs chordotonal organ formation in the Drosophila peripheral nervous system. Cell *73*, 1307-1321.

Jarman, A.P., Sun, Y., Jan, L.Y., and Jan, Y.N. (1995). Role of the proneural gene, atonal, in formation of Drosophila chordotonal organs and photoreceptors. Development *121*, 2019-2030.

Jefferis, G.S., Marin, E.C., Stocker, R.F., and Luo, L. (2001). Target neuron prespecification in the olfactory map of Drosophila. Nature *414*, 204-208.

Jinushi-Nakao, S., Arvind, R., Amikura, R., Kinameri, E., Liu, A.W., and Moore, A.W. (2007). Knot/Collier and cut control different aspects of dendrite cytoskeleton and synergize to define final arbor shape. Neuron *56*, 963-978.

Kania, A., and Jessell, T.M. (2003). Topographic motor projections in the limb imposed by LIM homeodomain protein regulation of ephrin-A:EphA interactions. Neuron *38*, 581-596.

Kelsch, W., Mosley, C.P., Lin, C.W., and Lois, C. (2007). Distinct mammalian precursors are committed to generate neurons with defined dendritic projection patterns. PLoS Biol *5*, e300.

Kim, A.H., Puram, S.V., Bilimoria, P.M., Ikeuchi, Y., Keough, S., Wong, M., Rowitch, D., and Bonni, A. (2009). A centrosomal Cdc20-APC pathway controls dendrite morphogenesis in postmitotic neurons. Cell *136*, 322-336.

Kim, M.D., Jan, L.Y., and Jan, Y.N. (2006). The bHLH-PAS protein Spineless is necessary for the diversification of dendrite morphology of Drosophila dendritic arborization neurons. Genes Dev *20*, 2806-2819.

Kimura, H., Usui, T., Tsubouchi, A., and Uemura, T. (2006). Potential dual molecular interaction of the Drosophila 7-pass transmembrane cadherin Flamingo in dendritic morphogenesis. J Cell Sci *119*, 1118-1129.

Kitamoto, T. (2001). Conditional modification of behavior in Drosophila by targeted expression of a temperature-sensitive shibire allele in defined neurons. J Neurobiol *47*, 81-92.

Kolodziej, P.A., Timpe, L.C., Mitchell, K.J., Fried, S.R., Goodman, C.S., Jan, L.Y., and Jan, Y.N. (1996). frazzled encodes a Drosophila member of the DCC immunoglobulin subfamily and is required for CNS and motor axon guidance. Cell *87*, 197-204.

Komiyama, T., Johnson, W.A., Luo, L., and Jefferis, G.S. (2003). From lineage to wiring specificity. POU domain transcription factors control precise connections of Drosophila olfactory projection neurons. Cell *112*, 157-167.

Komiyama, T., and Luo, L. (2007). Intrinsic control of precise dendritic targeting by an ensemble of transcription factors. Curr Biol *17*, 278-285.

Komiyama, T., Sweeney, L.B., Schuldiner, O., Garcia, K.C., and Luo, L. (2007). Graded expression of semaphorin-1a cell-autonomously directs dendritic targeting of olfactory projection neurons. Cell *128*, 399-410.

Kypta, R.M., Su, H., and Reichardt, L.F. (1996). Association between a transmembrane protein tyrosine phosphatase and the cadherin-catenin complex. J Cell Biol *134*, 1519-1529.

Labrador, J.P., O'keefe, D., Yoshikawa, S., McKinnon, R.D., Thomas, J.B., and Bashaw, G.J. (2005). The homeobox transcription factor even-skipped regulates netrin-receptor expression to control dorsal motor-axon projections in Drosophila. Curr Biol *15*, 1413-1419.

Lai, H.C., Klisch, T.J., Roberts, R., Zoghbi, H.Y., and Johnson, J.E. (2011). In vivo neuronal subtype-specific targets of atoh1 (math1) in dorsal spinal cord. J Neurosci *31*, 10859-10871.

Latchman, D.S. (1999). POU family transcription factors in the nervous system. J Cell Physiol *179*, 126-133.

Lee, R., Petros, T.J., and Mason, C.A. (2008). Zic2 regulates retinal ganglion cell axon avoidance of ephrinB2 through inducing expression of the guidance receptor EphB1. J Neurosci *28*, 5910-5919.

Lee, T., and Luo, L. (1999). Mosaic analysis with a repressible cell marker for studies of gene function in neuronal morphogenesis. Neuron *22*, 451-461.

Li, N., Zhao, C.T., Wang, Y., and Yuan, X.B. (2010). The transcription factor cux1 regulates dendritic morphology of cortical pyramidal neurons. PLoS ONE *5*, e10596.

Li, W., Wang, F., Menut, L., and Gao, F.B. (2004). BTB/POZ-zinc finger protein abrupt suppresses dendritic branching in a neuronal subtype-specific and dosage-dependent manner. Neuron *43*, 823-834.

Lichtneckert, R., Nobs, L., and Reichert, H. (2008). Empty spiracles is required for the development of olfactory projection neuron circuitry in Drosophila. Development *135*, 2415-2424.

Liu, L., Johnson, W.A., and Welsh, M.J. (2003a). Drosophila DEG/ENaC pickpocket genes are expressed in the tracheal system, where they may be involved in liquid clearance. Proc Natl Acad Sci USA *100*, 2128-2133.

Liu, L., Leonard, A.S., Motto, D.G., Feller, M.A., Price, M.P., Johnson, W.A., and Welsh, M.J. (2003b). Contribution of Drosophila DEG/ENaC genes to salt taste. Neuron *39*, 133-146.

Livet, J., Sigrist, M., Stroebel, S., De Paola, V., Price, S.R., Henderson, C.E., Jessell, T.M., and Arber, S. (2002). ETS gene Pea3 controls the central position and terminal arborization of specific motor neuron pools. Neuron *35*, 877-892.

Lloyd, A., and Sakonju, S. (1991). Characterization of two Drosophila POU domain genes, related to oct-1 and oct-2, and the regulation of their expression patterns. Mech Dev *36*, 87-102.

London, M., and Häusser, M. (2005). Dendritic computation. Annu Rev Neurosci *28*, 503-532.

Long, H., Ou, Y., Rao, Y., and van Meyel, D.J. (2009). Dendrite branching and self-avoidance are controlled by Turtle, a conserved IgSF protein in Drosophila. Development *136*, 3475-3484.

Lowenstein, O. and Finlayson, L. (1959). The response of the abdominal stretch receptor of an insect to phasic stimulation. Comp Biochemistry and Physiology *1*, 56-61.

Luria, V., Krawchuk, D., Jessell, T.M., Laufer, E., and Kania, A. (2008). Specification of motor axon trajectory by ephrin-B:EphB signaling: symmetrical control of axonal patterning in the developing limb. Neuron *60*, 1039-1053.

Marin, E.C., Jefferis, G.S., Komiyama, T., Zhu, H., and Luo, L. (2002). Representation of the glomerular olfactory map in the Drosophila brain. Cell *109*, 243-255.

Markram, H., Toledo-Rodriguez, M., Wang, Y., Gupta, A., Silberberg, G., and Wu, C. (2004). Interneurons of the neocortical inhibitory system. Nat Rev Neurosci *5*, 793-807.

Masland, R.H. (2004). Neuronal cell types. Curr Biol *14*, R497-500.

Matthews, B., and Grueber, W. (2011). Dscam1-Mediated Self-Avoidance Counters Netrin-Dependent Targeting of Dendrites in Drosophila. Current Biology.

Matthews, B.J., Kim, M.E., Flanagan, J.J., Hattori, D., Clemens, J.C., Zipursky, S., and Grueber, W.B. (2007). Dendrite Self-Avoidance Is Controlled by Dscam. Cell *129*, 593-604.

Mauss, A., Tripodi, M., Evers, J.F., and Landgraf, M. (2009). Midline signalling systems direct the formation of a neural map by dendritic targeting in the Drosophila motor system. PLoS Biology *9*, e1000200.

Merritt, D.J. (1997). Transformation of external sensilla to chordotonal sensilla in the cut mutant of Drosophila assessed by single-cell marking in the embryo and larva. Microsc Res Tech *39*, 492-505.

Merritt, D.J., Hawken, A., and Whitington, P.M. (1993). The role of the cut gene in the specification of central projections by sensory axons in Drosophila. Neuron *10*, 741-752.

Merritt, D.J., and Whitington, P.M. (1995). Central projections of sensory neurons in the Drosophila embryo correlate with sensory modality, soma position, and proneural gene function. J Neurosci *15*, 1755-1767.

Mitchell, K.J., Doyle, J.L., Serafini, T., Kennedy, T.E., Tessier-Lavigne, M., Goodman, C.S., and Dickson, B.J. (1996). Genetic analysis of Netrin genes in Drosophila: Netrins guide CNS commissural axons and peripheral motor axons. Neuron *17*, 203-215.

Mohler, J., Seecoomar, M., Agarwal, S., Bier, E., and Hsai, J. (2000). Activation of knot (kn) specifies the 3-4 intervein region in the Drosophila wing. Development *127*, 55-63.

Moore, A.W., Jan, L.Y., and Jan, Y.N. (2002). hamlet, a binary genetic switch between single- and multiple- dendrite neuron morphology. Science *297*, 1355-1358.

Murphey, R.K., Possidente, D., Pollack, G., and Merritt, D.J. (1989). Modality-specific axonal projections in the CNS of the flies Phormia and Drosophila. J Comp Neurol *290*, 185-200.

Nair, A., Bate, M., and Pulver, S.R. (2010). Characterization of voltage-gated ionic currents in a peripheral sensory neuron in larval Drosophila. BMC Res Notes *3*, 154.

Nepveu, A. (2001). Role of the multifunctional CDP/Cut/Cux homeodomain transcription factor in regulating differentiation, cell growth and development. Gene *270*, 1-15.

Nern, A., Zhu, Y., and Zipursky, S.L. (2008). Local N-cadherin interactions mediate distinct steps in the targeting of lamina neurons. Neuron *58*, 34-41.

Neumann, C.J., and Cohen, S.M. (1998). Boundary formation in Drosophila wing: Notch activity attenuated by the POU protein Nubbin. Science *281*, 409-413.

Ng, M., Diaz-Benjumea, F.J., and Cohen, S.M. (1995). Nubbin encodes a POU-domain protein required for proximal-distal patterning in the Drosophila wing. Development *121*, 589-599.

Nieto, M., Monuki, E.S., Tang, H., Imitola, J., Haubst, N., Khoury, S.J., Cunningham, J., Gotz, M., and Walsh, C.A. (2004). Expression of Cux-1 and Cux-2 in the subventricular zone and upper layers II-IV of the cerebral cortex. J Comp Neurol *479*, 168-180.

Nott, A., Watson, P.M., Robinson, J.D., Crepaldi, L., and Riccio, A. (2008). S-Nitrosylation of histone deacetylase 2 induces chromatin remodelling in neurons. Nature *455*, 411-415.

O'Donnell, M., Chance, R.K., and Bashaw, G.J. (2009). Axon growth and guidance: receptor regulation and signal transduction. Annu Rev Neurosci *32*, 383-412.

Orgogozo, V., and Grueber, W.B. (2005). FlyPNS, a database of the Drosophila embryonic and larval peripheral nervous system. BMC Dev Biol *5*, 4.

Osborne, M.P. (1963). The sensory neurons and sensilla in the abdomen and thorax of the blowfly larva. Quarterly Journal of Microscopical Science *104*, 227-241.

Osborne, M.P., and Finlayson, L. (1962). The structue and topography of stretch recptors in representatives of seven orders of insects. Quarterly Journal of Microscopical Science *103*, 227-242.

Ou, Y., Chwalla, B., Landgraf, M., and van Meyel, D.J. (2008). Identification of genes influencing dendrite morphogenesis in developing peripheral sensory and central motor neurons. Neural development *3*, 16.

Parrish, J.Z., Emoto, K., Jan, L.Y., and Jan, Y.N. (2007a). Polycomb genes interact with the tumor suppressor genes hippo and warts in the maintenance of Drosophila sensory neuron dendrites. Genes Dev *21*, 956-972.

Parrish, J.Z., Emoto, K., Kim, M.D., and Jan, Y.N. (2007b). Mechanisms that regulate establishment, maintenance, and remodeling of dendritic fields. Annu Rev Neurosci *30*, 399-423.

Parrish, J.Z., Kim, M.D., Jan, L.Y., and Jan, Y.N. (2006). Genome-wide analyses identify transcription factors required for proper morphogenesis of Drosophila sensory neuron dendrites. Genes Dev *20*, 820-835.

Pfluger, H.J., Braunig, P., and Hustert, R. (1988). The Organization of Mechanosensory Neuropiles in Locust Thoracic Ganglia. Philosophical Trans Royal Soc of London *321*, 1-39.

Polleux, F., Ince-Dunn, G., and Ghosh, A. (2007). Transcriptional regulation of vertebrate axon guidance and synapse formation. Nat Rev Neurosci *8*, 331-340.

Polleux, F., Morrow, T., and Ghosh, A. (2000). Semaphorin 3A is a chemoattractant for cortical apical dendrites. Nature *404*, 567-573.

Ramos, B., Gaudillière, B., Bonni, A., and Gill, G. (2007). Transcription factor Sp4 regulates dendritic patterning during cerebellar maturation. Proc Natl Acad Sci USA *104*, 9882-9887.

Reuter, J.E., Nardine, T.M., Penton, A., Billuart, P., Scott, E.K., Usui, T., Uemura, T., and Luo, L. (2003). A mosaic genetic screen for genes necessary for Drosophila mushroom body neuronal morphogenesis. Development *130*, 1203-1213.

Roll-Mecak, A., and Vale, R.D. (2005). The Drosophila homologue of the hereditary spastic paraplegia protein, spastin, severs and disassembles microtubules. Curr Biol *15*, 650-655.

Rolls, M.M. (2010). Neuronal polarity in drosophila: Sorting out axons and dendrites. Dev Neurobiol.

Rolls, M.M., Satoh, D., Clyne, P.J., Henner, A.L., Uemura, T., and Doe, C.Q. (2007). Polarity and intracellular compartmentalization of Drosophila neurons. Neural development *2*, 7.

Rosenfeld, M.G. (1991). POU-domain transcription factors: pou-er-ful developmental regulators. Genes Dev *5*, 897-907.

Ryan, A.K., and Rosenfeld, M.G. (1997). POU domain family values: flexibility, partnerships, and developmental codes. Genes Dev *11*, 1207-1225.

Sabatier, C., Plump, A.S., Ma, L., Brose, K., Tamada, A., Murakami, F., Lee, E.Y., and Tessier-Lavigne, M. (2004). The divergent Robo family protein rig-1/Robo3 is a negative regulator of slit responsiveness required for midline crossing by commissural axons. Cell *117*, 157-169.

Satoh, D., Sato, D., Tsuyama, T., Saito, M., Ohkura, H., Rolls, M.M., Ishikawa, F., and Uemura, T. (2008). Spatial control of branching within dendritic arbors by dynein-dependent transport of Rab5-endosomes. Nat Cell Biol *10*, 1164-1171.

Schrader, S., and Merritt, D.J. (2000). Central projections of Drosophila sensory neurons in the transition from embryo to larva. J Comp Neurol *425*, 34-44.

Schrader, S., and Merritt, D.J. (2007). Dorsal longitudinal stretch receptor of Drosophila melanogaster larva - fine structure and maturation. Arthropod structure & development *36*, 157-169.

Schuurmans, C., Armant, O., Nieto, M., Stenman, J.M., Britz, O., Klenin, N., Brown, C., Langevin, L.M., Seibt, J., Tang, H.*, et al.* (2004). Sequential phases of cortical specification involve Neurogenin-dependent and -independent pathways. EMBO J *23*, 2892-2902.

Sepp, K., and Auld, V.J. (2003). Reciprocal interactions between neurons and glia are required for Drosophila peripheral nervous system development. J Neurosci *23*, 8221-8230.

Sepp, K.J., Schulte, J., and Auld, V.J. (2000). Developmental dynamics of peripheral glia in Drosophila melanogaster. Glia *30*, 122-133.

Sepp, K.J., Schulte, J., and Auld, V.J. (2001). Peripheral glia direct axon guidance across the CNS/PNS transition zone. Dev Biol *238*, 47-63.

Simon-Areces, J., Dopazo, A., Dettenhofer, M., Rodriguez-Tebar, A., Garcia-Segura, L.M., and Arevalo, M.A. (2011). Formin1 mediates the induction of dendritogenesis and synaptogenesis by neurogenin3 in mouse hippocampal neurons. PLoS ONE *6*, e21825.

Song, W., Onishi, M., Jan, L.Y., and Jan, Y.N. (2007). Peripheral multidendritic sensory neurons are necessary for rhythmic locomotion behavior in Drosophila larvae. Proc Natl Acad Sci USA *104*, 5199-5204.

Spletter, M.L., Liu, J., Liu, J., Su, H., Giniger, E., Komiyama, T., Quake, S., and Luo, L. (2007). Lola regulates Drosophila olfactory projection neuron identity and targeting specificity. Neural development *2*, 14.

Stegmuller, J., Konishi, Y., Huynh, M.A., Yuan, Z., Dibacco, S., and Bonni, A. (2006). Cell-intrinsic regulation of axonal morphogenesis by the Cdh1-APC target SnoN. Neuron *50*, 389-400.

Steimel, A., Wong, L., Huarcaya Najarro, E., Ackley, B.D., Garriga, G., and Hutter, H. (2010). The Flamingo ortholog FMI-1 controls pioneer-dependent navigation of follower axons in C. elegans. Development.

Steinel, M.C., and Whitington, P.M. (2009). The atypical cadherin Flamingo is required for sensory axon advance beyond intermediate target cells. Dev Biol *327*, 447-457.

Stone, M.C., Roegiers, F., and Rolls, M.M. (2008). Microtubules have opposite orientation in axons and dendrites of Drosophila neurons. Mol Biol Cell *19*, 4122-4129.

Stork, T., Engelen, D., Krudewig, A., Silies, M., Bainton, R.J., and Klämbt, C. (2008). Organization and function of the blood-brain barrier in Drosophila. J Neurosci *28*, 587-597.

Sugimura, K., Satoh, D., Estes, P., Crews, S., and Uemura, T. (2004). Development of morphological diversity of dendrites in Drosophila by the BTB-zinc finger protein abrupt. Neuron *43*, 809-822.

Sugimura, K., Yamamoto, M., Niwa, R., Satoh, D., Goto, S., Taniguchi, M., Hayashi, S., and Uemura, T. (2003). Distinct developmental modes and lesion-induced reactions of dendrites of two classes of Drosophila sensory neurons. J Neurosci *23*, 3752-3760.

Suli, A., Mortimer, N., Shepherd, I., and Chien, C.B. (2006). Netrin/DCC signaling controls contralateral dendrites of octavolateralis efferent neurons. J Neurosci *26*, 13328-13337.

Sulkowski, M., Iyer, S., Kurosawa, M., Iyer, E., and Cox, D. (2011). Turtle functions downstream of cut in differentially regulating class specific dendrite morphogenesis in Drosophila. PLoS ONE *6*, e22611.

Sweeney, N.T., Li, W., and Gao, F.B. (2002). Genetic manipulation of single neurons in vivo reveals specific roles of flamingo in neuronal morphogenesis. Dev Biol *247*, 76-88.

Tahirovic, S., and Bradke, F. (2009). Neuronal polarity. Cold Spring Harb Perspect Biol *1*, a001644.

Takeichi, M. (2007). The cadherin superfamily in neuronal connections and interactions. Nat Rev Neurosci *8*, 11-20.

Tea, J.S., and Luo, L. (2011). The chromatin remodeling factor Bap55 functions through the TIP60 complex to regulate olfactory projection neuron dendrite targeting. Neural development *6*, 5.

Terriente, J., Perea, D., Suzanne, M., and Díaz-Benjumea, F.J. (2008). The Drosophila gene zfh2 is required to establish proximal-distal domains in the wing disc. Dev Biol *320*, 102-112.

Tessier-Lavigne, M. and Goodman, C.S. (1996). The molecular biology of axon guidance. Science *274*, 1123-33

Tian, L., Hires, S.A., Mao, T., Huber, D., Chiappe, M.E., Chalasani, S.H., Petreanu, L., Akerboom, J., McKinney, S.A., Schreiter, E.R.*, et al.* (2009). Imaging neural activity in worms, flies and mice with improved GCaMP calcium indicators. Nat Methods.

Umesono, Y., Hiromi, Y., and Hotta, Y. (2002). Context-dependent utilization of Notch activity in Drosophila glial determination. Development *129*, 2391-2399.

Usui, T., Shima, Y., Shimada, Y., Hirano, S., Burgess, R.W., Schwarz, T.L., Takeichi, M., and Uemura, T. (1999). Flamingo, a seven-pass transmembrane cadherin, regulates planar cell polarity under the control of Frizzled. Cell *98*, 585-595.

Vrieseling, E., and Arber, S. (2006). Target-induced transcriptional control of dendritic patterning and connectivity in motor neurons by the ETS gene Pea3. Cell *127*, 1439-1452.

Wagh, D.A., Rasse, T.M., Asan, E., Hofbauer, A., Schwenkert, I., Dürrbeck, H., Buchner, S., Dabauvalle, M.C., Schmidt, M., Qin, G.*, et al.* (2006). Bruchpilot, a protein with homology to ELKS/CAST, is required for structural integrity and function of synaptic active zones in Drosophila. Neuron *49*, 833-844.

Wang, Z., Singhvi, A., Kong, P., and Scott, K. (2004). Taste representations in the Drosophila brain. Cell *117*, 981-991.

Whitford, K.L., Dijkhuizen, P., Polleux, F., and Ghosh, A. (2002). Molecular control of cortical dendrite development. Annu Rev Neurosci *25*, 127-149.

Wilson, S.I., Shafer, B., Lee, K.J., and Dodd, J. (2008). A molecular program for contralateral trajectory: Rig-1 control by LIM homeodomain transcription factors. Neuron *59*, 413-424.

Winberg, M.L., Mitchell, K.J., and Goodman, C.S. (1998). Genetic analysis of the mechanisms controlling target selection: complementary and combinatorial functions of netrins, semaphorins, and IgCAMs. Cell *93*, 581-591.

Wong, A.M., Wang, J.W., and Axel, R. (2002). Spatial representation of the glomerular map in the Drosophila protocerebrum. Cell *109*, 229-241.

Wong, R.O., and Ghosh, A. (2002). Activity-dependent regulation of dendritic growth and patterning. Nat Rev Neurosci *3*, 803-812.

Wu, J.I., Lessard, J., Olave, I.A., Qiu, Z., Ghosh, A., Graef, I.A., and Crabtree, G.R. (2007). Regulation of dendritic development by neuron-specific chromatin remodeling complexes. Neuron *56*, 94-108.

Wu, Z., Sweeney, L., Ayoob, J., Chak, K., Andreone, B., Ohyama, T., Kerr, R., Luo, L., Zlatic, M., and Kolodkin, A. (2011). A Combinatorial Semaphorin Code Instructs the Initial Steps of Sensory Circuit Assembly in the Drosophila CNS. Neuron *70*, 281-298.

Xie, X., and Auld, V.J. (2011). Integrins are necessary for the development and maintenance of the glial layers in the Drosophila peripheral nerve. Development *138*, 3813-3822.

Xue, D., Finney, M., Ruvkun, G., and Chalfie, M. (1992). Regualtion of the mec-3 gene by the C. elegans homeoproteins UNC-86 and MEC-3. EMBO J *11*, 4969-79.

Yamamoto, M., Ueda, R., Takahashi, K., Saigo, K., and Uemura, T. (2006). Control of axonal sprouting and dendrite branching by the Nrg-Ank complex at the neuron-glia interface. Curr Biol *16*, 1678-1683.

Ye, B., Kim, J.H., Yang, L., McLachlan, I., Younger, S., Jan, L.Y., and Jan, Y.N. (2011). Differential regulation of dendritic and axonal development by the novel kruppel-like factor dar1. J Neurosci *31*, 3309-3319.

Ye, B., Zhang, Y., Song, W., Younger, S.H., Jan, L.Y., and Jan, Y.N. (2007). Growing dendrites and axons differ in their reliance on the secretory pathway. Cell *130*, 717-729.

Yeo, S.L., Lloyd, A., Kozak, K., Dinh, A., Dick, T., Yang, X., Sakonju, S., and Chia, W. (1995). On the functional overlap between two Drosophila POU homeo domain genes and the cell fate specification of a CNS neural precursor. Genes Dev *9*, 1223-1236.

Zhong, L., Hwang, R.Y., and Tracey, W.D. (2010). Pickpocket Is a DEG/ENaC Protein Required for Mechanical Nociception in Drosophila Larvae. Curr Biol.

Zhu, H., and Luo, L. (2004). Diverse functions of N-cadherin in dendritic and axonal terminal arborization of olfactory projection neurons. Neuron *42*, 63-75.

Zlatic, M., Landgraf, M., and Bate, M. (2003). Genetic specification of axonal arbors: atonal regulates robo3 to position terminal branches in the Drosophila nervous system. Neuron *37*, 41-51.

Zlatic, M., Li, F., Strigini, M., Grueber, W., and Bate, M. (2009). Positional cues in the Drosophila nerve cord: semaphorins pattern the dorso-ventral axis. PLoS Biol *7*, e1000135.